8-2-2022 2:00 PM

Complete Hopf and Bogdanov-Takens Bifurcation Analysis on Two Epidemic Models

Yuzhu Ruan, *The University of Western Ontario*

Supervisor: Yu, Pei, *The University of Western Ontario*

A thesis submitted in partial fulfillment of the requirements for the Master of Science degree in Applied Mathematics

Abstract

Infectious diseases are a global problem that harms people's health and well-being and severely threatens human survival. As an epidemiological model, the SIR model is commonly referred to as forecasting how illnesses will spread, how many people will become sick, and how long an epidemic will last. It is also possible to estimate other epidemiological parameters.

Bifurcation theory and limit cycle theory have played an important role in the study of nonlinear dynamical systems, especially for the infectious disease models. In particular, Hopf and Bogdanov-Takens (B-T) bifurcations are the two most prevalent bifurcations in real-world systems and should be considered in practical problems which require analysis of stability and bifurcation.

In this thesis, we reconsider two epidemic models and focus on the dynamical behaviours of the systems, which are not explored in the previous studies. Our main attention focuses on the stability and bifurcation of equilibrium solutions. Explicit conditions are obtained to classify different bifurcations, including forward bifurcation, backward bifurcation, Hopf bifurcation, and B-T bifurcation. The method of normal forms is applied to study Hopf, codimension-2 and codimension-3 B-T bifurcations, showing complex dynamics in these two models.

Keywords: SIR disease model, Stability, Limit cycle, Forward bifurcation, Backward bifurcation, Hopf bifurcation, Bogdanov-Takens bifurcation, Normal form

Lay Summary

Infectious diseases are a global problem that harms people's health and well-being and severely threatens human survival. In epidemiology, SIR models are widely used to predict the spread of diseases, the number of infected individuals, epidemic duration, and other factors.

We have studied the stability of epidemic SIR models, the conditions for the existence of limit cycle bifurcations, as well as Hopf and B-T bifurcations as a result of the increasing interest in the dynamic behavior of epidemic anaysis. We therefore examined the dynamics of the systems in this paper and reconsider the two epidemic models. Our analysis focused on the equilibrium solutions, stability, and bifurcation of the two models and we obtained explicit conditions that permit us to classify each bifurcation. The center manifold theorem, normal form theory, bifurcation theory and limit cycle theory were used to demonstrate the complex dynamics of both models. Hopf, codimension 2 and codimension 3 B-T bifurcations were studied to demonstrate the complex dynamics of these models.

Acknowledgment

I am extremely horned and proud to have such an opportunity to express my honest appreciation to my supervisor, Professor Pei Yu. Professor Yu has been extremely patient in guiding and educating me from my second year of college to the end of my master's term. The amount of encouragement and support that I received from him has made me come this far. Particularly in helping me finish my thesis, his passion, knowledge, and honesty towards academic studies have always reminded me of what a true researcher should be. I would not reach what I have reached without Professor Yu.

I would also like to thank Professor Xingfu Zou for a tremendous amount of conductive suggestions during seminar talks. Many thanks to Professor Shu Li and Professor Tatyana Barron for pointing out my shortcomings and faults in my thesis, all those helpful comments and insights have made the thesis complete.

I would also like to thank Professor Rob Corless for the recommendation letter and Professor Khoa Nguyen for hosting my defense. Thanks also go to my course Professors, Dr. Greg Reid, Dr. David Jeffery, and Dr Linda Wahl for their generous help and support.

My appreciation extends to the Department of Applied Mathematics and the University of Western Ontario for providing me with such great facilities and opportunities to study. Your acceptance of my PhD application would allow me to fulfill my academic accomplishments. I will never regret spending the most beautiful years of my life to be in this outstanding community.

Contents

List of Figures

List of Tables

Chapter 1

Introduction

Infectious illnesses, as a worldwide concern, not only inflict considerable harm to people's bodily and mental health but also constitute a significant danger to human survival and progress and have piqued the international community's interest. Today, infectious diseases are widely distributed worldwide, especially the COVID 19 pandemic. Tens of millions of people suffer from physical and mental health, leading to increased social problems.

1.1 Research Background

The classic infectious disease model is the famous SIR compartment model developed in the early 20th century, particularly by Ross in 1916 [23], Ross and Hudson in 1917 [24], Kermack and McKendrick in 1927 [15], and Kendall in 1956 [16] with S denoting the susceptible, I the infectious, R the recovered individuals who are immune to the disease ever, and patients are able to move between compartments [41]. At the time t, the number of people not infected by the disease but at risk of infection demonstrated by $S(t)$, the number of people infected and infectious demonstrated by $I(t)$, and the number of people who are out of infectiousness demonstrated by $R(t)$.

With general assumptions, the population of susceptibles at a given time is constant, the number of susceptibles infected by a patient at a given time is proportional to the total number of susceptibles, which is denoted by β, and the number of patients removed per unit time equals the number of infected patients, with the proportionality factor denoted as γ [16]. Thus, a fundamental epidemic SIR differential system model can be written as

$$\begin{aligned} \frac{dS}{dt} &= -\beta S I \\ \frac{dI}{dt} &= \beta S I - \gamma I \\ \frac{dR}{dt} &= \gamma I \end{aligned} \tag{1.1}$$

According to the above SIR model, people are considered immune to a disease for the rest of their lives upon recovery. However, an individual's immunity may wane with time for other airborne diseases. As a result, the SIRS model has been introduced, which is derived from the SIR model, with the recovered patient having the ability to revert to a susceptible state. In recent years, comparative epidemiological models have been widely used to study infectious disease dynamics. Various infectious disease problems have been analyzed using various mathematical models. Models based on ordinary differential equations are the most popular for describing infectious disease dynamics.

As one of the most effective methods to analyze infectious illnesses, more and more scholars are using dynamical systems approach to analyze factors such as the diffusion spread of infectious diseases. An SIR model is widely recognized as the most important epidemiological model because it is capable of predicting how diseases will spread, how many people will be affected, and how long an epidemic will persist throughout a particular population. It can also estimate other epidemiological factors, such as reproductive capacity.

Several studies have been conducted in recent years on the Hopf bifurcation and Bogdanov-Takens (B-T) bifurcation of epidemic models. A 2-dimensional disease model has been developed by Yu *et al.* [35] , which can be used for both epidemiologic and in-host disease modeling, by focusing on diverse dynamical behaviors of the system. A simple HIV SIR model with a convex incidence and four real parameters was studied by Yu *et al.* [36] to analyze multiple limit cycles that emerge from Hopf bifurcation, and a unique method was developed to determine the normal forms of codimension-2 and codimension-3 B-T bifurcations. A saturated incidence rate and saturated treatment function were considered by Zhang *et al.* in [37]. It was demonstrated that a backward bifurcation between the endemic and disease-free equilibrium is observed when there is a strong effect on treatment. There were two studies [3, 14], in which the authors focused on the stability analysis and the existence of bifurcations in an epidemic model with a nonlinear incidence rate. Wang *et al.* [29] investigated a bilinear incidence rate and density-dependent SIR model with a saturated treatment function, concentrating on the model's dynamical bifurcation analysis, particularly the stability of equilibirum solutions and supercritical Hopf bifurcation. Rao *et al.* [22] studied an SIRS epidemic model with a generalised incidence rate function representing illness transmission processes with an emphasis on equilibria, as well as on forward and backward bifurcations.

An increased interest in the dynamic behaviors of epidemic models motivated us to study

stability and bifurcation of the models in epidemiology, especially the existence condition on the bifurcation of limit cycles, and Hopf and B-T bifurcations. For the purpose of analysis of these questions, we have chosen to examine the following epidemic models: an SIR model with saturated treatment function introduced in [29], and an SIRS model with a generalized incidence introduced in [22]. The focus of this study will be on the relation between susceptible and infectious within the system since we are able to analyze the dynamical behaviors of the systems by examining the reduced system, since these two systems are topologically equivalent.

With regard to the SIR model with a saturated treatment function [29], we will utilize the fact that the third function is independent from the first two functions. Specifically, we will address the gap part of their study in this thesis, which is the determination of the codimension of the Hopf bifurcation, and the maximum number of limit cycles that can bifurcate simultaneously from the Hopf critical point, and also the B-T bifurcation.

For SIRS model with a generalized incidence [22], on the other hand, we will assume that the total population is constant, which reduces the system to two dimensions, and then analyze the Hopf and B-T bifurcations of the reconstructed system using the new hierarchical parametric approach proposed in [39].

1.2 Methodology

Before describing the methodology to be used in this thesis, we first introduce some mathematical concepts related to dynamical analysis, such as equilibrium solutions and their stability, followed by an explanation of the importance on the bifurcation of limit cycles. Then, we will discuss the conditions for generating Hopf bifurcations and Bogdanov-Takens bifurcations.

1.2.1 Equilibrium Points and Stability

Studies of stability are a vital part of research on the SIR models of infectious diseases. In preparation for the investigation of stability, we followed the method introduced in [11], which is needed to compute the equilibrium solutions and the Jacobian matrix of our systems.

Consider the general 2-d system of differential equations:

$$\begin{aligned} \dot{x_1} &= f(x_1, x_2), \\ \dot{x_2} &= g(x_1, x_2). \end{aligned} \tag{1.2}$$

The equilibrium solutions or equilibrium points can be found by solving the nonlinear equations: $f(x_1^*, x_2^*) = g(x_1^*, x_2^*) = 0$ for some (x_1^*, x_2^*).

The Jacobian matrix of the system (1.2) evaluated at the equilibrium point (x_1^*, x_2^*) is given by

$$J(x_1^*, x_2^*) = \begin{bmatrix} \frac{\partial f}{\partial x_1}(x_1^*, x_2^*) & \frac{\partial f}{\partial x_2}(x_1^*, x_2^*) \\ \frac{\partial g}{\partial x_1}(x_1^*, x_2^*) & \frac{\partial g}{\partial x_2}(x_1^*, x_2^*) \end{bmatrix}. \tag{1.3}$$

Then, the stability of the equilibrium point (x_1^*, x_2^*) can be determined by the eigenvalues of J, which are functions of the parameters of the system.

For our 2-d models, the dynamics of the equilibrium points can be classified in the following theorem.

Theorem 1.2.1. Let J be the Jacobian matrix of the dynamical system at equilibrium point (x_1^*, x_2^*) with eigenvalues λ_1 and λ_2. Then, the equilibrium is

(i) a **saddle** if both λ_1 and λ_2 are real and have opposite signs;

(ii) a **stable node** if λ_1 and λ_2 are are distinct, non-zero and both negative, and an **unstable node** if λ_1 and λ_2 are are distinct, non-zero and both positive;

(iii) a **stable focus** if both λ_1 and λ_2 are a pair of complex conjugates with negative real part; an **unstable focus** if both λ_1 and λ_2 are a pair of complex conjugates with positive real part.

If the real parts of the eigenvalues are changed to zero with respect to system parameters, then the quilibrim point becomes singular and bifurcations occur from the equilibrium solutions.

1.2.2 Limit cycle theory

In studying nonlinear dynamical systems, limit cycle theory plays a very important role in the well-known phenomenon of self-oscillations arising from physical science and engineering [10, 13]. Hopf and B-T bifurcations are two main bifurcations that generate limit cycles in real-world systems. The main task in such studies is to derive the normal form (NF) of the system and determine the codimension of the associated bifurcation, since the codimension is directly related to the maximal number of limit cycles which determines complex behaviors of the system. This is not easy for higher-codimension bifurcation problems. In reality, the parameters involved in real systems often have physical limitations, yielding additional difficulty in the bifurcation analysis such that the analysis becomes very difficult even for 2-dimensional dynamical systems.

Very recently, a hierarchical parametric analysis has been proposed to overcome this difficulty in dealing with the stability and bifurcation analysis related to Hopf bifurcation [39].

In this article, the authors use a simple epidemic model to demonstrate that this new approach is efficient when traditional methods are not applicable, which is to determine the limit cycle from the normalized dimensionless model. Here is the example for the 2d model mentioned in [39]

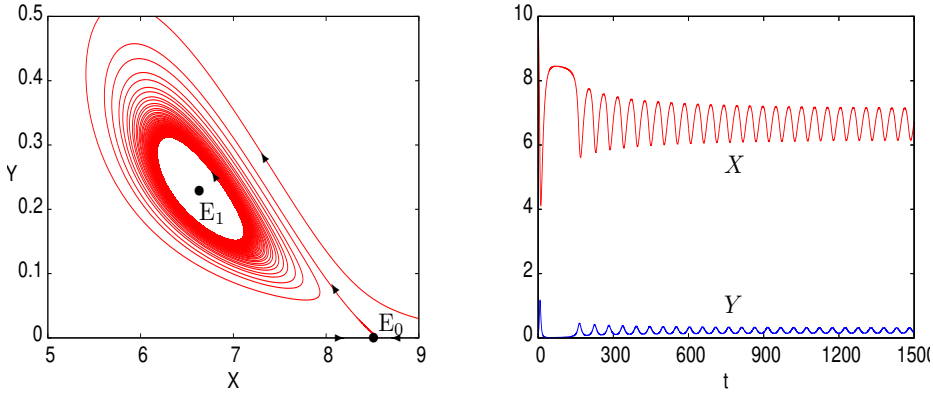

Figure 1.1: Simulation of one stable limit cycle for the 2-d HIV model in [36]

In the following, we use the limit cycle bifurcation examples given in [36] to illustrate the codimension of Hopf bifurcation, and to show the significant difference between the bifurcations of one and two limit cycles.

For the case with one limit cycle depicted in Figure 1.1, it is shown in [36] that there exists a degenerate saddle point (which is not shown in this figure), an unstable focus E_{1-} and a stable limit cycle. The whole 2-d phase space is divided into two parts by the limit cycle, all trajectories (both from inside and outside the limit cycle) converge to the stable limit cycle. This implies that the patient is under a relative stable situation.

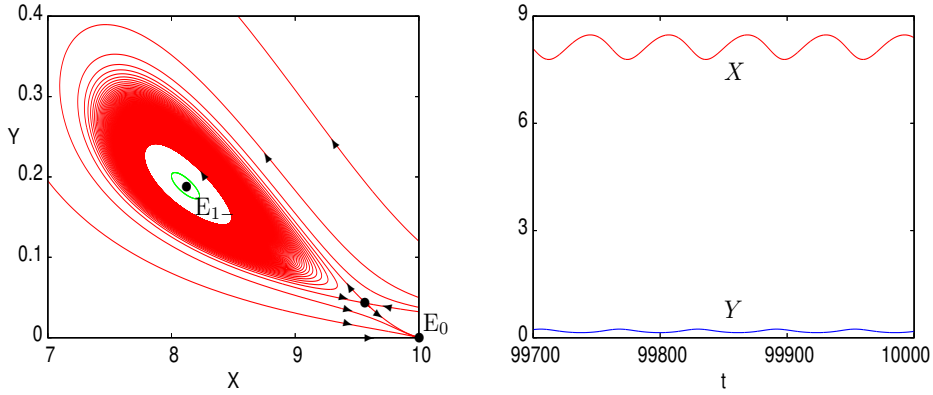

Figure 1.2: Simulation of two limit cycles for the 2-d HIV model in [36]

For the case with two limit cycles as shown in Figure 1.2 (see Figure 10 in [36]), on the other hand, it has three equilibria, E_0 which is a stable node, E_{1+} which is a saddle point, and E_{1-} which is a stable focus. There exist two limit cycles bifurcating from a Hopf critical point, with the outer one stable (in red color) and inner one unstable (in green color). Therefore, the whole 2-d phase plane is divided by the two limit cycles into three regions, and trajectories converge either to the stable node E_0, or to the stable focus E_{1-}, or to the satble limit cycle. These complex dynamical behaviours reflect more realistic situation, since the patient may experience different situations at different time.

1.2.3 Hopf bifurcation

Hopf bifurcation occurs from a critical point at which the equilibrium loses it stability and periodic solutions emerge, which is characterized by a pure imaginary pair of eigenvalues. Consequently, for autonomous differential systems, Hopf bifurcations can occur only in dynamical systems with a dimension of two or greater.

Consider the following differential n-d system:

$$\dot{x} = A(\mu)x + F(x,\mu), \quad x \in R^n, \ \ \mu \in R, \tag{1.4}$$

where μ is a parameter, and A denotes the linear part while F represents the nonlinear part with $F(0) = 0$, implying that the origin is an equilibrium solution. Suppose the one pair of complex conjugate eigenvalues of $A(\mu)$ is given by $\lambda_{1,2} = \alpha(\mu) \pm i\beta(\mu)$. Then, Hopf bifurcation is definded by the following two conditions:

(H_1) $\alpha(0) = 0$, and

(H_2) $\frac{d}{d\mu}\Big|_{\mu=\mu_0} \neq 0$, which is called transversal condition.

To consider the maximal limit cycles bifurcating from a Hopf critical point, we need to consider the codimension of Hopf bifurcation. To achieve this, the standard method is to use a computer algebraic system such as Maple or Mathematica to symbolically compute the conventional normal form (CNF) of the system at an equilibrium point resulting from a Hopf bifurcation, and then solving a multivariate polynomial system using that CNF.

There are two main difficulties in the computation of the CNF. The first one is due to the symbolic computational complexity in the CNF caused by the conventional approach used in stability and bifurcation analysis. The second difficulty comes from that real-world systems often have extra restrictions on the system parameters.

For instance, consider the maximal number of limit cycles arising from generalized Hopf bifurcation in a 2-dimensional nonlinear system. The system parameters, in general, must be positive or even restricted to certain limiting values. Suppose that the system under consideration contains 5 real parameters. In general, if these parameters are assumed to be real, then the maximal number of bifurcating limit cycles may be 5, which is the same as the number

of parameters. It should be noted, however, that if the system is a real biological one or other physical system with parameters that are limited, the maximum number of limit cycles might be 4, 3, 2, or even only 1. In this case, determining the codimension of the Hopf bifurcation becomes extremely difficult. The difficulty is mainly from solving the polynomial systems based on the normal form or focus values (suppose the normal form has been obtained), since one needs to determine the sign of the polynomials with respect to the variation of many variables (parameters).

Besides the above-mentioned difficulties in bifurcation analysis, another difficulty in Hopf bifurcation is determining the conditions for which a given system undergoes Hopf bifurcation. When more parameters are involved in the system, and equilibrium solutions cannot be showed distinctly in terms of the system parameters, determining the stability of the equilibrium solutions becomes very difficult, and in most cases, it is impossible to determine the Hopf critical point. Thus, in this case, it is not possible to compute the normal form (or the focus values), thereby making it impossible to give a theoretical study on the bifurcations except using numerical approaches to get some solutions for fixed parameter values.

1.2.4 Bogdanov-Takens bifurcation

The Bogdanov-Takens (B-T) bifurcation occurs when the system has a double-zero eigenvalue at the equilibrium. To analyze the B-T bifurcation, the equilibrium point needs to be translated to the origin and Taylor expansion should be used around the origin. Next, we need to apply an appropriate affine transformation to transform the original system to a new one whose linear part is in the Jordan canonical form. Further, nonlinear transformations should be applied [36] to find the codimension of B-T bifurcation. Consider the following normal form associated with the codimension-2 B-T bifurcation (for example, see [40]):

$$\begin{aligned} \dot{y_1} &= y_2, \\ \dot{y_2} &= \gamma_1 + \gamma_2 y_1 + y_1^2 - y_1 y_2, \end{aligned} \tag{1.5}$$

where γ_1 and γ_2 are two unfolding (bifurcation) parameters. When $\gamma_1 = \gamma_2 = 0$, the system has a unique equilibrium at the origin $(0, 0)$, with a zero eigenvalue of multiplicity two. Generally, Andronov-Hopf bifurcation curves and saddle homoclinic bifurcation curves typically occur around the origin of the critical equilibrium on saddle-node bifurcation curves [40]. The local bifurcation curves for the codimension-2 B-T bifurcation are desribed as follows.

Saddle-node bifurcation: SN = $\{\gamma \mid 4\gamma_1 - \gamma_2^2 = 0\}$;

Hopf bifurcation: H = $\{\gamma \mid \gamma_1 = 0,\ \gamma_2 < 0\}$;

Homoclinic loop bifurcation: HL = $\{\gamma \mid \gamma_1 = -\frac{6}{25}\gamma_2^2,\ \gamma_2 < 0\}$.

In this thesis, we will analyze the codimension of B-T bifurcations. For the codimension-2 B-T bifurcation, the analysis has become standard [10, 31]. However, for codimension-3 or

higher-codimension (or degenerate) B-T bifurcations, the computation of the normal forms becomes much more involved, particularly in order to establish the relation between the original system and the simplified system (the normal form). The codimension-3 degenerate cusp B-T bifurcation was studied by Dumortier *et al.* in 1987 [6], and the classical six-step transformation approach was developed and widely used by researchers in deriving the simplest normal form (SNF) with unfolding. However, the six transformations are usually quite complicated, and some of them are not even in algebraic form, which causes difficulty in applications.

Recently, the so-called one-step transformation method was proposed [36, 38], which provides the transformation for the state variables, the parameters, and the time rescaling in just one step. This enables one to obtain a direct relationship between the original system and the SNF, which not only greatly simplifies the analysis but also clearly shows the impact of the original system parameters on the dynamical behaviors of the system. This new method is based on the SNF theory, and the parametric simplest normal (PSNF) theory [33, 8, 9, 34, 7, 36]. The key step in this method is to choose the appropriate basis for the SNF and the PSNF, as well as that in the nonlinear transformations.

1.3 Research Objectives

The main objectives of this thesis include the following tasks.

1. Identify the required condition of stability in our epidemic models and analyze the dynamical behavior near the equilibrium points.

2. Determine the necessary bifurcation condition in our epidemic models and present a predictably curve with respect to parameter changes in the system to analyze the bifurcation performance.

3. Use the method of normal forms to determine the condimension of Hopf bifurcation, and thus find the maximal number of limit cycles bifurcating from a Hopf critical point.

4. Apply he method of normal form to determine the codimension of B-T bifurcation, and perform bifurcation alaysis for codimension-2 and codimension-3 B-T bifurcations.

1.4 Thesis outline and contribution

In this thesis, we will re-investigate two disease models: one is an infectious disease SIR model with a saturated treatment function, studied by Wang *et al.* [29], and the other is an SIRS model with a generalized incidence function, considered by Rao *et al.* [22]. In [29],

the authors consider equilibrium solutions and their stability and present some formulas for Hopf bifurcation. However, their analysis is incomplete for Hopf bifurcation, though some numerical simulations are given to show the bifurcation of a single limit cycle. Also, they did not study the codimension of the Hopf bifurcation, nor the B-T bifurcation. In [22], the authors provide an analytical study for different death rates on the existence and stability of equilibrium solutions. They also present some numerical simulations to verify their theoretical results. However, they do not consider Hopf and B-T bifurcations due to the difficulty caused by different death rates.

We will re-reconsider the SIR model [29] and the SIRS model [22] in Chapter 3 and Chapter 4, respectively. Our analysis confirms that there is a transcritical bifurcation between the disease-free equilibrium and the endemic equilibrium at the critical values of the basic reproduction number $R_0 = 1$. We apply the hierarchical parametric analysis [39] to provide a detailed study on the existence and stability of the endemic equilibrium, and show that the models can have forward bifurcation, backward bifurcation, Hopf bifurcation, and B-T bifurcation. We mainly focus on the difficult parts: studying the codimension of the Hopf bifurcation and B-T bifurcation, as well as on the dynamical behaviors around these bifurcation points. We derive the explicit conditions for the codimension of Hopf and B-T bifurcations. For the codimension-3 B-T bifurcation, we apply the one-step transformation approach to obtain the SNF and PSNF for bifurcation analysis, showing the advantage of this method compared to the classical six-step transformation approach. Numerical simulations are also presented to demonstrate the existence of multiple limit cycle bifurcations, showing an excellent agreement with the theoretical predictions.

The main contributions of this thesis are described as follows.

1. Explicit existence conditions for the endemic equilibrium of the two models are obtained.

2. Explicit conditions for determining the Hopf critical point are derived.

3. The CNF for the Hopf bifurcation is explicitly computed and used to determine the codimension of Hopf bifurcation.

4. The SNF and PSNF for the codimension2 and codimension-3 B-T bifurcations are derived, and a complete analysis is given for these two bifurcations.

5. For the SIR model [29], the center manifold reduction is considered, and the dynamical equation on the manifold is obtained to determine the stability of the degenerate node. Moreover, the codimension of Hopf bifurcation on the center manifold is determined on the basis of the normal form.

Chapter 2

An SIR model with a saturated treatment function

2.1 Introduction

In this chapter, we give a further analysis of the SIR model, which has been studied by Wang *et al.* [29]. The model is described by three ordinary differential equations (ODE):

$$\begin{aligned} \dot{S} &= S(A-S) - kIS, \\ \dot{I} &= kIS - \mu I - \frac{rI}{a+I}, \\ \dot{R} &= \frac{rI}{a+I} - \mu R, \end{aligned} \tag{2.1}$$

All of the parameters are positive and defined in Table 2.1.

In [29], the authors consider the equilibrium solutions and their stability. Also, they analyzed Hopf bifurcation and presented some simulations for bifurcation of single limit cycle. Their analysis is incomplete, particularly for Hopf bifurcation. They did not study the codimension of the Hopf bifurcation, that is, they did not answer the question: What is the maximal number of limit cycles which can bifurcate simultaneously from the Hopf critical point. Also, they did not consider Bogdanov-Takens (B-T) bifurcation at all.

In this section, we will reconsider this model and give a complete analysis of the Hopf and B-T bifurcation, showing the complex dynamics of this model. We first simply summarize the solution properties and stability of the equilibrium solutions. Then we focus on Hopf and B-T bifurcations. Simulations are given to illustrate our theoretical results.

First, it is easy to note that the first two equations in model (2.1) are independent from the third equation, since the variable R is not included in the first two equations. Since our main concern is the prevalence of the disease, only the first two equations are relevant. Thus, the

Table 2.1: Definitions of parameters of system (2.1)

Variable	Description	Resource
S	The number of susceptible individuals	[41]
I	The number of infectious individuals	[41]
R	The number of recovered individuals	[41]
A	The population's carrying capacity without disease	[29]
μ	The natural mortality of the population	[28]
k	The infection coefficient	[28]
r	The cure rate	[29]
a	Evaluate the impact of a delay in treating the infected patients.	[29]

dimensionless 2-d model of the system (2.1) is obtained as follows.

$$\begin{aligned} \dot{S} &= S(A-S) - kIS, \\ \dot{I} &= kIS - \mu I - \frac{rI}{a+I}. \end{aligned} \tag{2.2}$$

Unlike the analysis in [29], we first perform a dimensionless change to simplify the analysis. To achieve this, introducing the changes of state variables: $S = AX$, $I = AY$, the parametrization: $r = \tilde{r}A$, $a = \tilde{a}A$, and the time scaling $t = \frac{1}{A}\tau$, into (2.2) we obtain the following dimensionless model (with $\tilde{r}$, $\tilde{a}$ and τ being still denoted by r, a and t, respectively, for simplicity):

$$\begin{aligned} \dot{X} &= X(1 - X - kY), \\ \dot{Y} &= Y\Big(kX - \mu - \frac{r}{a+Y}\Big). \end{aligned} \tag{2.3}$$

2.2 Property of solutions

First, we consider the property of solutions of the model (2.3) and have the following result.

Theorem 2.2.1. *The solution of the model (2.3) is positive if the given initial condition is positive; and the solution is bounded.*

Proof. Using the method of constant variations, the solution of the initial value for the model can be written as

$$\begin{aligned} X(t) &= X(0)\exp\left\{\int_0^t [1 - X(s) - k\,Y(s)]\,ds\right\}, \\ Y(t) &= Y(0)\exp\left\{\int_0^t [k\,X(s) - \mu - \frac{r}{a+Y(s)}]\,ds\right\}, \end{aligned} \tag{2.4}$$

which clearly shows that $X(t) > 0$, $Y(t) > 0$ for any $t > 0$ if $X(0) > 0$ and $Y(0) > 0$.

To prove the boundedness of the solution, we construct a simple Lyapunov function:

$$V(X, Y) = X + Y, \tag{2.5}$$

which is certainly positive definite for $X > 0$, $Y > 0$. Then, differentiating V with respect to time t and evaluating it on the trajectory of the model yields

$$\begin{aligned}\frac{dV}{dt} = \dot{X} + \dot{Y} &= X(1 - X) - Y\Big(\mu + \frac{r}{a + Y}\Big) \\ &= -\Big(X - \frac{1}{2}\Big)^2 - Y\Big(\mu + \frac{r}{a + Y}\Big) + \frac{1}{4}.\end{aligned}$$

It is clear that $\frac{dV}{dt} < 0$ for $X \geq 1,\ Y > 0$. For $X < 1,\ Y > 0$, we choose Y such that

$$-Y\Big(\mu + \frac{r}{a + Y}\Big) + \frac{1}{4} \leq 0,$$

yielding $\frac{dV}{dt} < 0$ for $X < 1,\ Y > 0$. From the above equation, we have

$$Y\Big(\mu + \frac{r}{a + Y}\Big) > Y\mu \geq \frac{1}{4},$$

which implies that when $X < 1,\ Y > 0$, choosing $Y \geq \frac{1}{4\mu}$ guarantees that $\frac{dV}{dt} < 0$.

Therefore, we construct the trapping region Ω as the triangle area, bounded by the X-axis, the Y-axis, and the straight line L:

$$\mathrm{L}: \quad X + Y = 1 + \frac{1}{4\mu}. \tag{2.6}$$

The proof is complete. □

2.3 Equilibrium solutions and their stability

Simply letting $\dot{X} = \dot{Y} = 0$ yields three equilibrium solutions:

$$\begin{aligned}&\mathrm{E}_0 = (0, 0), && \text{Trivial Equilibrium (Population-Free Equilibrium)}, \\ &\mathrm{E}_1 = (1, 0), && \text{Disease-Free Equilibrium}, \\ &\mathrm{E}_2 = (X_2, Y_2) = \Big(X_2, \frac{1 - X_2}{k}\Big), && \text{Endemic Equilibrium}.\end{aligned} \tag{2.7}$$

The model always admits the trivial equilibrium and disease-free equilibrium (DFE) E_0 and E_1. The existence of the endemic equilibrium requires that $0 < X_2 < 1$, where X_2 is determined from the quadratic polynomial:

$$F_2 = X_2^2 - \Big(ak + 1 + \frac{\mu}{k}\Big)X_2 + \frac{(ak + 1)\mu}{k} + r. \tag{2.8}$$

Solving X_2 from $F_2 = 0$ we have

$$X_{2\pm} = \frac{1}{2}\Big[ak + 1 + \frac{\mu}{k} \pm \sqrt{(ak + 1 - \tfrac{\mu}{k})^2 - 4r}\Big], \tag{2.9}$$

which exist if $(ak + 1 - \frac{\mu}{k})^2 - 4r \geq 0$. Denote the endemic equilibria as

$$\mathrm{E}_{2\pm} = (X_{2\pm},\, Y_{2\pm}) = \Big(X_{2\pm},\, \frac{1 - X_{2\pm}}{k}\Big). \tag{2.10}$$

The basic reproduction number can be defined as

$$\mathrm{R}_0 = \frac{k}{\mu + \frac{r}{a}}. \tag{2.11}$$

Then, we have the following two theorems for the existence of E_2 and the stability of the equilibrium solutions, with the proof given after the second theorem. More details on the Hopf bifurcation will be given in the next theorem.

Theorem 2.3.1. *The existence conditions for the equilibrium solutions of the model (2.3) are given as follows.*

(1) *The trivial equilibrium* E_0 *and the disease-free equilibrium* (DFE) E_1 *always exists for positive parameter values.*

(2) *For the endemic equilibrium* E_2*, there are three cases:*

   (a) *when* $\mu > k(1 - ak)$ *while* $r < a(k - \mu)$*, only* E_{2-} *exists;*

   (b) *when* $\mu < k(1 - ak), ak < 1$ *while* $r = \frac{1}{4}(ak + 1 - \frac{\mu}{k})^2$*, both* $E_{2+} = E_{2-}$ *exists; and*

   (c) *when* $\mu < k(1 - ak), ak < 1$ *while* $r < \frac{1}{4}(ak + 1 - \frac{\mu}{k})^2$*, both* E_{2+} *and* E_{2-} *exist.*

Theorem 2.3.2. *The stability conditions of the equilibrium solutions of the model (2.3) are given below.*

(1) *The trivial equilibrium* E_0 *is always unstable (a saddle).*

(2) *The disease-free equilibrium* (DFE) E_1 *is asymptotically stable(a node) for* $R_0 < 1$*, and unstable (a saddle) for* $R_0 > 1$.

(3) *For the endemic equilibrium* E_2*, there are three cases:*

   (a) *A transcritical bifurcation occurs between* E_1 *and* E_2 *at the critical point* $\mathrm{R}_0 = 1$ *(or* $k = \mu + \frac{r}{a}$*).*

   (b) *The endemic equilibrium* E_{2+} *is a saddle when it exists.*

(c) *One Hopf or two Hopf bifurcations may occur from the endemic equilibrium* E_{2-} *when it exists.*

Note that one solution $E_{2+} = E_{2-} = E_2$ *exists with* $X_{2+} = X_{2-} = X_2 = \frac{1}{2}(ak + 1 + \frac{\mu}{k})$ *if* $\mu < k(1-ak)$ *and* $r = \frac{1}{4}(ak+1-\frac{\mu}{k})^2$*; and two solutions* E_{2+} *and* E_{2-} *exist if* $\mu < k(1-ak)$ *and* $r < \frac{1}{4}(ak + 1 - \frac{\mu}{k})^2$.

Proof. The stability of the equilibrium solutions is determined from the Jacobian matrix of system (2.3), which is given by

$$J(X,Y) = \begin{bmatrix} 1-2X-kY & -kX \\ kY & kX-\mu-\dfrac{ar}{(a+Y)^2} \end{bmatrix}. \tag{2.12}$$

It is easy to see that E_0 is a saddle since its corresponding eigenvalues are 1 and $-\mu$. Evaluating J at E_1 yields two eigenvalues: $\lambda_1 = -1$ and $\lambda_2 = k - \mu - \frac{r}{a}$. Thus, E_1 is a stable node for $k < \mu + \frac{r}{a}$, and a saddle for $k > \mu + \frac{r}{a}$. The reproduction number R_0 can be easily obtained from the eigenvalue λ_2, which can be rewritten as

$$\lambda_2 = \Big(\mu + \frac{r}{\mu}\Big)\,(\,R_0 - 1\,).$$

To find the transcritical point between E_1 and E_2, we compute the determinant $\det(J_2)$ of the Jacobian J at E_2 and eliminate X_2 from $\det(J_2) = 0$ and $F_2 = 0$ to obtain

$$\tilde{X}_2 = \frac{(k-\mu)(ak+1)(ak^2+k-\mu) - kr(ak^2+3k-\mu)}{(k-\mu)(ak^2+k-\mu) - 2k^2r},$$

$$T_c = ark^2\Big(k-\mu-\frac{r}{a}\Big)\Big[\Big(ak+1-\frac{\mu}{k}\Big)^2 - 4r\Big].$$

It is easy to see that $T_c = 0$ gives the solution $k = \mu + \frac{r}{a}$, which is substituted into $\tilde{X}_2$ to yield $\tilde{X}_2 = 1$. Moreover, substituting $X_2 = 1$ into the determinant $\det(J_2)$ we have

$$\det(J_2)|_{X_2=1} = -\Big(k-\mu-\frac{r}{a}\Big).$$

Comparing the above expression with the eigenvalue associated with the equilibrium E_1, $\lambda_2 = k - \mu - \frac{r}{a}$, clearly shows that a transcritical bifurcation occurs between at $k = \mu + \frac{r}{a}$.

To consider the existence condition for the endemic equilibrium E_2, we define the discriminant of F_2 as

$$\Delta = \Big(ak + 1 - \frac{\mu}{k}\Big)^2 - 4r.$$

Then, it is easy to get that

(1) F_2 does not have real roots if $\Delta < 0$, i.e., $r > \frac{1}{4}(ak + 1 - \frac{\mu}{k})^2$;

(2) F_2 has one positive root if $\Delta = 0$, i.e., $r = \frac{1}{4}(ak + 1 - \frac{\mu}{k})^2$; and

(3) F_2 has two positive roots if $\Delta > 0$, i.e., $r < \frac{1}{4}(ak + 1 - \frac{\mu}{k})^2$.

We treat r as a bifurcation parameter and other parameters as controlling parameters. The quadratic equation (2.8) shows that the graph of $F_2 = 0$ represents a parabolic relation between r and X_2 in the r-X_2 plane, with a vertex at $(X_2, Y_2) = (\frac{1}{2}(ak + 1\frac{\mu}{k}),\ \frac{1}{2k}(1 - ak - \frac{\mu}{k}))$, at which the saddle-node bifurcation happens.

Therefore, when $\mu > k(1 - ak)$, E_{2+} is biologically meaningless, and only E_{2-} exists, which shows a *forward bifurcation*. When $\mu < k(1 - ak)$, both E_{2+} and E_{2+} exist.

Now, suppose E_{2+} exists and consider the stability of E_{2+}. For this case, both E_{2+} and E_{2-} exist, corresponding to the backward bifurcation. The condition $X_{2+} < 1$ yields

$$\sqrt{\Delta} \le 1 - ak - \frac{\mu}{k} \quad \Longrightarrow \quad k < \mu + \frac{r}{a}, \quad (\text{or } r > a(k - \mu)).$$

Combining the condition $\Delta > 0$ we have the existence condition for E_{2+}:

$$\mu < k(1 - ak) \quad \text{and} \quad a(k - \mu) < r < \frac{1}{4}\Big(ak + 1 - \frac{\mu}{k}\Big)^2. \tag{2.13}$$

To find the stability of E_{2+}, computing the determinant of the Jacobian J in (2.12) at E_{2+} we obtain

$$\begin{aligned} \det(J(E_{2+})) = {} & \frac{\sqrt{\Delta}}{2k(ak^2 + k - \mu - \sqrt{(ak^2 + k - \mu)^2 - 4k^2 r})} \\ & \times (ak^2 + k + \mu + k\sqrt{\Delta})[\, -k(1 - ak) + \mu + \sqrt{(ak^2 + k - \mu)^2 - 4k^2 r}\,]. \end{aligned} \tag{2.14}$$

Since we have $ak < 1$ and $\mu < k(1 - ak)$, we have $-k(1 - ak) + \mu < 0$. The sign of $-k(1 - ak) + \mu + \sqrt{(ak^2 + k - \mu)^2 - 4k^2 r}$ is the same as that of

$$\frac{-4k^2[r - a(k - \mu)]}{\sqrt{(ak^2 + k - \mu)^2 - 4k^2 r} + k(1 - ak) - \mu} < 0, \quad \text{due to } \ r > a(k - \mu) \ \text{ in } \ (2.13),$$

which shows that E_{2+} is a saddle when it exists.

Now, we turn to consider E_{2-}. There are two cases:

(A) $\mu > k(1 - ak)$ and $r < a(k - \mu)$,

(B) $\mu < k(1 - ak)$ and $r < \frac{1}{4}(ak + 1 - \frac{\mu}{k})^2$.

As pointed out above, only E_{2-} exists for Case (A), leading to forward bifurcation; while both E_{2+} and E_{2-} exist for the Case (B), leading to the backward bifurcation.

We first consider the Case (A). $X_{2-} < 1$ yields

$$\sqrt{\Delta} > ak - 1 + \frac{\mu}{k} > 0 \quad \Longrightarrow \quad r < a(k - \mu) \ \Big(\text{or } k > \mu + \frac{r}{a}\Big). \tag{2.15}$$

So the existence condition of E_{2-} for the Case (A) is

$$\mu > k(1-ak) \quad \text{and} \quad r < a(k-\mu). \tag{2.16}$$

For the Case (B) with $\mu < k(1-ak)$, $(ak < 1)$, it is easy to use (2.15) to verify that $X_{2-} < 1$ since $ak - 1 + \frac{\mu}{k} < 0$. Hence, the existence condition of E_{2-} for the Case (B) is

$$ak < 1, \quad \mu < k(1-ak) \quad \text{and} \quad r < \frac{1}{4}\Big(ak + 1 - \frac{\mu}{k}\Big)^2. \tag{2.17}$$

To consider the stability of E_{2-}, similarly computing the the determinant and trace of the Jacobian J at E_{2-} we obtain

$$\begin{aligned} \det(J(E_{2-})) = &- \frac{\sqrt{\Delta}}{2k(ak^2 + k - \mu - \sqrt{(ak^2+k-\mu)^2 - 4k^2r})} \\ &\times(ak^2 + k + \mu - k\sqrt{\Delta})[-k(1-ak) + \mu + \sqrt{(ak^2+k-\mu)^2 - 4k^2r}] \end{aligned} \tag{2.18}$$

and

$$\begin{aligned} \mathrm{Tr}(J_{2-}) = &- \frac{2}{k[ak^2 + k - \mu + \sqrt{(ak^2+k-\mu)^2 - 4k^2r}]^2} \\ &\times\{k[(\mu - k(1-ak)) + \mu + k(ak+1)] + \mu[(ak^2+k-\mu)^2 - 4k^2r] \\ &+[\mu(k(1+ak) - \mu) + k^2(1-k)r]\sqrt{(ak^2+k-\mu)^2 - 4k^2r}\}. \end{aligned} \tag{2.19}$$

Similar to prove that $\det(J(E_{2+})) < 0$, we can show that $\det(J(E_{2-})) > 0$. Thus the stability of E_{2-} is determined by $\mathrm{Tr}(J_{2-})$: E_{2-} is asymptotically stable if $\mathrm{Tr}(J_{2-}) < 0$, and unstable if $\mathrm{Tr}(J_{2-}) > 0$. Hopf bifurcation can occur from E_{2-} at the critical point determined by $\mathrm{Tr}(J_{2-})$. Hence, from E_{2-}, besides the transcritical bifurcation at the critical point $R_0 = 1$, Hopf bifurcation may also happen.

This completes the proof of Theorems 2.3.1 and 2.3.2. □

The bifurcation diagrams for the model (2.3) are given in Figure 2.1, which clearly shows forward bifurcation, backward bifurcation, saddle-node bifurcation and Hopf bifurcations. Note that biologically meaningful bifurcations only occur in the first quadrant with $r > 0$ and $0 < X < 1$.

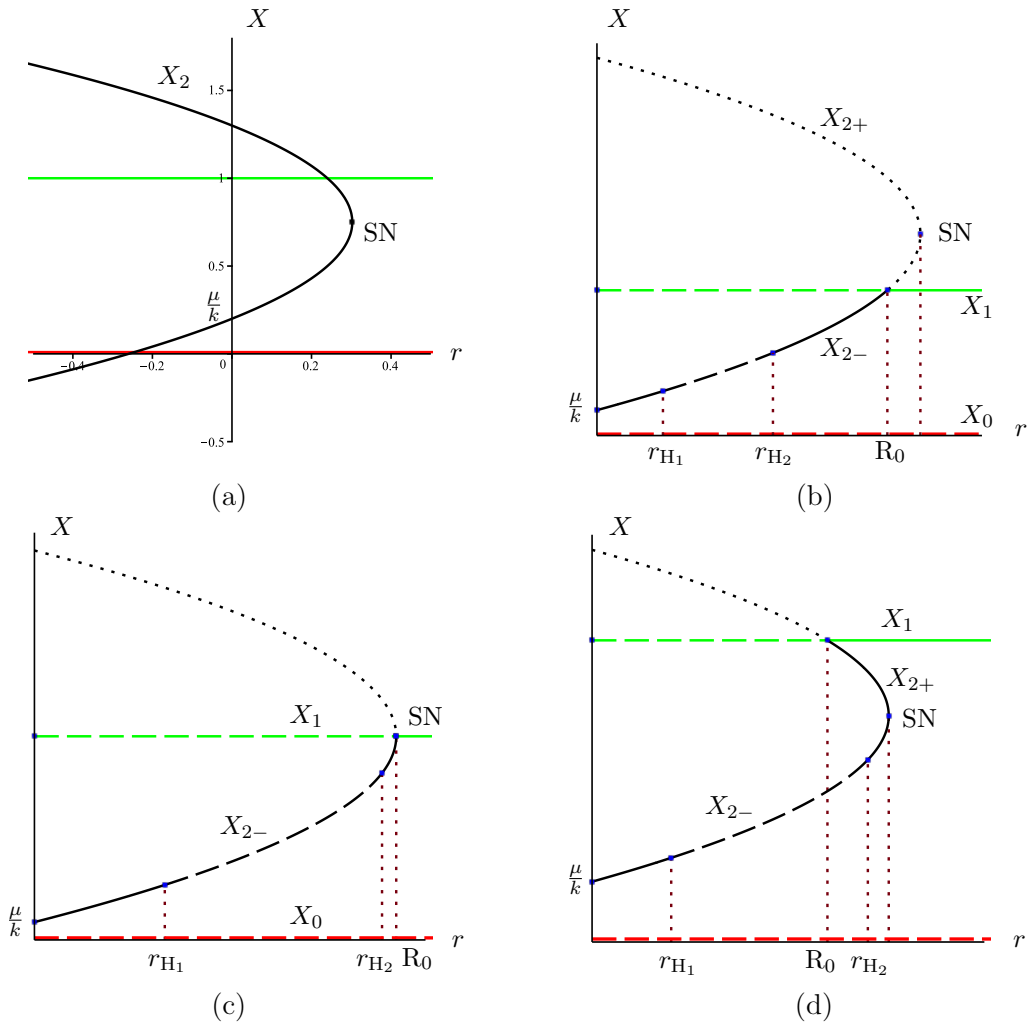

Figure 2.1: Bifurcation diagrams for system (2.3): (a) bifurcation curves in the whole $r - X$ plane; (b) forward bifurcation for $\mu > k(1-ak)$ and $r < a(k-\mu)$; (c) forward bifurcation for $\mu < k(1-ak), ak < 1$ while $r = \frac{1}{4}(ak+1-\frac{\mu}{k})^2$; and (d) backward bifurcation for $\mu < k(1-ak), ak < 1$ and $r < \frac{1}{4}(ak + 1 - \frac{\mu}{k})^2$. The red color, green color and black color curves denote the trivial equilibrium E_0, the disease-free equilibrium E_1, and the endemic equilibrium E_2, respectively. The stable and unstable equilibrium solutions are represented by the solid and dashed curves, respectively.

2.4 Hopf bifurcation

In this section, we consider Hopf bifurcation from the endemic equilibrium E_{2-}. We will derive a complete set of conditions for which system (2.3) undergoes Hopf bifurcation, which is not obtained in [29].

2.4.1 Conditions for Hopf bifurcation

As shown in the previous section, the Hopf bifurcation critical point is determined from $\mathrm{Tr}(J(\mathrm{E}_{2-})) = 0$. However, this condition is not convenient for application. We need to find the explicit expressions in terms of the system parameters. For convenience, define

$$\begin{aligned} \mu_{\max} &= \frac{2k(k^2-k+2) - 4k\sqrt{2k(k-1)}}{2(k+1)^2}, \\ a_{\min} &= \frac{(k-\mu)}{k^2}, \quad a_{\max} = \frac{k-1+\mu-2\sqrt{(k-1)\mu}}{k}. \end{aligned} \tag{2.20}$$

Then, we have the following theorem.

Theorem 2.4.1. *For the model (2.3), Hopf bifurcation can occur from the endemic equilibrium* E_{2-}*, if the following conditions are satisfied.*

For the Case (A) $\mu > k(1-ak)$ *and* $r < a(k-\mu)$ *(forward bifurcation) : Two Hopf bifurcations occur at the criritical points*:

$$r_{\mathrm{H}_\pm} = \frac{-F_{3b} \pm \sqrt{\Delta_1}}{2k(k-1)^2},$$

where F_{3b} *and* Δ_1 *are given in the following proof, if* $a \in (a_{\min}, a_{\max})$ *together with one of the following conditions to be held*:

(A-1) $2 < k \leq 2.8525454869$ *and* $0 < \mu < \mu_{\max}$*;*

(A-2) $2.8525454869 < k \leq 3$ *and* $\frac{k^2(3-k)}{6k-1-k^2} < \mu < \mu_{\max}$*; or*

(A-3) $k > 3$ *and* $0 < \mu < \mu_{\max}$.

The equilibrium E_{2-} *is asymptotically stable for* $r \in (0, r_{\mathrm{H}_-}) \bigcup (r_{\mathrm{H}_+}, a(k-\mu))$ *and unstable for* $r \in (r_{\mathrm{H}_-}, r_{\mathrm{H}_+})$.

For the Case (B) $\mu < k(1-ak)$ *and* $r < \frac{1}{4}(ak+1-\frac{\mu}{k})^2$ *(backward bifurcation) : One Hopf bifurcation occurs at the criritical point* r_{H_+} *if*

$$1 < k \leq 3, \quad a < \frac{k-1}{k(k+1)^2}, \quad \textit{and} \quad ak^3 < \mu < k(a+1) - 1 - 2\sqrt{ak(k-1)}.$$

The equilibrium E_{2-} *is asymptotically stable for* $r \in (0, r_{\mathrm{H}_+})$*, and unstable for* $r_{\mathrm{H}_+} < r < \frac{1}{4}(ak+1-\frac{\mu}{k})^2$.

Proof. First, we consider the Case (A): $\mu > k(1-ak)$ and $r < a(k-\mu)$. It is easy to see from (2.19) that for the Case (A), $\mathrm{Tr}(J(\mathrm{E}_{2-}) < 0$ when $k \leq 1$, implying that E_{2-} is asymptotically stable. Thus, in order to have Hopf bifurcation, it needs $k > 1$. For this case, we treat the

parameter k to be free. We rewrite the condition $\mu > k(1-ak)$ as $a > \frac{k-\mu}{k^2}$, and thus $ak^2+k-\mu > 2(k-\mu) > 0$. Further, it can be shown that $\mathrm{Tr}(J(\mathrm{E}_{2-})) = 0$ is equivalent to

$$F_3 = 4k^5 r F_{3a} = 0,$$

where

$$F_{3a} = k(k-1)^2 r^2 + F_{3b} r + a\mu(ak^2+k-\mu)^2, \tag{2.21}$$

in which

$$F_{3b} = k^4 a^2 - k[k^2(k-1-\mu) + (4k-1)\mu]a - \mu(k-1-\mu). \tag{2.22}$$

Define

$$\Delta_1 = F_{3b}^2 - 4ka\mu r^2 (k-1)^2 (ak^2+k-\mu)^2. \tag{2.23}$$

It is necessary to ensure that $F_{3b} < 0$ and $\Delta_1 > 0$ in order to have positive solutions of r for Hopf bifurcation. To have $F_{3b} < 0$, we need that

$$a_{1-} < a < a_{1+}, \tag{2.24}$$

where

$$a_{1\pm} = \frac{k^2(k-1-\mu) + (4k-1)\mu \pm \sqrt{[k^2(k-1-\mu)+(4k-1)\mu]^2 + 4k^2\mu(k-1-\mu)}}{2k^3}. \tag{2.25}$$

On the other hand, $\Delta_1 > 0$ yields

$$a < a_{2-} \quad \text{or} \quad a > a_{2+}, \tag{2.26}$$

where

$$a_{2\pm} = \frac{k-1+\mu \pm 2\sqrt{(k-1)\mu}}{k}. \tag{2.27}$$

A direct computation shows that

$$a_{2+} > a_{1+} > a_{2-} > a_{1-},$$

yielding the condition on a:

$$a_{1-} < a < a_{2-}. \tag{2.28}$$

Since $a > \mu > k(1-ak)$, define $a_{\min} = \frac{(k-\mu)}{k^2}$, $(k > \mu)$. Then,

$$\max\{a_{\min},\, a_{1-}\} < a < a_{2-},$$

which requires that $a_{2-} > a_{\min}$, leading to

$$\begin{aligned} & a_{2-} - a_{\min} = \frac{k(k-2)+(k+1)\mu - 2k\sqrt{(k-1)\mu}}{k^2} > 0 \\ \Longrightarrow \quad & k(k-2) + (k+1)\mu > 0 \\ \Longrightarrow \quad & \frac{k(2-k)}{k+1} < \mu < \frac{k(k-1)}{k+1}. \end{aligned}$$

To ensure the above inequality, $k > \frac{3}{2}$ must be satisfied. Further, $a_{2-} - a_{\min} > 0$ needs

$$(k+1)^2\mu^2 - 2k(k^2-k+2)\mu + k^2(k-2)^2 > 0,$$

which yields

$$\mu < \mu_- \quad \text{or} \quad \mu > \mu_+, \tag{2.29}$$

where

$$\mu_\pm = \frac{2k(k^2-k+2) \pm 4k\sqrt{2k(k-1)}}{2(k+1)^2}. \tag{2.30}$$

Simple direct computation shows that $\mu_+ > \frac{k(k-1)}{k+1}$ for $k > \frac{3}{2}$, and $m_- > \frac{k(2-k)}{k+1}$ for $k > 2$. Moreover, it is easy to show that $\frac{k(k-1)}{k+1} > \mu_-$ for $k > 2$. Therefore, we obtain the following conditions for the Case (A):

$$k > 2, \quad 0 < \mu < \mu_-, \quad \text{and} \quad \max\{a_{1-}, a_{\min}\} < a < a_{2-}.$$

Finally, we compare a_- and $\mu_{\min}$ depending upon the values of k:

$$a_{1-} - a_{\min} = -\frac{k^2(3-k) + \mu(k^2-6k+1) + \sqrt{(k^2(k-1-\mu)+(4k-1)\mu)^2 + 4k^2\mu(k-1-\mu)}}{2k^3}.$$

There are three cases: (i) $2 < k \le 3$, (ii) $3 < k \le 3+2\sqrt{2}$, and (iii) $k > 3+2\sqrt{2}$.

(i) When $2 < k \le 3$, we can show that $a_{1-} < a_{\min}$ regardless whether $\mu \ge \frac{k^2(3-k)}{6k-1-k^2}$ or $\mu < \frac{k^2(3-k)}{6k-1-k^2}$. On the other hand,

$$\frac{k^2(3-k)}{6k-1-k^2} - \mu_{1-} = \frac{2k(k-1)(7k^3-23k^2+9k-1)}{(k^2-6k+1)[(3k-1)(k-1)^2 + (6k-1-k^2)\sqrt{2k(k-1)}]}.$$

A unique positive root of the polynomial $7k^3 - 23k^2 + 9k - 1$ is $k = 2.852545487$. Then, it is easy to obtain that

$$\frac{k^2(3-k)}{6k-1-k^2} - \mu_{1-} \begin{cases} \ge 0 & \text{for } 2 < k \le 2.852545487 \implies 0 < \mu < \mu_{1-}, \\ \le 0 & \text{for } 2.852545487 < k \le 3 \implies \frac{k^2(3-k)}{6k-1-k^2} < \mu < \mu_{1-}. \end{cases}$$

(ii) When $3 < k \le 3+2\sqrt{2}$, we have $k^2(3-k) < 0$ and $k^2 - 6k + 1 \le 0$, and similarly we can show that $a_{1-} < a_{\min}$ for $\mu < \mu_{1-}$. Hence, for this case we have $0 < \mu < \mu_{1-}$ and $a_{1-} < a_{\min}$.

(iii) When $k > 3+2\sqrt{2}$, we have $k^2(3-k) < 0$, $k^2 - 6k + 1 \le 0$, and $7k^3 - 23k^2 + 9k - 1 > 0$. Similar to the case (ii), we can use a direct calculation to show that $0 < \mu < \mu_{1-}$ and $a_{1-} < a_{\min}$. Letting $a_{\max} = a_{2-}$ and $\mu_{\max} = \mu_{1-}$ proves for the Case (A).

Now we turn to consider the Case (B). With $ak < 1$ and $\mu < k(1-ak)$, which is equivalent to $a < \frac{k-\mu}{k^2}$, we rewrite the trace of J_{2-} given in (2.19) as

$$\mathrm{Tr}(J_{2-}) = -\frac{[I_2 + I_1\sqrt{(ak^2+k-\mu)^2 - 4k^2r}]}{k[ak^2+k-\mu+\sqrt{(ak^2+k-\mu)^2-4k^2r}]^2}, \tag{2.31}$$

where

$$\begin{aligned} I_1 &= \mu(ak^2 + k - \mu) - rk^2(k-1) \\ I_2 &= \mu(ak^2 + k - \mu)^2 + rk^2(k(ak(k+1) - (k-1)) + (k-3)\mu) \end{aligned} \tag{2.32}$$

To have solution from $\mathrm{Tr}(J_{2-}) = 0$, it needs $I_1 I_2 < 0$. A careful examination on the conditions for $I_1 > 0$, $I_2 < 0$ and $I_1 < 0$, $I_2 > 0$ gives the following categories:

(B-a) $k > 1$, $\frac{k-1}{k(k+1)} \le a < \frac{1}{k}$, $\mu < \min\{k(1-ak), \frac{k(k-1)(ak+1)}{k+3}\}$

and $\frac{\mu(ak^2-\mu+k)}{k^2(k-1)} < r < \frac{(ak+1-\frac{\mu}{k})^2}{4}$.

(B-b) $k > 1$, $\frac{k-1}{k(k+1)^2} < a < \frac{k-1}{k(k+1)}$, $\frac{k(k-1-ak(k+1))}{k+1} < \mu < \min\{k(1-ak), \frac{k(k-1)(ak+1)}{k+3}\}$

and $\frac{\mu(ak^2-\mu+k)}{k^2(k-1)} < r < \frac{(ak+1-\frac{\mu}{k})^2}{4}$.

(B-c) $1 < k < 3$, $a < \frac{k-1}{k(k+1)}$, $\mu < \frac{k(k-1)(ak+1)}{k+3}$

and $\frac{\mu(ak^2-\mu+k)}{k^2(k-1)} < r < \min\{\frac{\mu(ak^2-\mu+k)^2}{k^2(k(k-1-ak(k+1))+(3-k)\mu)}, \frac{(ak+1-\frac{\mu}{k})^2}{4}\}$.

(B-d) $1 < k \le 3$, $a < \min\{\frac{k-1}{k(k+1)}, \frac{1}{k(k+1)}\}$, $ak^3 < \mu < \frac{k(k-1-ak(k+1))}{k+1}$,

and $\frac{\mu(ak^2-\mu+k)^2}{k^2(k(k-1-ak(k+1))+(3-k)\mu)} < r < \min\{\frac{\mu(ak^2-\mu+k)}{k^2(k-1)}, \frac{(ak+1-\frac{\mu}{k})^2}{4}\}$.

(B-e) $k > 3$, $a < \frac{k-1}{k(k+1)^2}$, $ak^3 < \mu < \frac{k(k-1-ak(k+1))}{k+1}$,

and $\frac{\mu(ak^2-\mu+k)^2}{k^2(k(k-1-ak(k+1))-(k-3)\mu)} < r < \min\{\frac{\mu(ak^2-\mu+k)}{k^2(k-1)}, \frac{(ak+1-\frac{\mu}{k})^2}{4}\}$.

Define

$$r_{\min} = \frac{\mu(ak^2 + k - \mu)}{k^2(k-1)}, \quad r_{\max} = a(k-\mu), \tag{2.33}$$

which are substitutes into F_{3a} in (2.21) to obtain

$$\begin{aligned} F_{3a}|_{r=r_{\min}} &= \frac{\mu(ak^2 - \mu + k)(ak^3 - \mu)^2}{k^3(k-1)}, \\ F_{3a}|_{r=r_{\max}} &= a[k^5a^2 - k^2(k-1)(k-\mu)a + \mu(k-\mu)], \\ F_{3a}|_{\min} &= -\frac{\Delta_1(ak^3 - mu)^2}{4k(k-1)^2}. \end{aligned} \tag{2.34}$$

Then, two Hopf bifurcations only happens if

$$F_{3a}|_{r=r_{\min}} > 0, \quad F_{3a}|_{r=r_{\max}} > 0, \quad F_{3a}|_{\min} < 0, \quad \text{and} \quad r_{\min} < r_{\mathrm{H}_-} < r_{\mathrm{H}_+} < r_{\max},$$

otherwise there exists one or none Hopf bifurcation. Now, we solve $\Delta_1 = 0$ for μ and thus

$$\Delta_1 > 0 \quad \text{if} \quad \mu < \tilde{\mu}_- \quad \text{or} \quad \mu > \tilde{\mu}_+,$$

where

$$\tilde{\mu}_{\pm} = ak + k - 1 \pm 2\sqrt{ak(k-1)}. \tag{2.35}$$

Then, combining the above conditions with those in the categories (B-a)-(B-e), as well as the solutions for the Hopf critical points: r_{H_-} and r_{H_+}, we obtain that one Hopf bifurcation occurs at r_{H_+} if one of the following conditions holds.

(B-a) $k > 1$, $\frac{k-1}{k(k+1)} \le a < \frac{1}{k}$, $0 < \mu < \tilde{\mu}_-$.

(B-b) $k > 1$, $\frac{k-1}{k(k+1)^2} < a < \frac{k-1}{k(k+1)}$, $\frac{k(k-1-ak(k+1))}{k+1} < \mu < \tilde{\mu}_-$.

(B-c) (i) $1 < k < 3$, $\frac{k-1}{k(k+1)^2} < a < \frac{k-1}{k(k+1)}$, and $\frac{k(k-1-ak(k+1))}{k+1} < \mu < \tilde{\mu}_-$;

(ii) $1 < k < 3$, $a < \frac{k-1}{k(k+1)}$, $\mu < \min\{\frac{k(k-1-ak(k+1))}{k+1}, \frac{k(k-1)(ak+1)}{k+1}\}$.

(B-d) (i) $1 < k \le 2$, $a < \frac{k-1}{k(k+1)^2}$, $ak^3 < \mu < \tilde{\mu}_-$ and $\frac{\mu(ak^2-\mu+k)^2}{k^2(k(k-1-ak(k+1))+(3-k)\mu)}$;

(ii) $1 < k \le 2$, $a < \frac{k-1}{k(k+1)^2}$, $ak^3 < \mu < \tilde{\mu}_-$ and $\frac{\mu(ak^2-\mu+k)^2}{k^2(k(k-1-ak(k+1))+(3-k)\mu)}$;

(iii) $2 < k \le 3$, $a < \frac{k-1}{k(k+1)^2}$, $\frac{k(k-1)(ak+1)}{k+3} < \mu < \tilde{\mu}_-$;

(iv) $2 < k \le 3$, $a < \frac{k-1}{k(k+1)^2}$, $ak^3 < \mu < \frac{k(k-1)(ak+1)}{k+3}$.

Combining the above conditions we reach the conclusion for the Case (B).

This completes the proof of Theorem 3.2.3. □

2.4.2 Codimension of Hopf bifurcation

Having established the conditions in the previous section for Hopf bifurcation to occur from the endemic equilibrium E_{2-}, we now consider the codimension of the Hopf bifurcation. That is, we want to find the maximal number of limit cycles which can bifurcate from the Hopf critical point. We first consider the marginal case $R_0 = 1$ and then $R_0 \neq 1$.

For the Case $R_0 = 1$

When $R_0 = 1$, i.e., $k = \mu + \frac{r}{a}$, we obtain the equilibrium solutions:

$$E_1 = (1, 0) \quad \text{and} \quad \tilde{E}_2 = (X_2, Y_2) = \Big(a\mu + r + \frac{a\mu}{a\mu + r}, \frac{1 - X_2}{k}\Big). \tag{2.36}$$

Now E_1 is a degenerate node. In order to have positive solution E_2, it needs

$$X_2 < 1 \quad \Longrightarrow \quad a\mu + r + \frac{a\mu}{a\mu + r} < 1 \quad \Longrightarrow \quad a\mu < \sqrt{r} - r \ \ (r < 1).$$

We apply center manifold theorem to determine the stability of E_1 and study Hopf bifurcation from $\tilde{E}_2$.

Theorem 2.4.2. *For the model (2.3) with the basic reproduction number* $R_0 = 1$*, the equilibrium point* E_1 *is either a degenerate stable node if* $a\mu > max\{0, \sqrt{r} - r\}$*; or a degenerate unstable node if* $a\mu < \sqrt{r} - r$ $(r < 1)$*. Bifurcation occurs at the critical point* $a\mu < \sqrt{r} - r$ $(r < 1)$*.*

Proof. Introducing the following affine transformation,

$$\begin{pmatrix} X \\ Y \end{pmatrix} = \begin{pmatrix} 1 \\ 0 \end{pmatrix} + \begin{pmatrix} -\mu - \frac{r}{a} & 1 \\ 1 & 0 \end{pmatrix} \begin{pmatrix} x_1 \\ x_2 \end{pmatrix}, \tag{2.37}$$

with $k = \mu + \frac{r}{a}$, into (2.3) yields

$$\begin{aligned} \dot{x}_1 &= -\Big[\Big(\mu + \frac{r}{a}\Big)^2 - \frac{r}{a^2}\Big](x_1^2 + x_2^2) + \Big(\mu + \frac{r}{a}\Big)x_1x_2 + O(|(x_1, x_3)|^3), \\ \dot{x}_2 &= -x_2 - \Big(\mu + \frac{r}{a}\Big)\Big[\Big(\mu + \frac{r}{a}\Big)^2 - \frac{r}{a^2}\Big](x_1^2 + x_2^2) + \Big(\mu + \frac{r}{a}\Big)\Big(\mu + 1 + \frac{r}{a}\Big)x_1x_2 \\ &\quad + O(|(x_1, x_3)|^3). \end{aligned} \tag{2.38}$$

Then applying center manifold theory and letting $x_2 = c_1x_1^2$, and using $\dot{x}_2 = 2c_2x_1\dot{x}_1$ yields

$$c_1 = -\Big(\mu + \frac{r}{a}\Big)\Big[\Big(\mu + \frac{r}{a}\Big)^2 - \frac{r}{a^2}\Big].$$

Hence, the center manifold up to the second order is given by

$$W^c = \{(x_1, x_2) | x_2 = c_1x_1^2 + O(x_1^3)\}, \tag{2.39}$$

and the differential equation describing the dynamics on the center manifold is

$$\dot{x}_1 = -\frac{1}{a^2}[(a\mu + r)^2 - r]\, x_1^2 + O(x_1^3), \tag{2.40}$$

which indicates that the equilibrium E_1 is a degenerate stable node if $(a\mu + r)^2 - r > 0$, which is equivalent to $a\mu > \max\{0, \sqrt{r} - r\}$, and is a degenerate unstable node when $(a\mu + r)^2 - r < 0$, which is equivalent to $0 < a\mu < \sqrt{r} - r$, $(r < 1)$. □

Next, we consider the endemic equilibrium $\tilde{E}_2$. We have the following result.

Theorem 2.4.3. *For the model (2.3) with basic reproduction number* $R_0 = 1$*, the endemic equilibrium point* $\tilde{E}_2$ *exists for* $0 < a\mu < \sqrt{r} - r$ $(0 < r < 1)$*, and its stability and bifurcation are described as follows.*

(i) $\tilde{E}_2$ *is asymptotically stable for* $(a\mu + r)^3[r - (a\mu + r)^2] < ar[(a\mu + r)^2 + a\mu]$.

(ii) $\tilde{E}_2$ *is unstable for* $(a\mu + r)^3[r - (a\mu + r)^2] > ar[(a\mu + r)^2 + a\mu]$.

(iii) *Transcritical bifurcation occurs between* E_1 *and* $\tilde{\mathrm{E}}_2$ *at the critical point* $a\mu = \sqrt{r} - r$ $(0 < r < 1)$.

(iv) *Hopf bifurcation occurs from* $\tilde{\mathrm{E}}_2$ *at the critical point defined by* $(a\mu + r)^3[r - (a\mu + r)^2] - ar[(a\mu + r)^2 + a\mu] = 0$.

Proof. Evaluating the Jacobian (2.12) at $\tilde{\mathrm{E}}_2$ with $k = \mu + \frac{r}{a}$ yields the trace and determinant as follows:

$$\mathrm{Tr}(J(\tilde{\mathrm{E}}_2)) = \frac{1}{(a\mu + r)^3}\{(a\mu + r)^3[r - (a\mu + r)^2] - ar[(a\mu + r)^2 + a\mu]\},$$
$$\det(J(\tilde{\mathrm{E}}_2)) = \frac{ar}{(a\mu + r)^5}[(a\mu + r)^2 + a\mu][r - (a\mu + r)^2]^2.$$

$\det(J(\tilde{\mathrm{E}}_2)) > 0$ for $(a\mu + r)^2 - r \neq 0$. Thus, the stability is determined by the sign of $\mathrm{Tr}(J(\tilde{\mathrm{E}}_2))$: $\tilde{\mathrm{E}}_2$ is asymptotically stable (respectively unstable) if $\mathrm{Tr}(J(\tilde{\mathrm{E}}_2)) < 0$ (respectively $\mathrm{Tr}(J(\tilde{\mathrm{E}}_2)) > 0$). $\det(J(\tilde{\mathrm{E}}_2)) = 0$ yields the transcritical bifurcation point $a\mu = \sqrt{r} - r$ $(0 < r < 1)$, and $\mathrm{Tr}(J(\tilde{\mathrm{E}}_2)) = 0$ determines the Hopf critical point. □

The remaining question of this section is the codimension of the Hopf bifurcation. We have the following result.

Theorem 2.4.4. *For the model* (2.3) *with* $\mathrm{R}_0 = 1$*, the codimension of the Hopf bifurcation arising from the equilibrium* $\tilde{\mathrm{E}}_2$ *is two.*

Proof. To simplify the analysis, let

$$r = C_1^2 + C_2, \quad a\mu = C_1 - C_2 - C_1^2, \tag{2.41}$$

which shows that $C_1 = r + a\mu > 0$, $C_2 = r - (a\mu + r)^2 > 0$, $C_1 > C_2$, and $C_2 < C_1(1 - C_1)$, implying that $0 < C_1 < 1$. Then, we have

$$\mathrm{Tr}(J(\tilde{\mathrm{E}}_2)) = \frac{1}{C_1^3}[C_1^3C_2 - a(C_1^2 + C_2)(C_1 - C_2)],$$

from which we can solve a to determine the Hopf critical point:

$$a_{\mathrm{H}} = \frac{C_1^3C_2}{(C_1^2 + C_2)(C_1 - C_2)}. \tag{2.42}$$

Therefore, at $a = a_{\mathrm{H}}$, introducing the affine transformation,

$$\begin{pmatrix} X \\ Y \end{pmatrix} = \begin{pmatrix} C_1 + \frac{C_1 - C_1^2 - C_2}{C_1} \\ -1 + \frac{1}{C_1} - \frac{C_1 - C_1^2 - C_2}{C_1^2} \end{pmatrix} + \begin{bmatrix} 1 & 0 \\ -\frac{C_1^2C_2}{(C_1^2+C_2)(C_1-C_2)} & \frac{C_1C_2\sqrt{C_2}}{(C_1^2+C_2)(C_1-C_2)} \end{bmatrix} \begin{pmatrix} u \\ v \end{pmatrix}, \tag{2.43}$$

with a time rescaling $\tau = \omega_c\, t$, where $\omega_c = \frac{C_2}{C_1}\sqrt{C_2}$, into (2.3) we obtain

$$\begin{aligned}
\frac{du}{d\tau} &= v - \tfrac{C_1(C_1-C_1^2-2C_2)}{(C_2+C_1^2)(C_1-C_2)}\,uv - \tfrac{\sqrt{C_2}}{C_2+C_1^2}\,v^2 - \tfrac{C_1^2}{(C_2+C_1^2)(C_1-C_2)}\,u^2v - \tfrac{C_1\sqrt{C_2}}{(C_2+C_1^2)(C_1-C_2)}\,uv^2\\
\frac{dv}{d\tau} &= -u + \tfrac{2C_1}{C_2}\,u^2 - \tfrac{C_1^2(C_1^3+C_2^2)+2C_2(C_2-C_1)(C_1^2+C_2)}{C_2\sqrt{C_2}(C_1^2+C_2)(C_1-C_2)}\,uv - \tfrac{C_1^3}{C_2(C_1^2+C_2)}\,v^2 - \tfrac{C_1^2}{C_2^2}\,u^3\\
&\quad - \tfrac{C_1[C_1^2(2C_1-3C_2)+2C_2(C_1-C_2)]}{C_2\sqrt{C_2}(C_1^2+C_2)(C_1-C_2)}\,u^2v - \tfrac{C_1^2(C_1-2C_2)+C_2(C_1-C_2)}{C_2(C_1^2+C_2)(C_1-C_2)}\,uv^2
\end{aligned} \tag{2.44}$$

Then we apply the Maple program [32] to the above system to obtain the following focus values:

$$\begin{aligned}
v_1 &= -\frac{1}{8C_2(C_1^2+C_2)(C_1-C_2)}\,v_{1a},\\
v_2 &= -\frac{1}{192C_2^4(C_1^2+C_2)^3(C_1-C_2)^3}\,v_{2a},
\end{aligned} \tag{2.45}$$

where

$$\begin{aligned}
v_{1a} &= C_1^3(C_1^2+C_2) - C_2^2(C_1-C_2),\\
v_{2a} &= C_2^9 - C_1(14C_1+3)C_2^8 - C_1^2(34C_1^2-52C_1-3)C_2^7\\
&\quad - C_1^3(31C_1^3-55C_1^2+89C_1+1)C_2^6 + C_1^5(22C_1^2-52C_1+51)C_2^5\\
&\quad - C_1^7(41lC_1^2+25C_1-4)C_2^4 - C_1^9(27C_1^2+42C_1+46)C_2^3\\
&\quad - C_1^{11}(13C_1-5)C_2^2 + 16C_1^{13}C_2 + C_1^{15}.
\end{aligned} \tag{2.46}$$

Since there are two free parameters C_1 and C_2, there may exist solutions such that $v_1 = v_2 = 0$, and $v_2 \neq 0$, yields three limit cycles. However, eliminating C_2 from the equations $v_{1a} = v_{2a} = 0$ we obtain a solution,

$$C_2 := -\frac{C_1^2(7C_1^2+133C_1+174)}{(31C_1^2+265C_1+282)},$$

and a resultant $\mathrm{R}_{12} = C_1(C_1+1)(C_1-2)(C_1-15)$. Since $C_1 > C_2 > 0$, it is obvious that no feasible parameter values satisfying $C_2 > 0$. Thus, three limit cycles are not possible. The existence of two limit cycles only needs $v_1 = 0$ or $v_{1a} = 0$ which certainly has solutions since $C_1^3(C_1^2+C_2) > 0$ and $C_2^2(C_1-C_2) > 0$, and there exist an infinite number of solutions for bifurcating two limit cycles. This indicates that the codimension of the Hopf bifurcation is two when the reproduction number $\mathrm{R}_0 = 1$.

This completes the proof of Theorem 3.4.2. □

An example of the two limit cycle simulation for the model (2.3) is shown in Figure 2.2, by choosing the following parameter values:

$$a = 0.061758641, \quad k = 2.430000932, \quad \mu = 0.367779398, \quad r = 0.12736.$$

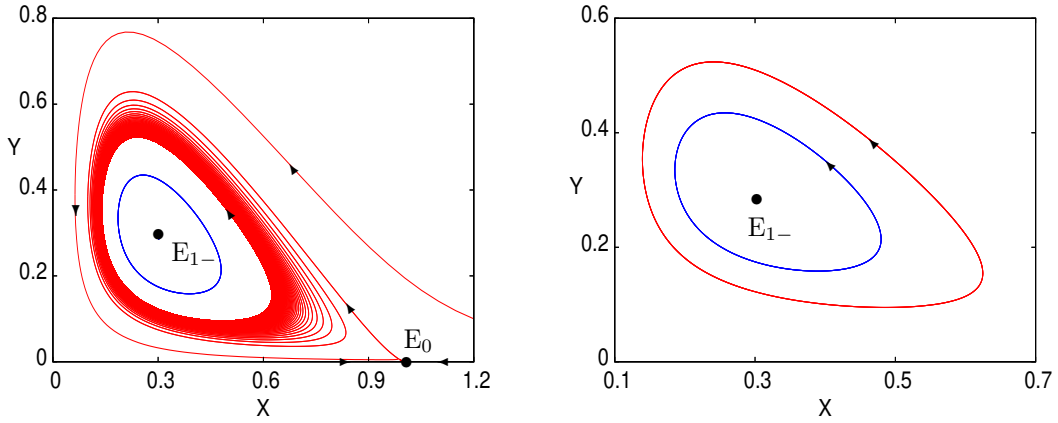

(a) (b)

Figure 2.2: Simulation of the model (2.3) with $a = 0.061758641$, $k = 2.430000932$, $\mu = 0.367779398$, $r = 0.12736$, showing bifurcation of two limit cycles: (a) a global picture of the phase portrait; and (b) the zoomed region near the stable equilibrium E_{2-}, with the outer limit cycle stable (in red color) and the inner one unstable (in blue color), both of them enclosing the stable equilibrium E_{1-}.

For the Case $\mathrm{R}_0 \neq 1$

Now, we consider the codimension of the Hopf bifurcation arising from E_{2-} for the case $\mathrm{R}_0 \neq 1$, and have the following theorem.

Theorem 2.4.5. *For the model* (2.3) *with* $\mathrm{R}_0 \neq 1$*, the codimension of the Hopf bifurcation arising from the equilibrium* $\tilde{\mathrm{E}}_2$ *is two.*

Proof. The existence conditions for the existence of E_{2-} are

$$k > 1, \quad 0 < X_2 < \frac{k}{k+1}, \quad \text{and} \quad 0 < r < \frac{(k-1)X_2(ak - X_2 + 1)^2}{ak^2}.$$

For this case, it is impossible or extremely difficulty to compute the focus values if we solve X_2 explicitly from the equation $F_2 = 0$. Instead, we use μ to solve the determinant of the Jacobian evaluated at E_{2-} and treated X_{2-} as a parameter in the stability and bifurcation analysis. To find the focus values, we first apply the affine transform,

$$\begin{pmatrix} X \\ Y \end{pmatrix} = \begin{pmatrix} X_2 \\ \dfrac{1 - X_2}{k} \end{pmatrix} + \begin{bmatrix} 1 & 0 \\ -\dfrac{1}{k} & \dfrac{\sqrt{-X_2(X_2k + X_2 - k)}}{k X_2} \end{bmatrix} \begin{pmatrix} u \\ v \end{pmatrix}, \tag{2.47}$$

where X_2 denotes the endemic equilibrium solution. Then, similar to the case $R_0 = 1$, we apply the the Maple program [32] into the resulting system to obtain the first-order value:

$$v_1 = \frac{(k-1)(1-X_2)^2 - ak(1+2k-2(1+k)X_2)}{8((ak+1-X_2)(k(1-X_2)-X_2))}.$$

The conditions $k > 1$ and $X_2 < \frac{k}{k+1}$ ensures that $v_1 = 0$ has a positive solution for a:

$$a = \frac{(k-1)(1-X_2)^2}{k[1+2k-2(1+k)X_2]}, \tag{2.48}$$

under which v_2 and v_3 become

$$v_2 = \frac{4X_2(k-1)(1-X_2)^5(k-kX_2-X_2)^2}{(2k-2kX_2+1-2X_2)^2}[2(k+1)(3k^2+3k+1)X_2^2 - 3k(2k+3)(2k+1)X_2 + 6k^2(k+2)],$$
$$v_3 = \frac{4X_2(k-1)(1-X_2)^5(k-kX_2-X_2)^2}{(2k-2kX_2+1-2X_2)^2}[\cdots].$$

Eliminating X_2 from the equations $v_2 = v_3 = 0$ yields a solution $X_2 = X_2(k)$, and a resultant equation:

$$R_{23} = k(k^2-1)(8k^2-5)(k^2-4) = 0,$$

which has a positive solution $k = 2 > 1$, which in turn yields $X_2 = 1$. Thus, there are no feasible parameter values satisfying $v_2 = v_3 = 0$, implying that there are no four limit cycles due to the Hopf bifurcation. Next, examine if three limit cycles can exist, which only needs $v_2 = 0$. Solving $v_2 = 0$ for X_2 gives

$$X_2^{\pm} = \frac{k[3(2k+3)(2k+1) \pm \sqrt{3(8k^2-5)}]}{4(k+1)(3k^2+3k+1)}, \quad (k > 1).$$

However, it is easy to show that

$$X_2^+ > X_2^- > \frac{k}{k+1},$$

implying that no feasible parameter values can be chosen to have three limit cycles. Therefore, the best result is two limit cycles, and so the codimension of the Hopf bifurcation is two.

The sign of the v_2 is easy to be verified as positive since it has been shown that $X_2 < \frac{k}{k+1} < X_2^-$, indicating $v_2 < 0$. Thus, the outer bifurcating limit cycle is stable and the inner one is unstable, both of them enclose a stable focus E_{2-}. □

2.4.3 B-T bifurcation of system (2.3)

In this section, we present an analysis on the B-T bifurcation of the model (2.3). We first determine the codimension of the B-T bifurcation, and then present the bifurcation results for codimension-2 and codimension-3 B-T bifurcations.

In order to find the B-T bifurcation critical point from E_2, we solve the polynomial F_2 for r to obtain

$$r = \frac{1}{k}(ak + 1 - X_2)(kX_2 - \mu).$$

Then, evaluating J at E_2 results in the trace and determinant as

$$\begin{aligned} \mathrm{Tr}_{E_2} &= \frac{X_2[(k-1)(1-X_2) - ak] - (1-X_2)\mu}{ak + 1 - X_2}, \\ \det_{E_2} &= \frac{X_2(1-X_2)(ak^2 + k - 2kX_2 + \mu)}{ak + 1 - X_2}. \end{aligned} \tag{2.49}$$

Solving μ from $\det_{E_2} = 0$ we obtain

$$\mu = k(2X_2 - 1 - ak),$$

which is substituted into $\mathrm{Tr}_{E_2} = 0$ gives

$$k - (1 + k)X_2 = 0,$$

which yields

$$X_2 = \frac{k}{k+1}, \quad \text{and then } Y_2 = \frac{1}{k(k+1)}, \quad r = \frac{(1+ak)^2}{(k+1)^2}, \quad \mu = \frac{k[k - 1 - ak(k+1)]}{k+1}. \tag{2.50}$$

$\mu > 0$ requires that

$$a < \frac{k-1}{k(k+1)}, \quad k > 1. \tag{2.51}$$

2.4.4 Determining the codimension of B-T bifurcation

We apply the SNF theory [33, 34, 36] to determine the codimension of B-T bifurcation. To achieve this, introduce the following affine transformation:

$$\begin{pmatrix} X \\ Y \end{pmatrix} = \begin{pmatrix} \frac{k}{k+1} \\ \frac{1}{k(k+1)} \end{pmatrix} + \begin{bmatrix} \frac{-k}{k+1} & 1 \\ \frac{1}{k+1} & 0 \end{bmatrix} \begin{pmatrix} u \\ v \end{pmatrix} \tag{2.52}$$

into (2.3) yields

$$\begin{aligned} \frac{du}{dt} &= \frac{(ku+1)\{ak^3v + k^2[(2a+u)v - u^2] + k(a+u+1)v + v\}}{(k+1)[ak^2 + k(a+u) + 1](k+1)}, \\ \frac{dv}{dt} &= \frac{1}{(k+1)^2[ak^2 + k(a+u) + 1]}\{ak^5uv - k^4[u^3 - (3a+u)uv + av^2] \\ &\quad -k^3[u^2 + (3a+u)v^2 - (2u^2 + (3a+1)u)v] - k^2[(3a+2u+1)v - (a+u+2)u]v \\ &\quad -k[(a+u+2)v - u]v - v^2\} \end{aligned} \tag{2.53}$$

Next, applying the 5th-order change of variables:

$$\begin{aligned} u =& y_1 + \tfrac{[ak(k^2-1)+2k-1]}{4[ak(k+1)+1]}\, y_1^2 + \tfrac{(k+1)[k^2(k-1)(k+1)^3a^2+k(k+1)(5k^2+7k-2)a-2k^2+7k-1]}{12k^2[ak(k+1)+1]}\, y_1y_2 \\ & -\tfrac{1}{240k^4[ak(k+1)+1]}\{(k+1)^2[4k^3(k-1)(k+1)^5a^3+k^2(k+1)^2(25k^3-86k^2+9k-12)a^2 \\ & \qquad -2k(k+1)(38k^3+27k^2-15k+6)a+20k^3+36k^2+17k-4]\}\, y_2^2+\cdots \\ v =& y_2 + \tfrac{k^2}{((k+1)[ak(k+1)+1]}\, y_1^2 - y_1y_2 \\ & + \tfrac{(k+1)[k^2(k-1)(k+1)^3a^2+k(k+1)(5k^2+7k-2)a-2k^2+7k-1]}{12k^2[ak(k+1)+1]}\, y_2^2+\cdots \end{aligned} \tag{2.54}$$

and the time scaling:

$$t = \left(1 + \frac{[ak(k^2-1)-1]}{2[ak(k+1)+1]} y_1 + t_{30}\, y_1^3\right)\tau_1,$$

where t_{30} is a function in a and k, into (2.53) yields the SNF up to 5-th order:

$$\begin{aligned} \frac{dy_1}{d\tau_1} &= y_2, \\ \frac{dy_2}{d\tau_1} &= c_{20}\, y_1^2 + c_{11}\, y_1y_2 + c_{31}\, y_1^3y_2 + c_{41}\, y_1^4y_2, \end{aligned} \tag{2.55}$$

in which

$$c_{20} = -\frac{k^3}{(k+1)^2[ak(k+1)+1]}, \quad c_{11} = -\frac{k[k-1-ak(k+1)^2]}{(k+1)[ak(k+1)+1]}, \quad c_{31} = \cdots, \quad c_{41} = \cdots, \tag{2.56}$$

which shows that $c_{20} < 0$, and $c_{11} \neq 0$ if $a \neq \frac{k-1}{k(k+1)^2}$. Since $a = \frac{k-1}{k(k+1)^2} < \frac{k-1}{k(k+1)}$ $(k > 1)$, we see that c_{11} can reach zero under the condition (2.51) if $a = \frac{k-1}{k(k+1)^2}$ at which

$$c_{31} = \frac{k(k^2-1)}{8} > 0, \quad c_{41} = -\frac{k(k+5)(k^2-1)}{64} < 0.$$

Thus, we have the following theorem.

Theorem 2.4.6. *For system* (2.3)*,* B-T *bifurcation occurs from the equilibrium* E_2*:* $(\frac{k}{k+1}, \frac{1}{k(k+1)})$ *at the critical point* $(\mu, k) = (\frac{k[k-1-ak(k+1)]}{k+1}, \frac{(1+ak)^2}{(k+1)^2})$*, with* $k > 1$*. Moreover, the* B-T *bifurcation is*

(i) *codimension* 2 *if* $a \in (0, \frac{k-1}{k(k+1)^2}) \bigcup (\frac{k-1}{k(k+1)^2}, \frac{k-1}{k(k+1)})$*; or*

(ii) *codimension* 3 *if* $a = \frac{k-1}{k(k+1)^2}$.

2.4.5 Codimension-2 B-T bifurcation

In this subsection, we apply the one-step transformation approach to derive the parametric simplest normal form (PSNF) [8, 9, 7, 36]. Let

$$\mu = \frac{k[k-1-ak(k+1)]}{k+1} + \mu_1, \quad r = \frac{(ak+1)^2}{(k+1)^2} + \mu_2, \tag{2.57}$$

which, together with the transformation (2.54), is substituted into (2.3) to yield the following system up to second-order terms:

$$\begin{aligned}\frac{du}{d\tau} &= v - \tfrac{1}{k}\mu_1 - \tfrac{k+1}{ak(k+1)+1}\mu_2 - \left[\mu_1 + \tfrac{k^2(k+1)^2a}{[ak(k+1)+1]^2}\mu_2\right]u - \tfrac{k^2}{(k+1)[ak(k+1)+1}u^2 + kuv,\\ \frac{dv}{d\tau} &= \tfrac{1}{k+1}\mu_1 - \tfrac{k}{[ak(k+1)+1]}\mu_2 - \left[\tfrac{k}{k+1}\mu_1 + \tfrac{k^3(k+1)a}{[ak(k+1)+1]^2}\mu_2\right]u\\ &\quad - \tfrac{k^3}{(k+1)^2[ak(k+1)+1]}u^2 + kuv - v^2,\end{aligned} \tag{2.58}$$

Next, applying the change of variables:

$$\begin{aligned}u =& -\tfrac{(k+1)^2[ak(k+1)+1]}{k^3}y_1 + \tfrac{1}{k}\gamma_2\\ &-\tfrac{(k+1)^2[ak(k+1)+1]}{k^8}\{(k+1)^4[ak(k+1)+1]\gamma_1 + (k-1)k^4\gamma_2\}y_1\\ &+\tfrac{(k-1)(k+1)^4[ak(k+1)+1]^2}{2k^6}y_1^2 + \tfrac{2(k+1)^5[ak(k+1)+1]^2}{3k^7}y_1y_2,\\ v =& -\tfrac{(k+1)^2[ak(k+1)+1]}{k^3}y_2 + \tfrac{(k+1)^3[ak(k+1)+1]}{k^4}\gamma_1 + \tfrac{2(k+1)^5[ak^2+ak+1]^2}{3k^7}\gamma_1 y_1\\ &-\tfrac{(k+1)^2[ak(k+1)+1]}{k^8}\{(k+1)^4[ak(k+1)+1]\gamma_1 - k^4\gamma_2\}y_2 + \tfrac{(k+1)^3[ak(k+1)+1]}{k^4}y_1^2\\ &-\tfrac{(k+1)^4[ak(k+1)+1]^2}{k^6}y_1y_2 + \tfrac{2(k+1)^5[ak(k+1)+1]^2}{3k^7}y_2^2,\end{aligned} \tag{2.59}$$

and the parametrization:

$$\begin{aligned}\mu_1 &= \frac{(k+1)^3[ak(k+1)+1]}{k^3}\gamma_1 - \frac{2k}{k+1}\gamma_2,\\ \mu_2 &= \frac{2[ak(k+1)+1]}{(k+1)^2}\gamma_2 + \frac{1}{(k+1)^2}\gamma_2^2,\end{aligned} \tag{2.60}$$

into (2.58), we obtain the PSNF as follows:

$$\begin{aligned}\frac{dy_1}{d\tau} &= y_2,\\ \frac{dy_2}{d\tau} &= \gamma_1 + \gamma_2 y_2 + y_1^2 + C_{11}y_1y_2,\end{aligned} \qquad \text{for } a \in (0, \tfrac{k-1}{k(k+1)^2}) \bigcup (\tfrac{k-1}{k(k+1)^2}, \tfrac{k-1}{k(k+1)}), \tag{2.61}$$

where

$$C_{11} = \frac{(k+1)[k-1-ak(k+1)^2]}{k^2}. \tag{2.62}$$

Note from the above equation that the coefficient C_{11} is not normalized into ± 1 in order to show the direct effect of the original system parameters on the dynamics of the system. It is clear that $C_{11} > 0$ for $a \in (0, \frac{k-1}{k(k+1)^2})$ and $C_{11} < 0$ for $a \in (\frac{k-1}{k(k+1)^2}, \frac{k-1}{k(k+1)})$. Also, note that there is a negative multiplier $-\frac{(k+1)^2[ak(k+1)+1]}{k^3}$ in the transformation from (u, v) to (y_1, y_2).

Based on the PSNF (2.61), we have the following bifurcation result.

Theorem 2.4.7. *For the epidemic model* (2.3)*, codimension-*2 B-T *bifurcation occurs from the equilibrium* E_2*:* $(X, Y) = (\frac{k}{k+1}, \frac{1}{k(k+1)})$ *when* $\mu = \frac{k[k-1-ak(k+1)]}{k+1}$ *and* $r = \frac{(ak+1)^2}{(k+1)^2}$ *if* $a \in (0, \frac{k-1}{k(k+1)^2}) \bigcup (\frac{k-1}{k(k+1)^2}, \frac{k-1}{k(k+1)})$*. Moreover, three local bifurcations with the representations of the bifurcation curves are given below.*

(1) *Saddle-node bifurcation occurs from the bifurcation curve:*

$$\mathrm{SN} = \left\{(\gamma_1, \gamma_2) \mid \gamma_1 = 0, \begin{cases} \gamma_2 > 0 \ (C_{11} > 0) \\ \gamma_2 < 0 \ (C_{11} < 0) \end{cases}\right\}.$$

(2) *Hopf bifurcation occurs from the bifurcation curve:*

$$\mathrm{H} = \left\{(\gamma_1, \gamma_2) \middle| \gamma_1 = -\frac{1}{C_{11}^2}\gamma_2^2, \begin{cases} \gamma_2 > 0 \ (C_{11} > 0), \ \text{subcritical} \\ \gamma_2 < 0 \ (C_{11} < 0), \ \text{supercritical} \end{cases}\right\}.$$

(3) *Homoclinic loop bifurcation occurs from the bifurcation curve:*

$$\mathrm{HL} = \left\{(\gamma_1, \gamma_2) \middle| \gamma_1 = -\frac{49}{25}\frac{1}{C_{11}^2}\gamma_2^2, \begin{cases} \gamma_2 > 0 \ (C_{11} > 0), \ \text{unstable} \\ \gamma_2 < 0 \ (C_{11} < 0), \ \text{stable} \end{cases}\right\}.$$

The above formulas for bifurcation curves can be expressed in terms of the original perturbation parameters μ_1 and μ_2 by using (2.60). The bifurcation diagram is depicted in Figure 2.3.

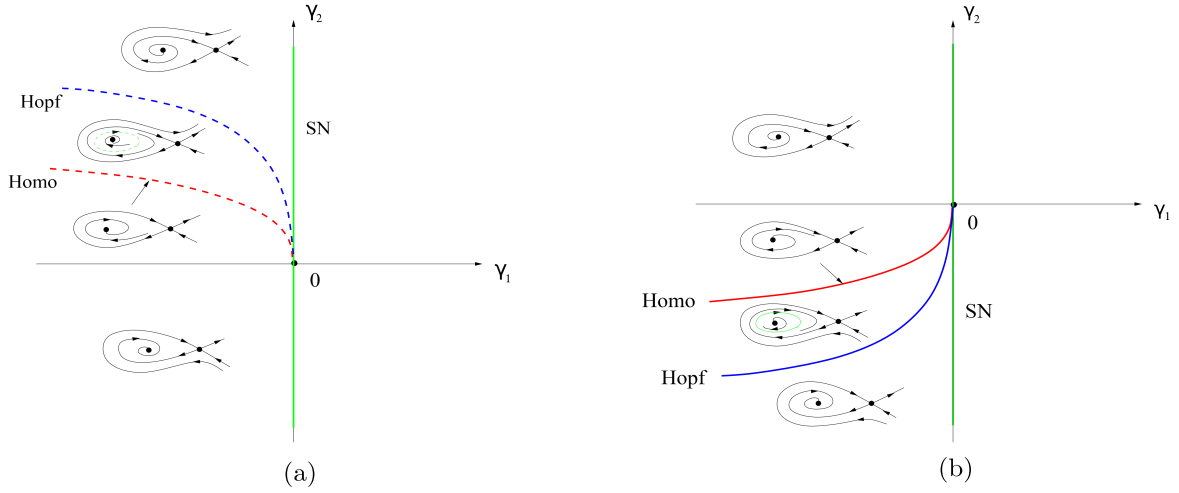

Figure 2.3: Bifurcation diagrams for the codimension-2 B-T bifurcation of the epidemic model (2.3) based on the normal form (2.61): (a) for $a \in (0, \frac{k-1}{k(k+1)^2})$ $(C_{11} > 0)$; and (b) for $a \in (\frac{k-1}{k(k+1)^2}, \frac{k-1}{k(k+1)})$ $(C_{11} < 0)$.

2.4.6 Codimension-3 B-T bifurcation

Now we turn to consider codimension-3 B-T bifurcation for the model (2.3), and we again apply the one-step transformation approach, based on the parametric simplest normal form (PSNF) [34, 7, 36]. The main difficulty of this method is how to determine the basis for nonlinear transformations, since different systems require different forms of transformations.

We first introduce the transformation,

$$\begin{aligned} &X = \tfrac{k}{k+1} + u, \quad Y = \tfrac{1}{k(k+1)} \\ &\mu = \tfrac{k^2(k-1)}{(k+1)^2}, \quad r = \tfrac{4k^2}{(k+1)^4}, \quad a = \tfrac{k-1}{k(k+1)^2} + \mu_3, \end{aligned} \tag{2.63}$$

into (2.3) to obtain the following system:

$$\begin{aligned} \frac{du}{dt} &= -\frac{1}{k+1}(kv+u)(ku+k+u), \\ \frac{dv}{dt} &= \tfrac{1}{k(k+1)[k^2(\mu_3+v)+2k(\mu_3+v)+v+\mu_3+2]}\,[kv(k+1)+1]\{k^4\mu_3 v + k^3[(u+2\mu_3)v+\mu_3 u] \\ &\quad +k^2[(2u-\mu_1+\mu_3+2)v+(2u-\mu_1)\mu_3-\mu_2] \\ &\quad +k[(u-2\mu_1)v+(u-2\mu_1)\mu_3+2u-2\mu_2]-\mu_1 v-\mu_1\mu_3-2\mu_1-\mu_2\} \end{aligned} \tag{2.64}$$

Then, applying the change of variables:

$$\begin{aligned} u &= -\tfrac{2}{k+1}(\tfrac{k+1}{k-1})^{\frac{2}{5}} y_1 - \tfrac{k-3}{2(k^2-1)}(\tfrac{k-1}{k+1})^{\frac{1}{5}}\gamma_1 - \tfrac{1}{k-1}(\tfrac{k-1}{k+1})^{\frac{4}{5}}\gamma_2 \\ &\quad + \tfrac{3k-1}{2(k+1)^2}(\tfrac{k+1}{k-1})^{\frac{4}{5}} y_1^2 - \tfrac{2}{3(k-1)} y_1 y_2 + \tfrac{9k^2+42k-143}{40(k-1)(k^2-1)}(\tfrac{k-1}{k+1})^{\frac{4}{5}} y_2^2 \\ &\quad + \sum_{i+j+k+l+s=3}^{4} a_{ijkls}\, y_1^i y_2^j \gamma_1^k \gamma_2^l \gamma_3^s, \\ v &= \tfrac{2k}{(k+1)^2}(\tfrac{k+1}{k-1})^{\frac{3}{5}} y_2 + \tfrac{2k}{(k+1)^2}(\tfrac{k+1}{k-1})^{\frac{4}{5}}\gamma_1 + \tfrac{2k}{(k+1)^2}(\tfrac{k+1}{k-1})^{\frac{4}{5}} y_1^2 + \tfrac{4k}{(k+1)(k^2-1)} y_1 y_2 \\ &\quad + \tfrac{2k}{3(k^2-1)}(\tfrac{k+1}{k-1})^{\frac{1}{5}} y_2^2 + \sum_{i+j+k+l+s=3}^{4} b_{ijkls}\, y_1^i y_2^j \gamma_1^k \gamma_2^l \gamma_3^s, \end{aligned} \tag{2.65}$$

the parametrization:

$$\begin{aligned}
\mu_1 =& \tfrac{4k^2}{(k+1)^2}\big(\tfrac{k-1}{k+1}\big)^{\frac{1}{5}}\gamma_1 + \tfrac{2k^2}{(k+1)^2}\big(\tfrac{k+1}{k-1}\big)^{\frac{1}{5}}\gamma_2 - \tfrac{k^2(5k^2+54k-47)}{2(k-1)(k+1)^3}\big(\tfrac{k-1}{k+1}\big)^{\frac{2}{5}}\gamma_1^2 \\
&- \tfrac{k^2(k^2+7)}{3(k-1)(k-3)(k+1)^2}\big(\tfrac{k-1}{k+1}\big)^{\frac{3}{5}}\gamma_2^2 - \tfrac{2k^2(k^3+14k^2-11k+8)}{3(k-1)(k-3)(k+1)^3}\gamma_1\gamma_2 \\
&- \tfrac{k^2(k^2+22k-11)}{3(k-3)(k+1)^3}\big(\tfrac{k+1}{k-1}\big)^{\frac{3}{5}}\gamma_1\gamma_3 - \tfrac{2k^2(k-1)}{3(k-3)(k+1)^2}\gamma_2\gamma_3 + \sum_{i+j+k=3}^{4}\alpha_{1ijk}\,\gamma_1^i\gamma_2^j\gamma_3^k, \\
\mu_2 =& -\tfrac{4k^2(k-3)}{(k-1)(k+1)^4}\big(\tfrac{k-1}{k+1}\big)^{\frac{1}{5}}\gamma_1 - \tfrac{4k^2}{(k+1)^4}\big(\tfrac{k+1}{k-1}\big)^{\frac{1}{5}}\gamma_2 + \tfrac{k^2(k-3)(7k^2+20k-19)}{(k-1)^2(k+1)^5}\big(\tfrac{k-1}{k+1}\big)^{\frac{2}{5}}\gamma_1^2 \\
&+ \tfrac{2k^2(7k^2-24k+25)}{3(k-3)(k+1)^5}\big(\tfrac{k+1}{k-1}\big)^{\frac{2}{5}}\gamma_2^2 + \tfrac{2k^2(13k^2-24k+19)}{3(k-1)(k+1)^5}\gamma_1\gamma_2 \\
&- \tfrac{2k^2(k-7)}{3(k-3)(k+1)^4}\gamma_1\gamma_3 + \sum_{i+j+k=3}^{4}\alpha_{2ijk}\,\gamma_1^i\gamma_2^j\gamma_3^k, \\
\mu_3 =& -\tfrac{k-3}{(k+1)^3}\big(\tfrac{k+1}{k-1}\big)^{\frac{1}{5}}\gamma_1 + \tfrac{3k-5}{2(k+1)^2}\big(\tfrac{k+1}{k-1}\big)^{\frac{1}{5}}\gamma_2 + \tfrac{1}{(k+1)^2}\big(\tfrac{k-1}{k+1}\big)^{\frac{1}{5}}\gamma_3 \\
&- \tfrac{6997k^4-43778k^3+103308k^2+31570k-53393}{720(k-1)(k+1)^5}\big(\tfrac{k+1}{k-1}\big)^{\frac{3}{5}}\gamma_1^2 \\
&+ \tfrac{(3k-1)(k^2-6k+13)}{6(k-3)(k+1)^4}\big(\tfrac{k+1}{k-1}\big)^{\frac{2}{5}}\gamma_2^2 + \tfrac{(k-1)^2}{3(k-3)(k+1)^3}\big(\tfrac{k+1}{k-1}\big)^{\frac{3}{5}}\gamma_3^2 \\
&- \tfrac{79k^3+4385k^2-49019k+10739}{1200(k-1)(k+1)^4}\gamma_1\gamma_2 - \tfrac{143k^2-826k+359}{120(k+1)^4}\big(\tfrac{k+1}{k-1}\big)^{\frac{3}{5}}\gamma_1\gamma_3 \\
&- \tfrac{(k-5)(5k-3)}{6(k-3)(k+1)^3}\gamma_2\gamma_3 + \sum_{i+j+k=3}^{4}\alpha_{3ijk}\,\gamma_1^i\gamma_2^j\gamma_3^k,
\end{aligned} \tag{2.66}$$

and the time rescaling:

$$dt = \big[-\tfrac{k}{k+1}\big(\tfrac{k+1}{k-1}\big)^{\frac{1}{5}} + \tfrac{k(k-3)}{2(k+1)^2}\big(\tfrac{k+1}{k-1}\big)^{\frac{3}{5}}y_1 + \tfrac{k(k^2+7)}{6(k-3)(k+1)^2}\big(\tfrac{k+1}{k-1}\big)^{\frac{2}{5}}\gamma_2 + \tfrac{k(k-1)}{3(k+1)(k-3)}\gamma_3\big]\,d\tau_1, \tag{2.67}$$

into (2.64) yields the following PSNF up to 4th-order terms:

$$\begin{aligned}
\frac{dy_1}{d\tau_1} &= y_2, \\
\frac{dy_2}{d\tau_1} &= \gamma_1 + \gamma_2\, y_2 + \gamma_3\, y_1 y_2 + y_1^2 + y_1^3 y_2 + O(|(y_1, y_2, \gamma)|^5).
\end{aligned} \tag{2.68}$$

Here, a_{ijkls}'s, b_{ijkls}'s and α_{mijk}'s are coefficients given in terms of k, and $\gamma = (\gamma_1, \gamma_2, \gamma_3)$.

It is easy to verify that

$$\det\left[\frac{\partial(\mu_1,\mu_2,\mu_3)}{\partial(\gamma_1,\gamma_2,\gamma_3)}\right]_{\gamma=0} = -\tfrac{8k^4}{(k+1)^8}\Big(\frac{k+1}{k-1}\Big)^{\frac{4}{5}} \neq 0, \tag{2.69}$$

which shows that near the critical point $\mu = 0$, system (2.3) has the same bifurcation set with respect to μ as system (2.68) has with respect to γ, up to a homeomorphism in the parameter space.

Now, following the method described in [6], and the computations in [36] we apply the method of normal forms and Abelian integral (or the Melnikov function method) to derive the

bifurcations for the codimension-3 B-T bifurcation. For the convenience of readers, in the following we briefly describe the derivations. First of all, it is easy to see that system (2.64) has two equilibrium solutions $E_\pm$:

$$E_\pm = (y_{1\pm}, 0), \quad \text{where} \quad y_{1\pm} = \pm\sqrt{-\gamma_1} \quad \text{for} \quad \gamma_1 < 0. \tag{2.70}$$

Evaluating the Jacobian of (2.64) at $E_\pm$ gives

$$J_\pm = \begin{bmatrix} 0 & 1 \\ 2y_{1\pm} & \gamma_2 + \gamma_3 y_{1\pm} + y_{1\pm}^3 \end{bmatrix}, \tag{2.71}$$

which shows that E_{1+} is a saddle, and E_{1-} is either a focus or node. It follows from the Jacobian that the plane

$$\text{SN} = \{(\gamma_1, \gamma_2, \gamma_3) \mid \gamma_1 = 0\}, \tag{2.72}$$

excluding the origin in the parameter space is the saddle-node bifurcation surface. Hopf bifurcation occurs from E_- on the critical surface, determined by setting the trace to equal zero, given by

$$\gamma_2 - (\gamma_3 - \gamma_1)\sqrt{-\gamma_1} = 0, \quad (\gamma_1 < 0). \tag{2.73}$$

With Hopf bifurcation theory, a direct computation (e.g., with the Maple program in [32]) leads to the following focus values:

$$v_1 = \frac{\gamma_3 + 3\gamma_1}{16\sqrt{-\gamma_1}} \quad \text{and} \quad v_2|_{v_1=0} = \frac{5}{96\sqrt{-\gamma_1}} > 0,$$

indicating that generalized Hopf bifurcation occurs on the surface, defined by $v_1 = 0$:

$$\gamma_3 + 3\gamma_1 = 0, \quad (\gamma_1 < 0), \tag{2.74}$$

giving rise to two limit cycles, with the outer one unstable and the inner one stable, and both them enclose the unstable focus E_-.

Next, in order to find the homoclinic and degenerate homoclinic bifurcations, we apply the Melnikov function method [13]. To achieve this, introducing the scaling:

$$y_1 = \varepsilon^{\frac{2}{5}} w_1, \;\; y_2 = \varepsilon^{\frac{3}{5}} w_2, \;\; \gamma_1 = \varepsilon^{\frac{4}{5}} \nu_1, \;\; \gamma_2 = \varepsilon^{\frac{6}{5}} \nu_2, \;\; \gamma_3 = \varepsilon^{\frac{4}{5}} \nu_3, \;\; \tau_2 = \varepsilon^{\frac{1}{5}} \tau_1, \;\; (0 < \varepsilon \ll 1), \tag{2.75}$$

together with the following transformation,

$$w_1 = \bar{\nu}_1 + z_1, \quad w_2 = \sqrt{2\bar{\nu}_1}\, z_2, \quad \tau_3 = \sqrt{2\bar{\nu}_1}\, \tau_3, \quad \nu_1 = -\bar{\nu}_1^2, \;\; (\bar{\nu}_1 > 0), \tag{2.76}$$

into (2.64) one obtains

$$\begin{aligned} \frac{dz_1}{d\tau_2} &= z_2, \\ \frac{dz_2}{d\tau_2} &= z_1 + \frac{1}{2\bar{\nu}_1} z_1^2 + \varepsilon\, q(z_1, z_2, \bar{\nu}), \end{aligned} \tag{2.77}$$

where

$$q(z_1, z_2, \bar{\nu}) = \frac{1}{\sqrt{2\bar{\nu}_1}}\left[(\nu_2 + \bar{\nu}_1\,\nu_3 + \bar{\nu}_1^3)z_2 + (\nu_3 + 3\bar{\nu}_1^2)z_1 z_2 + 3\bar{\nu}_1 z_1^2 z_2 + z_1^3 z_2\right], \tag{2.78}$$

with $\bar{\nu} = (\bar{\nu}_1, \nu_2, \nu_3)$.

When $\varepsilon = 0$, the system (2.77) is a Hamiltonian system which has two equilibrium points:

$$\widetilde{\mathrm{E}}_- = (-2\bar{\nu}_1, 0) \quad \text{and} \quad \widetilde{\mathrm{E}}_0 = (0, 0), \tag{2.79}$$

which are center and saddle, respectively. These two equilibria correspond to the $\mathrm{E}_\pm$ defined in (2.64). The Hamiltonian of (2.77) is given by

$$H(z_1, z_2) = \frac{1}{2}(z_2^2 - z_1^2) - \frac{1}{6\bar{\nu}_1} z_1^3, \tag{2.80}$$

and the homoclinic orbit connecting E_0 is described by

$$\Gamma_0: \quad H(z_1, z_2) = \frac{1}{2}(z_2^2 - z_1^2) - \frac{1}{6\bar{\nu}_1} z_1^3, \quad \text{with } H(0,0) = 0, \tag{2.81}$$

and $H(-2\bar{\nu}_1, 0) = -\frac{2}{3}\bar{\nu}_1^2$. Thus, any closed orbits of the Hamiltonian system $(2.77)|_{\varepsilon=0}$ inside the homoclinic loop Γ_0 can be described by

$$\Gamma_\mathrm{h}: \quad H(z_1, z_2, h) = \frac{1}{2}(z_2^2 - z_1^2) - \frac{1}{6\bar{\nu}_1} z_1^3 - h = 0, \quad h \in \Big(-\frac{2}{3}\bar{\nu}_1^2, 0\Big). \tag{2.82}$$

Then, the Abelian integral or the (first-order) Melnikov function for the perturbed system (2.77) can be expressed as [13]

$$\begin{aligned} M(h, \nu) &= \oint_{\Gamma_\mathrm{h}} q(z_1, z_2, \nu)\, dz_1 - p(z_1, z_2, \nu)\, dz_2 \,|_{\varepsilon=0} \qquad (p = 0) \\ &= \oint_{\Gamma_\mathrm{h}} q(z_1, z_2, \nu)\,|_{\varepsilon=0}\; dz_1 = \oint_{\Gamma_\mathrm{h}} H_{z_2} q(z_1, z_2, \nu)\,|_{\varepsilon=0}\; dt \\ &= \frac{1}{\sqrt{2\bar{\nu}_1}} \oint_{\Gamma_\mathrm{h}} z_2^2\left[\nu_2 + \bar{\nu}_1\,\nu_3 + \bar{\nu}_1^3 + (\nu_3 + 3\bar{\nu}_1^2)z_1 + 3\bar{\nu}_1 z_1^2 + z_1^3\right] dt \\ &= M(h, \nu) = C_0(\nu) + C_1(\nu)\, h \ln|h| + C_2(\nu)\, h + C_3(h)\, h^2 \ln|h| + \cdots, \end{aligned} \tag{2.83}$$

for $0 < -h \ll 1$, where

$$\begin{aligned} C_0(\nu) &= \frac{1}{\sqrt{2\bar{\nu}_1}} \oint_{\Gamma_0} z_2^2[\nu_2 + \bar{\nu}_1\,\nu_3 + \bar{\nu}_1^3 + (\nu_3 + 3\bar{\nu}_1^2)z_1 + 3\bar{\nu}_1 z_1^2 + z_1^3]\, dt, \\ C_1(\nu) &= a_{10} + b_{01}, \end{aligned} \tag{2.84}$$

in which a_{10} and b_{01} are the coefficients in the functions $p(z_1, z_2, \nu)$ and $q(z_1, z_2, \nu)$, given by

$$a_{10} = 0, \quad b_{01} = \frac{1}{\sqrt{2\bar{\nu}_1}}(\nu_2 + \bar{\nu}_1\,\nu_3 + \bar{\nu}_1^3). \tag{2.85}$$

To compute $C_0(\nu)$, we introduce the parametric transformation:

$$z_1(t) = -3\,\bar{\nu}_1\,\mathrm{sech}^2(t), \quad z_2(t) = 3\,\bar{\nu}_1\,\mathrm{sech}^2(t)\tanh(t), \tag{2.86}$$

into $C_0(\nu)$ with a direct integration to obtain

$$C_0(\nu) = \frac{6\bar{\nu}_1\sqrt{2\bar{\nu}_1}}{5}\left[\nu_2 - \frac{5}{7}\bar{\nu}_1\,\nu_3 - \frac{103}{77}\,b_1\bar{\nu}_1^3\right]. \tag{2.87}$$

Further, we express $C_0(\nu)$ and $C_1(\nu)$ in terms of the original perturbation parameters γ_j by using

$$\bar{\nu}_1 = \sqrt{-\nu_1} = \sqrt{-\varepsilon^{-\frac{4}{5}}\,\gamma_1} = \varepsilon^{-\frac{2}{5}}\sqrt{-\gamma_1}, \quad \nu_2 = \varepsilon^{-\frac{6}{5}}\gamma_2, \quad \nu_3 = \varepsilon^{-\frac{4}{5}}\gamma_3,$$

as

$$\begin{aligned} C_0(\gamma) &= \frac{6\bar{\nu}_1\sqrt{2\bar{\nu}_1}}{5}\,\varepsilon^{-\frac{6}{5}}\Big[\gamma_2 - \Big(\frac{5}{7}\,\gamma_3 - \frac{103}{77}\,\gamma_1\Big)\sqrt{-\gamma_1}\Big], \\ C_1(\gamma) &= \frac{1}{\sqrt{2\bar{\nu}_1}}\,\varepsilon^{-\frac{6}{5}}\left[\gamma_2 + (\gamma_3 - \gamma_1)\sqrt{-\gamma_1}\,\right]. \end{aligned} \tag{2.88}$$

Therefore, the homoclinic and degenerate homoclinic bifurcation surfaces are defined by $C_0(\gamma) = 0$ and $C_1(\gamma) = 0$, respectively.

Summarizing the above results yields the following theorem.

Theorem 2.4.8. *For the model (2.3), codimension-3 B-T bifurcation occurs from the equilibrium* E_2*:* $(X, Y) = (\frac{k}{k+1}, \frac{k-1}{k(k+1)})$ *when* $\mu = \frac{k^2(k-1)}{(k+1)^2}$, $r = \frac{4k^2}{(k+1)^4}$ *and* $a = \frac{k-1}{k(k+1)^2}$. *Moreover, six local bifurcations with the representations of the bifurcation surfaces/curves are obtained, as given below.*

(1) *Saddle-node bifurcation occurs from the critical surface:*

$$\mathrm{SN} = \{(\gamma_1, \gamma_2, \gamma_3) \mid \gamma_1 = 0\}.$$

(2) *Hopf bifurcation occurs from the critical surface:*

$$\mathrm{H} = \{(\gamma_1, \gamma_2, \gamma_3) \mid \gamma_1 < 0,\ \gamma_2 = (\gamma_3 - \gamma_1)\sqrt{-\gamma_1}\}.$$

(3) *Homoclinic loop bifurcation occurs from the critical surface:*

$$\mathrm{HL} = \left\{(\gamma_1, \gamma_2, \gamma_3) \mid \gamma_1 < 0,\ \gamma_2 = (\tfrac{5}{7}\,\gamma_3 - \tfrac{103}{77}\gamma_1)\sqrt{-\gamma_1}\right\}.$$

(4) *Generalized Hopf bifurcation occurs from the critical curve:*

$$\mathrm{GH} = \left\{(\gamma_1, \gamma_2, \gamma_3) \mid \gamma_1 < 0,\ \gamma_2 = -4\gamma_1\sqrt{-\gamma_1},\ \gamma_3 = -3\gamma_1\right\}.$$

(5) *Degenerate homoclinic bifurcation occurs from the critical curve:*

$$\mathrm{DHL} = \left\{(\gamma_1, \gamma_2, \gamma_3) \,\middle|\, \gamma_1 < 0,\ \gamma_2 = -\tfrac{4}{11}\,\gamma_1\sqrt{-\gamma_1},\ \gamma_3 = \tfrac{15}{11}\,\gamma_1\right\}.$$

(6) *Double limit cycle bifurcation occurs from a critical surface, which is tangent to the Hopf bifurcation surface* H *on the critical curve* GH*, and tangent to the homoclinic bifurcation surface* HL *on the critical curve* DHL.

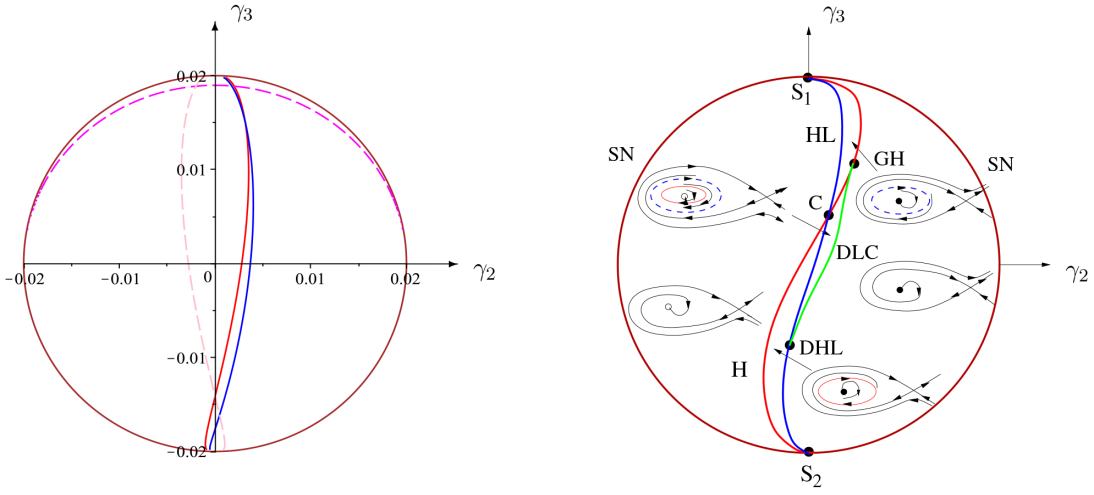

Figure 2.4: Bifurcation diagram for the codimension-3 B-T bifurcation based on the normal form (2.64), displayed in the intersection of the cone and the 2-sphere $\gamma_1^2 + \gamma_2^2 + \gamma_3^2 = \sigma^2$, with the brown color curve for saddle-node, red curve for Hopf and blue curve for homoclinic loop bifurcations, respectively: (a) with $\sigma = 0.02$, where the intersection point of the pink and red curve is the degenerate Hopf bifurcation, and the intersection point of the pale pink and blue curves denotes the degenerate homoclinic loop bifurcation; and (b) a schematic bifurcation diagram, where the GH and DHL represent the generalized Hopf critical point and the degenerate homoclinic critical point, respectively.

The bifurcation diagram projected on a 2-sphere is shown in Figure 2.4. Figure 2.4(a) is an exact bifurcation diagram for $\sigma = 0.02$, in which the intersection points C, GH and DHL, as shown in Figure 2.4(a), are given by

$$\begin{aligned}
\mathrm{C} &= (\sigma_2, \sigma_3)_{\mathrm{C}} &&= (0.0031, 0.0151), && \text{for } \sigma_1 = -0.0128,\\
\mathrm{GH} &= (\sigma_2, \sigma_3)_{\mathrm{GH}} &&= (0.0020, 0.0189), && \text{for } \sigma_1 = -0.0063,\\
\mathrm{DHL} &= (\sigma_2, \sigma_3)_{\mathrm{DHL}} &&= (0.0005, -0.0161), && \text{for } \sigma_1 = -0.0118.
\end{aligned} \tag{2.89}$$

For a better view of bifurcations, a schematic general bifurcation diagram is shown in Fig. 2.4(b) with typical phase portraits, which is similar to Figure 3 in [6] and Figure 2 in [18].

Chapter 3

An SIRS model with a generalized incidence

3.1 Introduction

In this chapter, we reconsider a disease system studied by Rao *et al.* [22], in which a generalized incidence function, $f(I) = \frac{\beta I}{\pi(I)}$ is proposed to model the transmission of disease. It implies that susceptible individuals become infected at this rate. The function f is non-monotone when the psychological influence is considered. The model is described by the following equations:

$$\begin{aligned} \dot{S} &= (1-p)b - \mu_1 S - \lambda S I + \gamma R, \\ \dot{I} &= \lambda S I - (\mu_2 + \alpha) I - T(I), \\ \dot{R} &= pb - (\mu_3 + \gamma) R + \alpha I + T(I), \end{aligned} \tag{3.1}$$

where S, I and R represent the numbers of the susceptible, infected, and recovered populations, respectively[41]. Among the factors that affect the transmission of diseases is the infection force which is given by $f(I) = \frac{\beta}{/pi(I)}$, whereas $\frac{1}{\pi(I)}$ represents the effect of intervention measures on the lowering of valid contact coefficient β. $T(I)$ is the treating function, and is assumed in the form $T(I) = \frac{rI}{1+kI}$, which is used in [29]. With this T, system (3.1) becomes

$$\begin{aligned} \dot{S} &= (1-p)b - \mu_1 S - \lambda S I + \gamma R, \\ \dot{I} &= \lambda S I - (\mu_2 + \alpha) I - \frac{rI}{1+kI}, \\ \dot{R} &= pb - (\mu_3 + \gamma) R + \alpha I + \frac{rI}{1+kI} \end{aligned} \tag{3.2}$$

The total population at time t is given by $N(t) = S(t) + I(t) + R(t)$. All the parameters are assumed to be positive and typical values are shown in Table 3.1.

Table 3.1: Definitions and value of parameters of system (3.2)[22]

Variable	Description	Value	Resource
b	The population's recruitment rate	1 or 50	[30, 4, 28]
p	The proportion of susceptible populations that is vaccinated remains constant	[0, 1]	[17]
α	The recovery rate of infectious individuals	0.1	[4]
λ	The individuals' treatment rate	0.1	[4]
γ	The immune loss rate	0.25	[4]
μ_1	The mortality rate among the susceptible population	0.2	[30]
μ_2	The mortality rate among the infected population	0.2	[30]
μ_3	The mortality rate among the recovered population	0.2	[30]
r	The capacity of treatment for infected individuals	varies	[28]
k	The impact of delays in treating infected	varies	[28]

In [22], the authors provide an analysis for different death rates μ_i on the existence and stability of equilibrium solutions, as well as numerical simulations to verify their theoretical results. However, the important Hopf and B-T bifurcations are not discussed due to the difficulty caused the different death rates.

In general, the three death rates μ_i should be different. But in the reality, the difference in the rates can be ignored, and in the literature, they are taken the same values (see Table 3.1). As a matter of fact, all simulations given in [22] use the same value 0.2 for the three death rates. Therefore, we assume that $\mu_1 = \mu_2 = \mu_3 = \mu$ in our study so that we can perform a more complex bifurcation analysis. Adding the equations in (3.2) results in a different equation for N: $\dot{N} = b - \mu N$, which gives the solution

$$N(t) = \frac{b}{\mu} + \Big(N(0) - \frac{b}{\mu}\Big)e^{-\mu t},$$

showing that $N(t) \to \frac{b}{\mu}$ as $t \to \infty$. Thus, with $R = \frac{b}{\mu} - S - I$, the dynamics of the limiting system is described by the following 2-d differential system,

$$\begin{aligned} \dot{S} &= (1-p)b - \mu S - \lambda S I + \gamma\Big(\frac{b}{\mu} - S - I\Big) \\ \dot{I} &= \lambda S I - (\mu + \alpha)I - \frac{rI}{Ik+1} \end{aligned} \tag{3.3}$$

To further simplify the mathematical analysis, we introduce the scaling transformation:

$$S = \frac{X}{k}, \quad I = \frac{Y}{k}, \quad \tau = rt, \tag{3.4}$$

into (3.3) to obtain the dimensionless system,

$$\begin{aligned} \dot{X} &= A - BXY - (C+D)X - CY, \\ \dot{Y} &= BXY - (D+E)Y - \frac{Y}{Y+1}, \end{aligned} \tag{3.5}$$

where the new parameters are defined as

$$A = \frac{kb}{r}\Big(1 - p + \frac{r}{\mu}\Big), \quad B = \frac{\lambda}{rk}, \quad C = \frac{\gamma}{r}, \quad D = \frac{\mu}{r}, \quad E = \frac{\alpha}{r}. \tag{3.6}$$

The positivity of the solution of the system can be easily proved using the method of variation constant, and the boundedness of the solution can be shown using a Lyapunov function $V(X,Y) = X + Y$ to find the trapping region bounded by the X-axis, the Y-axis and the straight line L, defined by

$$\mathrm{L}: \quad X + Y = \frac{A}{C+D}. \tag{3.7}$$

3.2 Equilibrium solutions and their stability

Setting $\dot{X} = \dot{Y} = 0$ yields two equilibrium solutions:

$$\begin{aligned} &\mathrm{E}_0 = \Big(\frac{A}{C+D}, 0\Big), && \text{Disease free equilibrium (DFE),} \\ &\mathrm{E}_1 = (X_1, Y_1) = \Big(\frac{D}{B} + \frac{E}{B} + \frac{1}{B(Y_1+1)}, Y_1\Big), && \text{Endemic equilibrium,} \end{aligned} \tag{3.8}$$

where Y_1 is determined from the quadratic polynomial,

$$F_2 = -\frac{F_{2a}}{B(Y_1+1)}, \quad \text{where} \quad F_{2a} = M_2 Y_1^2 + M_2 Y_1 + M_0, \tag{3.9}$$

where

$$\begin{aligned} M_0 &= B(C+D+E) > 0, \\ M_1 &= (C+D)(D+E) + B(C+D+E+1-A), \\ M_2 &= (C+D)(D+E+1) - AB. \end{aligned} \tag{3.10}$$

The Jacobian matrix of system (3.5) can be used to determine the stability of equilibrium solutions, which is given by

$$J(X,Y) = \begin{bmatrix} -BY - C - D & -BX - C \\ BY & BX - D - E - \dfrac{1}{Y+1} + \dfrac{Y}{(Y+1)^2} \end{bmatrix}. \tag{3.11}$$

For the DFE E_0, we have the following result.

Theorem 3.2.1. *For system (3.5), the* DFE *is asymptotically stable (a stable node) if* $AB < (C+D)(1+D+E)$*; and unstable (a saddle) if* $AB > (C+D)(1+D+E)$*. A bifurcation occurs at the critical point, defined by* $AB = (C+D)(1+D+E)$*.*

Proof. Evaluating the Jacobian J at E_0 gives two eigenvalues:

$$\lambda_1 = -(C+D) < 0, \quad \lambda_2 = \frac{AB}{C+D} - (D+E+1),$$

which clearly shows that E_0 is a stable node if $AB < (C+D)(D+E+1)$ ($\lambda_2 < 0$), and a saddle if $AB > (C+D)(D+E+1)$ ($\lambda_2 > 0$). At the critical point defined by $AB = (C+D)(D+E+1)$, E_0 loses its stability and bifurcates into E_1 (as shown in the next theorem). □

The basic reproduction number R_0 can be easily obtained from λ_2 as

$$\begin{aligned}\lambda_2 = \frac{AB}{C+D} - (1+D+E) &= (D+E+1)\Big[\frac{AB}{(C+D)(1+D+E)} - 1\Big] \\ &\triangleq (D+E+1)(\mathrm{R}_0 - 1),\end{aligned}$$

implying that $\lambda_2 \lesseqgtr 0 \iff \mathrm{R}_0 \lesseqgtr 1$.

Similarly, we can obtain stability conditions for the endemic equilibrium, but the analysis is much more involved. Define

$$\begin{aligned} B_1 &= \tfrac{(C+D)(D+E+1)}{A}, \\ B_2 &= \tfrac{(C+D)(D+E)}{A-C-D-E-1}, \\ B_\pm &= \tfrac{(C+D)\{(D+E)(A+C+D+E+1)+2C \pm 2\sqrt{(C+D+E)[(A+C)(D+E)+C]}\}}{(A-1)^2+(C+D+E)(C+D+E+2A+2)}, \\ Y_{1\pm} &= \tfrac{1}{2M_0}(-M_1 \pm \sqrt{\Delta_1}), \\ E_{1\pm} &= (X_{1\pm}, Y_{1\pm}), \end{aligned} \tag{3.12}$$

where

$$\begin{aligned}\Delta_1 = M_1^2 - 4M_0M_2 &= \big[(A-1)^2 + (C+D+E)(C+D+E+2A+2)\big]B^2 \\ &\quad - 2(C+D)\big[(D+E)(A+C+D+E+1)+2C\big]B + (D+E)^2(C+D)^2.\end{aligned}$$

$\Delta_1 > 0$ if $B < B_-$ or $B > B_+$, for which the quadratic polynomial F_{2a} has real solutions for Y_1. We have the following theorem.

Theorem 3.2.2. *For the system (3.5), the following holds for the existence of the endemic equilibrium solution.*

(1) *No solution if* $B < B_-$*, or* $A \le C+D+E+1$ *and* $B_+ < B < B_1$*, or* $C+D+E+1 < A < (D+E+1)(C+D+E+1)$ *and* $B_+ < B < \min\{B_1, B_2\}$*,*

(2) *Two solutions* $\mathrm{E}_{1\pm}$ *if* $A > (D+E+1)(C+D+E+1)$ *and* $\max\{B_+, B_2\} < B < B_1$.

(3) *One solution* E_{1+} *if* $B > B_1$, *or* $A > (D+E+1)(C+D+E+1)$ *and* $B = B_1$.

Proof. We first prove that F_{2a} has no real roots if $B < B_-$. Note that the constant coefficient in F_{2a}, $M_0 < 0$ for $B > B_1$ and $M_0 \geq 0$ for $B \leq B_1$. A direct computation shows that $B_1 > B_+$. Hence, $M_0 > 0$ for $B < B_-$ ($< B_+ < B_1$).

Next, consider the sign of M_1, the coefficient of linear term in F_2. If $C+D+E+1-A \geq 0$, then $M_1 > 0$, indicating that all the three coefficients M_i are positive, and so F_{2a} has no real roots.

If $C+D+E+1-A < 0$, we have

$$\begin{aligned} M_1 &> (C+D)(D+E) + B_-(C+D+E+1-A) \\ &= \frac{2(C+D)}{(A-1)^2+(C+D+E)(C+D+E+2A+2)}\big[(D+E)^3 + 2(C+1)(D+E)^2 \\ &\quad + C(C+1) + (C^2+3C+1)(D+E) + A(D+E-1)(C+D+E) \\ &\quad + (A-C-D-E-1)\sqrt{(C+D+E)[(A+C)(D+E)+C]}\,\big]. \end{aligned}$$

It is obvious that $M_1 > 0$ if $D+E-1 \geq 0$. When $D+E-1 < 0$, $M_1 > 0$ if

$$C+D+E+1 < A \leq \frac{(D+E)^3 + 2(C+1)(D+E)^2 + C(C+1) + (C^2+3C+1)(D+E)}{(1-D-E)(C+D+E)}.$$

When

$$A > \frac{(D+E)^3 + 2(C+1)(D+E)^2 + C(C+1) + (C^2+3C+1)(D+E)}{(1-D-E)(C+D+E)},$$

A direct computation shows that $M_1 > 0$.

Summarizing the above discussions, we have that $F_{2a} = 0$ does not have real positive solutions for Y_1 if $B < B_-$.

Now, we consider $B > B_+$. We have three cases:

(a) No solution if $B_+ < B \leq B_1$ and $M_1 \geq 0$.

(b) Two solutions if $B_+ < B \leq B_1$ and $M_1 < 0$.

(c) One solution if $B > B_1$.

(d) One solution if $B = B_1$ and $M_1 < 0$.

For the Case (d), we have $M_2 \geq 0$. Thus $A \leq C+D+E+1$ yields $M_1 > 0$. When $A > C+D+E+1$, $M_1 \geq 0$ results in $B \leq B_2$ and thus $B_+ < B < \min\{B_1, B_2\}$. This requires $B_2 > B_+$. Then, similar to the proof for the case $B < B_-$, we discuss two sub-cases: $D+E \geq 1$ and $D+E < 1$ to obtain that

$$C+D+E+1 < A < (D+E+1)(C+D+E+1).$$

This finishes the proof for the case (a). Proving the case (b) and (d) needs to find the condition for $B_1 > B_2$, which is equivalent to

$$B_1 - B_2 = \frac{(C+D)[A-(D+E+1)(C+D+E+1)]}{A(A-C-D-E-1)} > 0,$$

yielding $A > (D+E+1)(C+D+E+1)$.

The proof is complete. □

For the stability of E_1, it is difficult to obtain the explicit conditions expressed in terms of system parameters. Instead of Y_1, we use A to solve $F_{2a} = 0$ and then treat Y_1 (representing both $Y_{1\pm}$ as a *parameter* in the following stability analysis. Note that since the solutions $Y_{1\pm}$ are computed at the equilibrium E_1, expressed in terms of the system parameters, Y_1 indeed represents parameters in an implicit form. Solving $F_{2a} = 0$ for A yields

$$A = \frac{B(C+D+E)Y_1^2 + [B(C+D+E+1)+(C+D)(D+E)]Y_1 + (D+E+1)(C+D)}{B(Y_1+1)}, \tag{3.13}$$

which is positive for positive parameter values and $Y_1 \geq 0$.

Then, we have the following result.

Theorem 3.2.3. *For the system (3.5), we have the following results for the stability of the endemic equilibrium* E_1.

(i) E_1 *is asymptotically stable for*

$$0 < C < -Y_1 B - D + \frac{Y_1}{(Y_1+1)^2} \quad \textit{and} \quad E > \max\{\frac{-B+C+D}{(Y_1+1)^2 B} - (C+D),\, 0\}.$$

(ii) E_1 *is unstable for*

$$\begin{aligned} &\textit{either} \quad C > B(C+D+E)(Y_1+1)^2 - D \\ &\textit{or} \qquad C > \max\{-BY_1 - D + \frac{Y_1}{(Y_1+1)^2},\, 0\} \ \textit{and} \ E > \max\{\frac{-B+C+D}{B(Y_1+1)^2} - (C+D),\, 0\}. \end{aligned}$$

(iii) *Transcritical bifurcation occurs at the critical point* $R_0 = 1$ *between* E_0 *and* E_1.

(iv) *Hopf bifurcation occurs at the critical point, defined by*

$$\begin{aligned} &C = -BY_1 - D + \frac{Y_1}{(Y_1+1)^2}, \quad D < \frac{Y_1[1-B(Y_1+1)^2]}{(Y_1+1)^2}, \quad B < \frac{1}{(Y_1+1)^2}, \\ &E > \frac{Y_1[B(Y_1+1)^2-1]^2 - B(Y_1+1)^2}{B(Y_1+1)^4}. \end{aligned}$$

(v) *Bogdanov-Takens bifurcation at the critical point, defined by*

$$C = -BY_1 - D + \frac{Y_1}{(Y_1+1)^2}, \quad D < \frac{Y_1[1 - B(Y_1+1)^2]}{(Y_1+1)^2}, \quad B < \frac{1}{(Y_1+1)^2},$$
$$E = \frac{Y_1[B(Y_1+1)^2 - 1]^2 - B(Y_1+1)^2}{B(Y_1+1)^4}.$$

Proof. Using Y_1, the Jacobian matrix (3.11) becomes

$$J(\mathrm{E}_1) = \begin{bmatrix} -BY_1 - C - D & \dfrac{(-C-D-E)Y_1 - C - D - E - 1}{Y_1+1} \\ BY_1 & \dfrac{Y_1}{(Y_1+1)^2} \end{bmatrix},$$

which gives the trace and determinant as follows:

$$\begin{aligned} \mathrm{Tr}(J(\mathrm{E}_1)) &= -BY_1 - C - D + \frac{Y_1}{(Y_1+1)^2}, \\ \det(J(\mathrm{E}_1)) &= \frac{Y_1}{(Y_1+1)}[B(C+D+E)(Y_1+1)^2 + B - C - D]. \end{aligned} \tag{3.14}$$

Then, based on $\det(J(\mathrm{E}_1))$ and $\mathrm{Tr}(J(\mathrm{E}_1))$, we use the parameters C and E to determine the stability conditions and bifurcations.

Case (i) E_1 is asymptotically stable if $\mathrm{Tr}(J(\mathrm{E}_1)) < 0$ and $\det(J(\mathrm{E}_1)) > 0$. Solving the inequality $\mathrm{Tr}(J(\mathrm{E}_1)) < 0$ gives the condition on C, and then solving the inequality $\det(J(\mathrm{E}_1)) > 0$ yields the condition on E.

Case (ii) E_1 is unstable if either $\det(J(\mathrm{E}_1)) < 0$, or $\det(J(\mathrm{E}_1)) > 0$ and $\mathrm{Tr}(J(\mathrm{E}_1)) > 0$. $\det(J(\mathrm{E}_1)) < 0$ leads to $C > B(C+D+E)(Y_1+1)^2 - D$. Similar to the Case I, the second condition can be easily derived.

Case (iii) Transcritical bifurcation occurs from E_1 if $\mathrm{Tr}(J(\mathrm{E}_1)) < 0$ and $\det(J_1) = 0$. $\det(J_1) = 0$ gives $Y_1 = 0$, and then (3.13) yields the critical point,

$$A = \frac{(C+D)(D+E+1)}{B},$$

under which $\mathrm{Tr}(J(\mathrm{E}_1)) = -(C+D) < 0$, and in addition,

$$X_1 = \frac{D+E+1}{B} = \frac{A}{C+D},$$

which indicates that a transcritical bifurcation happens at $AB = (C+D)(D+E+1)$, i.e., $\mathrm{R}_0 = 1$, between E_0 and E_1.

Case (iv) Hopf bifurcation occurs if $\mathrm{Tr}(J(\mathrm{E}_1)) = 0$ and $\det(J(\mathrm{E}_1)) > 0$, which requires

$$C = \frac{Y_1}{(Y_1+1)^2} - D - BY_1.$$

$C > 0$ needs

$$B < \frac{1}{(Y_1+1)^2} \quad \text{and} \quad D < Y_1\left[(Y_1+1)^2 - B\right]. \tag{3.15}$$

$\det(J(\mathrm{E}_1)) > 0$ yields

$$E > \frac{Y_1[B(Y_1+1)^2-1]^2 - B(Y_1+1)^2}{B(Y_1+1)^4}. \tag{3.16}$$

Case (v) B-T bifurcation occurs if $\mathrm{Tr}(J(\mathrm{E}_1)) = \det(J(\mathrm{E}_1)) = 0$, which directly leads to

$$C = \frac{Y_1}{(Y_1+1)^2} - D - BY_1 \quad \textit{and} \quad E = \frac{Y_1[B(Y_1+1)^2-1]^2 - B(Y_1+1)^2}{B(Y_1+1)^4},$$

together with the condition (3.15).

□

3.3 Codimension of Hopf bifurcation

In this section, we consider the codimension of the Hopf bifurcation. We have the following result.

Theorem 3.3.1. *For the model (3.5), the codimension of Hopf bifurcation is two.*

Proof. To determine the codimension of Hopf bifurcation, we use the method of normal forms to compute the focus values. To achieve this, we first use the parameter A to solve the polynomial $F_{2a} = 0$ to obtain the solution given in (3.14). Then, to simplify the computation of focus values, we introduce the time scaling

$$dt = (Y+1)d\tau$$

into (3.5) to obtain

$$\begin{aligned} \frac{dX}{d\tau} &= [A - BXY - (C+D)X - CY](Y+1), \\ \frac{dY}{d\tau} &= [BXY - (D+E)Y](Y+1) - Y. \end{aligned} \tag{3.17}$$

The stability of the equilibrium solution E_1 is determined from the Jacobian matrix of system (3.17), which is evaluated at E_1 to yield

$$J(\mathrm{E}_1) = \begin{bmatrix} -(Y_1+1)(BY_1+C+D) & -(C+D+E)(Y_1+1) - 1 \\ BY_1(Y_1+1) & \dfrac{Y_1}{Y_1+1} \end{bmatrix}, \tag{3.18}$$

where (3.14) has been used.

Next, let the trace of the J equal to zero yields the Hopf critical point, defined by

$$C_{\mathrm{H}} = \frac{Y_1}{(Y_1+1)^2} - D - BY_1. \tag{3.19}$$

$C_{\mathrm{H}} > 0$ requires the condition given in (3.15).

Now, introducing the following affine transformation:

$$\begin{pmatrix} X \\ Y \end{pmatrix} = \begin{pmatrix} \frac{1}{B}(D+E+\frac{1}{Y_1+1}) \\ Y_1 \end{pmatrix} + \begin{bmatrix} 1 & 0 \\ -\frac{(Y_1+1)(BY_1+C+D)}{(C+D+E)(Y_1+1)+1} & \frac{\omega_c}{(C+D+E)(Y_1+1)+1} \end{bmatrix} \begin{pmatrix} u \\ v \end{pmatrix}, \tag{3.20}$$

where

$$\omega_c = \frac{1}{Y_1+1}\sqrt{Y_1[-Y_1(1-B(Y_1+1)^2)^2 + B(Y_1+1)^2 + EB(Y_1+1)^4]}. \tag{3.21}$$

into (3.17) we obtain the following system,

$$\begin{aligned}
\frac{du}{dt} &= v - \tfrac{BY_1(Y_1+1)}{Q_1\omega_c}u^2 - \tfrac{B(Y_1+1)^3-Y_1}{Q_1(Y_1+1)}uv + \tfrac{\omega_c}{Q_1}v^2 - \tfrac{BY_1^2}{Q_1^2\omega_c}u^3 \\
&\quad - \tfrac{2BY_1(Y_1+1)}{Q_1^2}u^2v - \tfrac{B\omega_c(Y_1+1)^2}{Q_1^2}uv^2, \\
\frac{dv}{dt} &= -u + \tfrac{Y_1}{(Y_1+1)^2\omega_c^2}[B(Y_1+1)(2Y_1+1)+1+\tfrac{E(Y_1+1)^2+3Y_1+1}{Q_1}]u^2 \\
&\quad + \tfrac{1}{(Y_1+1)^2\omega_c^2}\{(Y_1+1)[B(Y_1+1)(2Y_1+1)+1] + \tfrac{E(Y_1+1)^3+3Y_1^2+5Y_1+1}{Q_1}\}uv \\
&\quad + \tfrac{1}{Q_1(Y_1+1)}v^2 + \tfrac{1}{Q_1(Y_1+1)}u^3 + \tfrac{BY_1^2[(BY_1-E)(Y_1+1)-1]}{Q_1^2\omega_c^2}u^2v \\
&\quad + \tfrac{2BY_1(Y_1+1)[(BY_1-E)(Y_1+1)-1]}{Q_1^2\omega_c}uv^2 + \tfrac{B(Y_1+1)^2[(BY_1-E)(Y_1+1)-1]}{Q_1}v^3,
\end{aligned} \tag{3.22}$$

where

$$Q_1 = (BY_1 - E)(Y_1+1)^2 - 2Y_1 - 1.$$

The transversal condition can be obtained as

$$v_0 = -\frac{Y_1+1}{2}. \tag{3.23}$$

Now, applying the Maple program [32] for computing the normal forms of Hopf and generalized Hopf bifurcations, we obtain the following focus values:

$$\begin{aligned}
v_1 = &-\frac{BY_1}{8(Y_1+1)Q_1[B(Y_1+1)^2Q_1+Y_1}[B(Y_1-2)(Y_1+1)^4E - B^2(2Y_1^2+1)(Y_1+1)^4 \\
&+B(2Y_1^2-2Y_1-1)(Y_1+1)^2+Y_1], \\
v_2 = &\cdots, \\
v_3 = &\cdots.
\end{aligned} \tag{3.24}$$

Solving $v_1 = 0$ for E yields

$$E = \frac{B^2(2Y_1^2+1)(Y_1+1)^4 - B(2Y_1^2-2Y_1-1)(Y_1+1)^2 - Y_1}{B(Y_1-2)(Y_1+1)^4}. \tag{3.25}$$

Substituting the solution E into v_2 we have

$$v_2 = -\frac{B^4 Y_1 (Y_1-2)^2 (Y_1+1)^3 [2B(2Y_1-1)(Y_1+1)^3 - (Y_1^2-4Y_1-2)]}{[B^2(Y_1+1)^6 - B(Y_1+1)^3 - Y_1]^2 [B(Y_1+1)^3 + Y_1 - 1]}.$$

Similarly, solving $v_1 = 0$ for B we obtain

$$B = \frac{Y_1^2 - 4Y_1 - 2}{2(2Y_1-1)(Y_1+1)^3}. \tag{3.26}$$

With the solutions E and B, the 3rd-order focus values become

$$v_3 = -\frac{(Y_1+2)(Y_1^2-4Y_1-2)^6 (Y_1^2-Y_1-1)}{800 Y_1^3 (Y_1+1)^{13} (Y_1^2-26Y_1-6)^3}. \tag{3.27}$$

Four limit cycles may bifurcate from the Hopf critical point if $v_3 = 0$. It is seen from (3.26) that $Y_1^2 - 4Y_1 - 2 \neq 0$ due to $B \neq 0$. Thus, the only possibility for $v_3 = 0$ is the solution from the equation $Y_1^2 - Y_1 - 1 = 0$, which gives

$$Y_1 = \frac{1+\sqrt{5}}{2}.$$

However, this solution leads to

$$B = \frac{3\sqrt{5}-7}{4} = \frac{-1}{3\sqrt{5}+7} < 0,$$

implying that there do not exist solutions such that $v_3 = 0$ and so four limit cycles are not possible.

Next, consider the possibility of three limit cycles, which only needs $v_1 = v_2 = 0$. Substituting B in (3.26) into E in (3.33) we have

$$\begin{aligned} E &= -\frac{(Y_1+2)(6Y_1^4 - 4Y_1^3 + 3Y_1^2 + 6Y_1 + 2)}{2(Y_1^2-4Y_1-2)(2Y_1-1)(Y_1+1)^3} \\ &= -\frac{Y_1+2}{4(Y_1+1)^3}\left[(6Y_1+23) + \frac{213Y_1^2-42}{(Y_1^2-4Y_1-2)(2Y_1-1)}\right]. \end{aligned}$$

It is easy to see that $B > 0$ requires that

$$(Y_1^2-4Y_1-2)(2Y_1-1) > 0 \quad \Longrightarrow \quad Y_1 > \frac{1+\sqrt{5}}{2},$$

under which $213Y_1^2 - 42 > 0$, yielding $E < 0$. Thus, the bifurcation of three limit cycles is not possible.

Finally, the existence of two limit cycles which can bifurcate from the Hopf critical point only needs $v_1 = 0$ and $v_2 \neq 0$. There is an infinite number of sets of parameter values for two limit cycles. For example, taking $Y_1 = 1$ and $B = \frac{1}{10}$ gives $E = \frac{3}{40}$, under which

$$v_1 = 0, \quad v_2 = -\frac{11}{107648}.$$

Note that the existence condition, $B(Y_1+1)^2 = 4B = \frac{2}{5} < 1$, is satisfied. Another existence condition needs $D < Y_1(\frac{1}{(Y1+1)^2} - B) = \frac{3}{20}$. So we choose $D = \frac{1}{10}$ and then $C_{\rm H} = \frac{1}{20}$. With these parameter values, in addition, taking the perturbations:

$$E = \frac{3}{20} - \varepsilon, \quad C = \frac{1}{20} + \xi, \quad \text{with } \varepsilon = 10^{-3}, \ \xi = 10^{-6},$$

we have the following normal form up to 5th order,

$$\dot{\rho} = \rho\,(v_0\,\xi + v_1\rho^2 + v_2 r^4) = \rho\Big(-\frac{1}{10^6} + \frac{25}{1146816}\rho^2 - \frac{11}{107648}\rho^4\Big). \tag{3.28}$$

Letting $\dot{(\rho)} = 0$ yields two positive solutions:

$$\rho_1 = 0.258402, \quad \rho_2 = 0.382834,$$

indicating that two limit cycles exist, and the outer one is stable, since $v_2 < 0$ and the inner one is unstable, and both of them enclose the stable focus E_1.

The proof is complete. □

With the parameter values, as discussed in the proof, given by

$$A = \frac{86750387}{50000000}, \quad B = D = \frac{1}{10}, \quad C = \frac{50001}{1000000}, \quad E = \frac{37}{500},$$

we perform the simulation as shown in Figure 3.1.

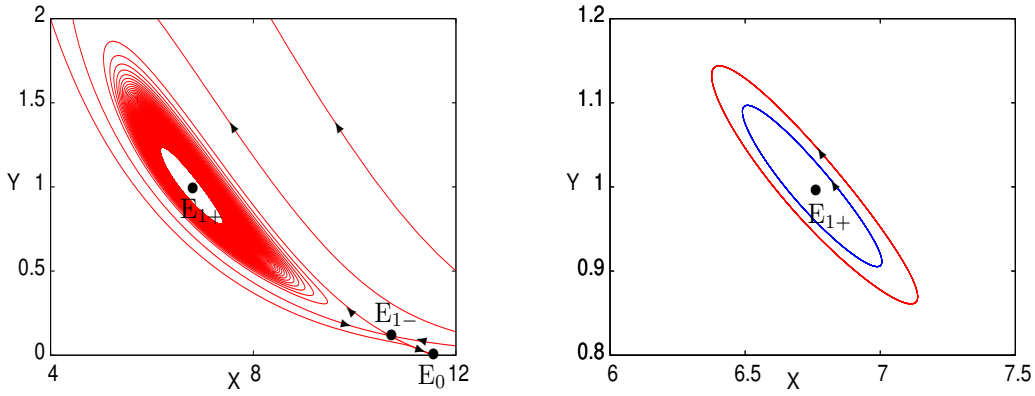

(a) (b)

Figure 3.1: Simulation of the model (3.5) with $A = \frac{86750387}{50000000}$, $B = D = \frac{1}{10}$, $E = \frac{37}{500}$, showing bifurcation of two limit cycles: (a) a global picture of the phase portrait; and (b) the zoomed region near the stable equilibrium E_{2+}, with the outer limit stable (in red color) and the inner one unstable (in blue color), both of them enclosing the stable equilibrium E_1.

3.4 B-T bifurcation of system (3.5)

In this section, we present an analysis on the B-T bifurcation of the model. We first determine the codimension of the B-T bifurcation, and then present the bifurcation results for codimension-2 and codimension-3 B-T bifurcations. In order to find the B-T bifurcation critical point from E_1, we use the solution A given in (3.13) and the critical point defined in item (v) of Theorem 3.2.3 to define

$$\begin{aligned} A &= \frac{B(C+D+E)Y_1^2 + [B(C+D+E+1)+(C+D)(D+E)]Y_1 + (C+D)(D+E+1)}{B(Y_1+1)} \triangleq \tilde{A}, \\ C &= \frac{Y_1}{(Y_1+1)^2} - D - BY_1 \triangleq \tilde{C}, \\ E &= \frac{Y_1(Y_1+1)^4B^2 - (2Y_1+1)(Y_1+1)^2B + Y_1}{B(Y_1+1)^4}, \end{aligned} \tag{3.29}$$

where $C > 0$ requires the condition (3.15), and $E > 0$ yields $B_- < B < B_+$, where

$$B_\pm = \frac{1}{2Y_1(1+Y_1)^2}\left[1 + 2Y_1 \pm \sqrt{1+4Y_1}\right]. \tag{3.30}$$

But it is easy to see that $B_+ > \frac{1}{(Y_1+1)^2}$. Hence, the existence conditions for the B-T bifurcation are

$$B < B_- \quad \text{and} \quad D < Y_1\Big(\frac{1}{(Y_1+1)^2} - B\Big). \tag{3.31}$$

3.4.1 Determining the codimension of B-T bifurcation

To find the codimension of the B-T bifurcation, we apply the SNF theory [33, 34, 36]. Define

$$B^* = \frac{1-Y_1}{(Y_1+1)^3}, \quad (Y_1 < 1), \quad Y_1^* = 0.5566930950. \tag{3.32}$$

Then, we have the following theorem.

Theorem 3.4.1. *For system* (3.5), B-T *bifurcation occurs from the equilibrium* E_1*:* $(\frac{1}{B}(D+E+\frac{1}{Y_1+1}), Y_1)$ *at the critical point:* $(A, C) = (\tilde{A}, \tilde{C})$*. Moreover, the* B-T *bifurcation is*

(i) *codimension* 2 *if* $Y_1 \in (0, Y_1^*]\bigcup[1, \infty)$*, or if* $Y_1 \in (Y_1^*, 1)$ *with* $B \neq B^*$*; or*

(ii) *codimension* 3 *if* $Y_1 \in (Y_1^*, 1)$ *with* $B = B^*$.

Proof. First, introduce the following affine transformation:

$$\begin{pmatrix} X \\ Y \end{pmatrix} = \begin{pmatrix} \frac{1}{B}\Big(D+E+\frac{1}{Y_1+1}\Big) \\ Y_1 \end{pmatrix} + \begin{bmatrix} \frac{-Y_1}{(Y_1+1)^2} & 1 \\ BY_1 & 0 \end{bmatrix} \begin{pmatrix} u \\ v \end{pmatrix} \tag{3.33}$$

into (3.5) we obtain the equations up to 5th order:

$$\begin{aligned}\frac{du}{dt} &= v - \tfrac{B}{(Y_1+1)^3}\,u\big[Y_1^2u - (Y_1+1)^3v\big] - \tfrac{B^2Y_1^2}{(Y_1+1)^4}\,u^3 + \tfrac{B^3Y_1^3}{(Y_1+1)^5}\,u^4 - \tfrac{B^4Y_1^4}{(Y_1+1)^6}\,u^5,\\ \frac{dv}{dt} &= -\tfrac{BY_1}{(Y_1+1)^5}\,u\{Y_1\big[Y_1 - B(Y_1+1)^3\big]u + (Y1+1)^3\big[B(Y_1+1)^2-1\big]v\}\\ &\quad -\tfrac{B^2Y_1^3}{(Y_1+1)^6}\,u^3 + \tfrac{B^3Y_1^4}{(Y_1+1)^7}\,u^4 - \tfrac{B^4Y_1^5}{(Y_1+1)^8}\,u^5.\end{aligned} \tag{3.34}$$

Then, applying the change of variables up to 5th-order:

$$\begin{aligned}u &= y_1 + \tfrac{B(2Y_1+1)}{4(1+Y_1)}\,y_1^2 - \tfrac{B(1+Y_1)[B(2Y_1-1)(Y_1+1)^3-2Y_1^2+5Y_1+1]}{12Y_1[B(Y_1+1)^3-Y_1]}\,y_1y_2\\ &\quad + \tfrac{B(2Y_1-1)(1+Y_1)^3(4B^2(Y_1+1)^6+B(6Y_1-17)(Y_1+1)^3-10Y_1^2+33Y_1+4)}{240Y_1^2[B(Y_1+1)^3-Y_1]^2}\,y_2^2 + \cdots\\ v &= y_2 + \tfrac{BY_1^2}{(Y_1+1)^3}\,y_1^2 - \tfrac{B(1+Y_1)[B(2Y_1-1)(Y_1+1)^3-2Y_1^2+5Y_1+1]}{12Y_1[B(Y_1+1)^3-Y_1]}\,y_2^2 + \cdots\end{aligned} \tag{3.35}$$

and the time scaling:

$$t = \left(1 + \frac{B}{2(Y_1+1)}\,y_1 + t_{30}\,y_1^3\right)\tau,$$

where t_{30} is a function in B and Y_1, into (3.34) yields the SNF up to 5th order:

$$\begin{aligned}\frac{dy_1}{d\tau} &= y_2,\\ \frac{dy_2}{d\tau} &= c_{20}\,y_1^2 + c_{11}\,y_1y_2 + c_{31}\,y_1^3y_2 + c_{41}\,y_1^4y_2,\end{aligned} \tag{3.36}$$

in which

$$\begin{aligned}c_{20} &= \frac{BY_1^2}{(Y_1+1)^5}[B(Y_1+1)^3 - Y_1],\\ c_{11} &= -\frac{BY_1}{(Y_1+1)^3}[B(Y_1+1)^3 + Y_1 - 1],\\ c_{31} &= \cdots, \quad c_{41} = \cdots.\end{aligned} \tag{3.37}$$

It is easy to show that $c_{20} < 0$ since

$$B(Y_1+1)^3 - Y_1 < B_-(Y_1+1)^3 - Y_1 = \frac{-2Y_1^2}{(Y_1+1)\sqrt{1+4Y_1} + 3Y_1 + 1} < 0.$$

Hence, codimension-3 B-T bifurcation can happen only if $c_{11} = 0$. First note that $c_{11} < 0$ for $Y_1 \geq 1$. When $Y_1 < 1$, it is easy to see that $c_{11} = 0$ has a unique solution $B = B^*$, and $c_{11} > 0$ for $B < B^*$ and $c_{11} < 0$ for $B > B^*$. Recall that the existence condition of the B-T bifurcation requires $B < B_-$, we compute $B_- - B^*$ to obtain

$$B_- - B^* = \frac{2(4Y_1^3 + Y_1^2 - 1)}{(Y_1+1)^3[4Y_1^2 + Y_1 + 1 + (Y_1+1)\sqrt{1+4Y_1}]},$$

implying that there exists a unique solution

$$Y_1 = Y_1^* = 0.5566930950, \tag{3.38}$$

at which $B_- = B^*$, and $B_- < B^*$ if $0 < Y_1 \leq Y_1^*$, and $B_- > B^*$ if $Y_1^* < Y_1 < 1$ for which B can reaches B^*. At $B = B^*$, we have

$$c_{31} = \frac{Y_1^3(1-Y_1)^3}{(Y_1+1)^{14}} > 0, \quad c_{41} = \frac{Y_1^3(1-2Y_1)(1-Y_1)^4}{4(1+Y_1)^{18}} < 0.$$

Therefore, the B-T bifurcation cannot have codimension higher than three.

The proof is complete. □

In the following two sections, we present the B-T bifurcation results using the parametric simplest normal form (PSNF) [8, 9, 7, 36], first for codimension two and then for codimension three.

3.4.2 Codimension-2 B-T bifurcation

Based on the PSNF theory, we can prove the following bifurcation results for the codimension-2 B-T bifurcation.

Theorem 3.4.2. *For the epidemic model (3.5), codimension-2 B-T bifurcation occurs from the equilibrium* E_1*:* $(X, Y) = (\frac{1}{B}(D + E + \frac{1}{Y_1+1}), Y_1)$ *when* $A = \tilde{A}$ *and* $C = \tilde{C}$ *if* $Y_1 \in (0, Y_1^*] \bigcup [1, \infty)$*, or if* $Y_1 \in (Y_1^*, 1)$ *with* $B \neq B^*$*. Further, three local bifurcations with the representations of the bifurcation curves are given as follows.*

(i) *Saddle-node bifurcation occurs from the bifurcation curve:*

$$\mathrm{SN} = \left\{ (\beta_1, \beta_2) \mid \beta_1 = 0, \begin{cases} \beta_2 < 0 \ (C_{11} < 0) \\ \beta_2 > 0 \ (C_{11} > 0) \end{cases} \right\}.$$

(ii) *Hopf bifurcation occurs from the bifurcation curve:*

$$\mathrm{H} = \left\{ (\beta_1, \beta_2) \,\middle|\, \beta_1 = -\frac{1}{C_{11}^2}\beta_2^2, \begin{cases} \beta_2 < 0 \ (C_{11} < 0), \ \text{supercritical} \\ \beta_2 > 0 \ (C_{11} > 0), \ \text{subcritical} \end{cases} \right\}.$$

(iii) *Homoclinic loop bifurcation occurs from the bifurcation curve:*

$$\mathrm{HL} = \left\{ (\beta_1, \beta_2) \,\middle|\, \beta_1 = -\frac{49}{25}\frac{1}{C_{11}^2}\beta_2^2, \begin{cases} \beta_2 < 0 \ (C_{11} < 0), \ \text{stable} \\ \beta_2 > 0 \ (C_{11} > 0), \ \text{unstable} \end{cases} \right\}.$$

Proof. Let

$$A = \tilde{A} + \mu_1, \quad C = \tilde{C} + \mu_2, \tag{3.39}$$

which, together with the transformation (3.35), is substituted into (3.5) to yield the following system up to second-order terms:

$$\begin{aligned} \frac{du}{dt} &= v - \tfrac{B}{(Y_1+1)^3}\, u[Y_1^2 u - (Y_1+1)^3 v], \\ \frac{dv}{d\tau} &= \mu_1 + \tfrac{1}{(Y_1+1)^5}\{BY_1^2[B(Y_1+1)^3 - Y_1]\, u^2 - (Y_1+1)^5\mu_2 v \\ &\qquad -Y_1(Y1+1)^3[B(Y_1+1)^2 - 1]\,(Bv+\mu_2)u\}. \end{aligned} \tag{3.40}$$

Now, to obtain the PSNF of the system, we further apply the change of variables:

$$\begin{aligned} u &= \tfrac{(Y_1+1)^5}{BY_1^2(B[(Y_1+1)^3-Y_1]}\, y_1 - \tfrac{[B(Y_1+1)^2-1]}{BY_1(Y_1+1)^3[B^2(Y_1+1)^5+2BY_1(Y_1+1)^2-3Y_1+1]}\,\beta_2 \\ &\quad -\tfrac{(Y_1+1)^8[B(Y_1+1)^2-1]}{BY_1^3[B(Y_1+1)^3-Y_1][B^2(Y_1+1)^5+2BY_1(Y_1+1)^2-3Y_1+1]}\beta_1\, y_1 + \tfrac{(Y_1+1)^{10}}{2BY_1^4[B(Y_1+1)^3-Y_1]^2}\, y_1^2, \\ v &= \tfrac{(Y_1+1)^5}{BY_1^2[B(Y_1+1)^3-Y_1]}\, y_2 + \tfrac{[B(Y_1+1)^2-1]^2(Y_1+1)^3}{B[B^2(Y_1+1)^5+2BY_1(Y_1+1)^2-3Y_1+1]^2}\,\beta_2^2 \\ &\quad -\tfrac{2(Y_1+1)^5[B(Y_1+1)^2-1]}{BY_1[B(Y_1+1)^3-Y1][B^2(Y_1+1)^5+2BY_1(Y_1+1)^2-3Y_1+1]}\,\beta_2\, y_1 + \tfrac{(Y_1+1)^7}{BY_1^2[B(Y_1+1)^3-Y_1]^2}\, y_1^2, \end{aligned} \tag{3.41}$$

and the parametrization:

$$\begin{aligned} \mu_1 &= \tfrac{(Y_1+1)^5}{BY_1^2(B(Y_1+1)^3-Y_1]}\beta_1 + \tfrac{(Y_1+1)[B(Y_1+1)^3-Y_1][B(Y_1+1)^2-1]^2}{B[B^2(Y_1+1)^5+2BY_1(Y_1+1)^2-3Y_1+1]^2}\,\beta_2^2, \\ \mu_2 &= -\tfrac{2[B(Y_1+1)^3-Y_1]}{B^2(Y_1+1)^5+2BY_1(Y_1+1)^2-3Y_1+1}\,\beta_2, \end{aligned} \tag{3.42}$$

into (3.40) to obtain the PSNF below:

$$\begin{aligned} \frac{dy_1}{d\tau} &= y_2, && \text{for } Y_1 \in (0, Y_1^*]\bigcup[1,\infty), \text{ or} \\ \frac{dy_2}{d\tau} &= \beta_1 + \beta_2 y_2 + y_1^2 + C_{11}\, y_1 y_2, && \text{for } Y_1 \in (Y_1^*, 1) \text{ with } B \neq B^*, \end{aligned} \tag{3.43}$$

where

$$C_{11} = \frac{(Y_1+1)^5(B-B^*)}{Y_1[Y_1 - B(Y_1+1)^3]}. \tag{3.44}$$

It should be pointed out that the coefficient C_{11} is not normalized into ± 1 in order to show the direct effect of the original system parameters on the dynamics of the system. It can be shown that since $Y_1 - B(Y_1+1)^3 > 0$ for $B < B_-$, $C_{11} > 0$ if $0 < Y_1 \le Y_1^*$ or if $Y_1^* < Y_1 < 1$ with $B < B^*$; and $C_{11} < 0$ if $Y_1 \ge 1$ or if $Y_1^* < Y_1 < 1$ with $B^* < B < B_-$. Also, note that there is a negative multiplier $\frac{(Y_1+1)^5}{BY_1^2[B(Y_1+1)^3-Y_1]}$ in the transformation from (u, v) to (y_1, y_2).

Since the normal form (3.43) is in the standard form (e.g., see [10, 36]), we can directly obtain the bifurcation results in Theorem 3.4.2.

This finishes the proof. □

The above formulas for bifurcation curves can be expressed in terms of the original perturbation parameters μ_1 and μ_2 by using (3.42). The bifurcation diagram is depicted in Figure 3.2.

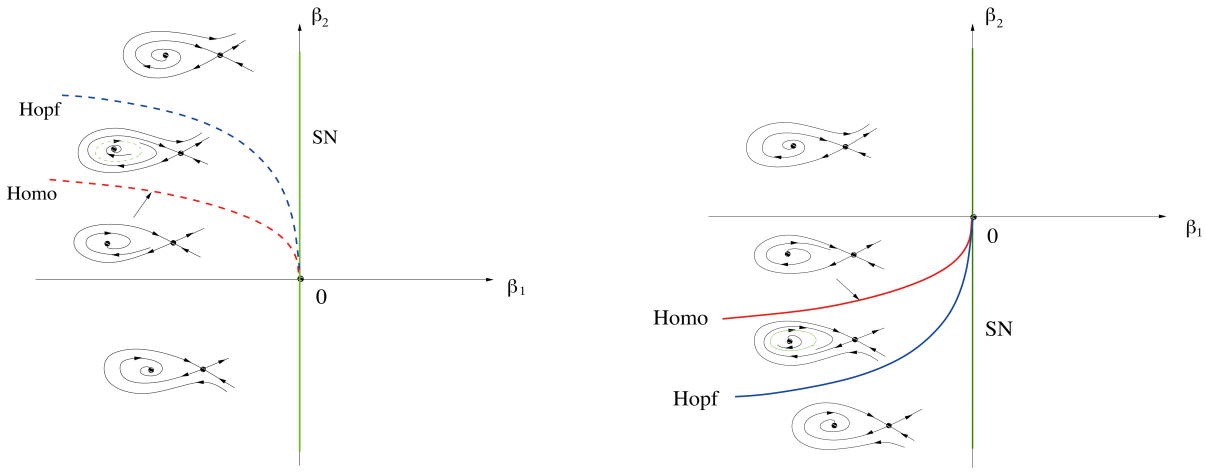

Figure 3.2: Bifurcation diagrams for the codimension-2 B-T bifurcation of the epidemic model (3.5) based on the normal form (3.43): (a) for $C_{11} < 0$; and (b) for $C_{11} > 0$.

3.4.3 Codimension-3 B-T bifurcation

In this section, we consider codimension-3 B-T bifurcation for the model (3.5), and again apply the parametric simplest normal form (PSNF) [34, 7, 36] associated with the one-step transformation approach. One needs to choose proper nonlinear transformations in order to determine the right basis for the PSNF, and therefore to overcome the difficulty in the application of this approach. We have the following theorem.

Theorem 3.4.3. *For the model (3.5), codimension-3 B-T bifurcation occurs from the equilibrium* E_1*:* $(X, Y) = (\frac{1}{B}(D + E + \frac{1}{Y_1+1}), Y_1)$ *when* $A = \tilde{A}$*,* $C = \tilde{C}$ *and* $B = B^*$*. Moreover, six local bifurcations with the representations of the bifurcation surfaces/curves are obtained, as given below.*

(1) *Saddle-node bifurcation occurs from the critical surface:*

$$\mathrm{SN} = \{(\beta_1, \beta_2, \beta_3) \mid \beta_1 = 0\}.$$

(2) *Hopf bifurcation occurs from the critical surface:*

$$\mathrm{H} = \{(\beta_1, \beta_2, \beta_3) \mid \beta_1 < 0,\ \beta_2 = (\beta_3 - \beta_1)\sqrt{-\beta_1}\}.$$

(3) *Homoclinic loop bifurcation occurs from the critical surface:*

$$\mathrm{HL} = \left\{(\beta_1, \beta_2, \beta_3) \mid \beta_1 < 0,\ \beta_2 = (\tfrac{5}{7}\beta_3 - \tfrac{103}{77}\beta_1)\sqrt{-\beta_1}\right\}.$$

(4) *Generalized Hopf bifurcation occurs from the critical curve:*

$$\mathrm{GH} = \left\{(\beta_1,\beta_2,\beta_3) \mid \beta_1 < 0,\ \beta_2 = -4\beta_1\sqrt{-\beta_1},\ \beta_3 = -3\beta_1\right\}.$$

(5) *Degenerate homoclinic bifurcation occurs from the critical curve:*

$$\mathrm{DHL} = \left\{(\beta_1,\beta_2,\beta_3)\,\middle|\,\beta_1 < 0,\ \beta_2 = -\tfrac{4}{11}\beta_1\sqrt{-\beta_1},\ \beta_3 = \tfrac{15}{11}\beta_1\right\}.$$

(6) *Double limit cycle bifurcation occurs from a critical surface, which is tangent to the Hopf bifurcation surface* H *on the critical curve* GH*, and tangent to the homoclinic bifurcation surface* HL *on the critical curve* DHL*.*

Proof. First, introducing the transformation,

$$\begin{aligned} &X = \frac{1}{B}\Big(D + E + \frac{1}{Y_1+1}\Big) + u, \quad Y = Y_1 + v,\\ &A = \tilde{A} + \mu_1, \quad C = \tilde{C} + \mu_2, \quad B = B^* + \mu_3, \end{aligned} \qquad \text{for } Y_1 \in (Y_1^*, 1), \tag{3.45}$$

into (3.5) yields the following system up to 4th-order terms:

$$\begin{aligned} \frac{du}{dt} &= v + \frac{(Y_1-1)}{(Y_1+1)^6}u[Y_1^2u - (Y_1+1)^3v]\\ &\quad -\frac{1}{(Y_1+1)^{10}}u[Y_1^2(Y_1-1)^2u^2 + Y_1^2(Y_1+1)^7\mu_3u - (Y_1+1)^{10}\mu_3v]\\ &\quad +\frac{Y_1^2(Y_1-1)}{(Y_1+1)^{14}}u^3[2(Y_1+1)^7\mu_3 - Y_1(Y_1-1)^2u],\\ \frac{dv}{dt} &= \frac{1}{(Y_1+1)^8}[Y_1^2(2Y_1-1)(Y_1-1)u^2 - 2Y_1^2(Y_1-1)(Y_1+1)^2uv\\ &\qquad +2Y_1^2(Y_1+1)^5\mu_2u - (Y_1+1)^8\mu_2v]\\ &\quad -\frac{Y_1}{(Y_1+1)^{12}}u[(Y_1+1)^{12}\mu_2\mu_3 + Y_1^2(Y_1-1)^2u^2\\ &\qquad +Y_1(3Y_1-2)(Y_1+1)^7\mu_3u - (3Y_1-1)(Y_1+1)^9\mu_3v]\\ &\quad -\frac{Y_1}{(Y_1+1)^{16}}u[Y_1^3(Y_1-1)^3u^3 - 2Y_1^2(Y_1-1)(Y_1+1)^7\mu_3u^2\\ &\qquad -Y_1(Y_1+1)^{14}\mu_3^2u + (Y_1+1)^{16}\mu_3^2v]. \end{aligned} \tag{3.46}$$

Next, we apply the change of variables:

$$
\begin{aligned}
u =& \tfrac{(Y_1+1)^4}{Y_1(Y_1-1)}[Y_1(2Y_1-1)]^{\frac{1}{5}}\, y_1 + \tfrac{(Y_1+1)^3(4Y_1^3-10Y_1^2-Y_1+1)}{4Y_1^2(2Y_1-1)(Y_1-1)}[Y_1(2Y_1-1)]^{\frac{2}{5}}\beta_1 \\
&- \tfrac{(Y_1+1)^3}{(Y_1-1)(2Y_1-1)}[Y_1(2Y_1-1)]^{\frac{3}{5}}\beta_2 - \tfrac{(Y_1+1)^4(2Y_1+1)}{4Y_1^2(Y_1-1)}[Y_1(2Y_1-1)]^{\frac{2}{5}}\, y_1^2 \\
&- \tfrac{(Y_1+1)^4(Y_1-2)}{3Y_1(Y_1-1)}\, y_1y_2 + \tfrac{(Y_1+1)^4(4Y_1^2-16Y_1+3)}{80Y_1^3(Y_1-1)}[Y_1(2Y_1-1)]^{\frac{3}{5}}\, y_2^2 \\
&- \{\tfrac{(Y1+1)^3(592Y_1^6-2960Y_1^5+4888Y_1^4-2776Y_1^3+381Y_1^2+56Y_1-21)}{80Y_1^3(2Y_1-1)^2(Y_1-1)^2}[Y_1(2Y_1-1)]^{\frac{3}{5}}\beta_1 \\
&\quad - \tfrac{(Y_1+1)^3(48Y_1^4-88Y_1^3+41Y_1^2-11Y_1+4)}{6Y_1^2(2Y_1-1)^2(Y_1-1)^2}[Y_1(2Y_1-1)]^{\frac{4}{5}}\beta_2 \\
&\quad + \tfrac{(Y_1+1)^4(7Y_1-4)}{3Y_1(Y_1-1)^2(2Y_1-1)}[Y_1(2Y_1-1)]^{\frac{3}{5}}\beta_3\}\, y_1 \\
&+ \{\tfrac{(Y_1+1)^3\, m_1}{180Y_1^2(2Y_1-1)^2(Y_1-1)^2(44Y_1^2+44Y_1+23)}[Y_1(2Y_1-1)]^{\frac{1}{5}}\beta_1 \\
&\quad - \tfrac{(Y_1+1)^3\, m_2}{180Y_1^2(44Y_1^2+44Y_1+23)(2Y_1-1)^2(Y_1-1)^2}[Y_1(2Y_1-1)]^{\frac{2}{5}}\beta_2 \\
&\quad \tfrac{(Y_1+1)^4(1352Y_1^4-3276Y_1^3-398Y_1^2+1365Y_1+117)}{18Y_l(44Y_1^2+44Y_1+23)(2Y_1-1)(Y_1-1)^2}[Y_1(2Y_1-1)]^{\frac{1}{5}}\beta_3\}\, y_2 \\
&+ \sum_{i+j+k+l+s=3} a_{ijkls}\, y_1^i y_2^j \beta_1^k \beta_2^l \beta_3^s, \\
v =& -\tfrac{(2Y_1-1)(Y_1+1)^2}{Y_1(Y_1-1)(2Y_1-1)}[Y_1(2Y_1-1)]^{\frac{4}{5}}\, y_2 - \tfrac{(Y_1+1)^2}{Y_1-1}[Y_1(2Y_1-1)]^{\frac{2}{5}}\, y_1^2 \\
&+ \tfrac{(Y_1-2)(Y_1+1)^2}{3Y_1(Y_1-1)}[Y_1(2Y_1-1)]^{\frac{3}{5}}\, y_2^2 \\
&- \{\tfrac{(Y_1+1)(8Y_1^3-24Y_1^2+3Y_1-1)}{6Y_1(Y_1-1)(2Y_1-1)}[Y_1(2Y_1-1)]^{\frac{3}{5}}\beta_1 - \tfrac{2Y_1(Y_1+1)}{(Y_1-1)(2Y_1-1)}[Y_1(2Y_1-1)]^{\frac{1}{5}}\beta_2\}\, y_1 \\
&+ \{\tfrac{(Y_1+1)(80Y_1^6-464Y_1^5+952Y_1^4-684Y_1^3+143Y_1^2+12Y_1-7)}{16Y_1^2(Y_1-1)^2(2Y_1-1)}[Y_1(2Y_1-1)]^{\frac{1}{5}}\beta_1 \\
&\quad - \tfrac{(Y_1+1)(6Y_1^3-8Y_1^2+Y_1-1)}{2Y_1(Y_1-1)^2}[Y_1(2Y_1-1)]^{\frac{2}{5}}\beta_2 + \tfrac{(2Y_1-1)(Y_1+1)^2}{(Y_1-1)^2}[Y_1(2Y_1-1)]^{\frac{1}{5}}\beta_3\}\, y_2 \\
&+ \sum_{i+j+k+l+s=3} b_{ijkls}\, y_1^i y_2^j \beta_1^k \beta_2^l \beta_3^s,
\end{aligned}
\tag{3.47}
$$

the parametrization:

$$
\begin{aligned}
\mu_1 =& \tfrac{2Y_1-1}{Y_1-1}[Y_1(2Y_1-1)]^{\frac{2}{5}}\beta_1 \\
&- \tfrac{(16Y_1^7-76Y_1^6+91Y_1^5+83Y_1^4-137Y_1^3+39Y_1^2+2Y_1-2)}{4Y_1^2(Y_1^2-1)^2(2Y_1-1)}[Y_1(2Y_1-1)]^{\frac{4}{5}}\beta_1^2 \\
&+ \tfrac{Y_1^3}{(Y_1-1)(Y_1+1)^2}[Y_1(2Y_1-1)]^{\frac{1}{5}}\beta_2^2 + \tfrac{(24Y_1^5+22Y_1^4-67Y_1^3+6Y_1^2+Y_1+2)}{6(Y_1^2-1)^2}\beta_1\beta_2 \\
&- \tfrac{(5Y_1-2)}{3(Y_1-1)^2}[Y_1(2Y_1-1)]^{\frac{4}{5}}\beta_1\beta_3 + \sum_{i+j+k=3}^{4} \alpha_{1ijk}\, \beta_1^i \beta_2^j \beta_3^k,
\end{aligned}
\tag{3.48}
$$

$$
\begin{aligned}
\mu_2 =& -\tfrac{Y_1-2}{(Y_1+1)^2}[Y_1(2Y_1-1)]^{\frac{1}{5}}\beta_1 + \tfrac{1}{(Y_1+1)^2}[Y_1(2Y_1-1)]^{\frac{3}{5}}\beta_2 \\
&- \tfrac{16Y_1^6-103Y_1^5+88Y_1^4+218Y_1^3-100Y_1^2+Y1+4}{4Y_1^2(2Y_1-1)^2(Y_1+1)^4}[Y_1(2Y_1-1)]^{\frac{4}{5}}\beta_1^2 \\
&- \tfrac{6Y_1^4-22Y_1^3-6Y_1^2+3Y_1-1}{6(2Y_1-1)(Y_1+1)^4}[Y_1(2Y_1-1)]^{\frac{1}{5}}\beta_2^2 - \tfrac{92Y_1^4-70Y_1^3+39Y_1^2-10Y_1+5}{12(2Y_1-1)(Y_1+1)^4}\beta_1\beta_2 \\
&- \tfrac{8Y_1^3-11Y_1^2+2Y_1+3}{6Y_1(2Y_1-1)(Y_1+1)^3}[Y_1(2Y_1-1)]^{\frac{4}{5}}\beta_1\beta_3 + \tfrac{Y_1(4Y_1+1)}{3(Y_1+1)^3}\beta_2\beta_3 \\
&+ \sum_{i+j+k=3}^{4}\alpha_{2ijk}\,\beta_1^i\beta_2^j\beta_3^k, \\
\mu_3 =& -\tfrac{2Y_1(Y_1-2)^2}{(Y_1+1)^4(2Y_1-1)}[Y_1(2Y_1-1)]^{\frac{2}{5}}\beta_1 + \tfrac{(4Y_1^3-6Y_1^2+Y_1-1)}{2Y_1(Y_1+1)^4(2Y_1-1)}[Y_1(2Y_1-1)]^{\frac{3}{5}}\beta_2 \\
&- \tfrac{1}{(Y_1+1)^3}[Y_1(2Y_1-1)]^{\frac{2}{5}}\beta_3 - \tfrac{m_3}{720Y_1^3(Y_1+1)^6(2Y_1-1)^3}[Y_1(2Y_1-1)]^{\frac{4}{5}}\beta_1^2 \\
&- \tfrac{72Y_1^7-208Y_1^6+72Y_1^5+32Y_1^4-63Y_1^3+27Y_1^2-13Y_1+1}{12Y_1(Y_1+1)^6(2Y_1-1)^2}[Y_1(2Y_1-1)]^{\frac{1}{5}}\beta_2^2 \\
&- \tfrac{2}{3(Y_1+1)^3(2Y_1-1)}[Y_1(2Y_1-1)]^{\frac{4}{5}}\beta_3^2 + \tfrac{m_4}{1200Y_1^2(Y_1+1)^6(2Y_1-1)^2}\beta_1\beta_2 \\
&- \tfrac{752Y_1^6-2616Y_1^5+1992Y_1^4+1844Y_1^3-1371Y_1^2+6Y_1+21}{120Y_1^2(2Y_1-1)^2(Y_1+1)^5}[Y_1(2Y_1-1)]^{\frac{4}{5}}\beta_1\beta_3 \\
&+ \tfrac{40Y_1^4-40Y_1^3-23Y_1^2+18Y_1-3}{6(2Y_1-1)(Y_1+1)^5}\beta_2\beta_3 + \sum_{i+j+k=3}^{4}\alpha_{3ijk}\,\beta_1^i\beta_2^j\beta_3^k,
\end{aligned}
\tag{3.49}
$$

and the time rescaling:

$$
\begin{aligned}
dt = \Big\{ &- \tfrac{1}{(Y_1+1)^2}[Y_1(2Y_1-1)]^{\frac{3}{5}} + \tfrac{1}{2Y_1(Y_1+1)^2}[Y_1(2Y_1-1)]^{\frac{4}{5}}\,y_1 \\
&- \tfrac{16Y_1^2-7Y_1+1}{6(2Y_1-1)(Y_1+1)^3}[Y_1(2Y_1-1)]^{\frac{1}{5}}\beta_2 - \tfrac{Y_1}{3(Y_1+1)^2}\beta_3\Big\}\,d\tau,
\end{aligned}
\tag{3.50}
$$

into (3.46) yields the following PSNF up to 4th-order terms:

$$
\begin{aligned}
\frac{dy_1}{d\tau} &= y_2, \\
\frac{dy_2}{d\tau} &= \beta_1 + \beta_2\,y_2 + \beta_3\,y_1y_2 + y_1^2 + y_1^3y_2 + O(|(y_1,y_2,\beta)|^5).
\end{aligned}
\tag{3.51}
$$

Here,

$$
\begin{aligned}
m_1 =\ & 19840Y_1^8 - 294032Y_1^7 + 968504Y_1^6 - 824808Y_1^5 - 712658Y_1^4 \\
&+ 1134587Y_1^3 - 307564Y_1^2 - 11187Y_1 + 10518, \\
m_2 =\ & 51200Y_1^7 - 135952Y_1^6 + 183440Y_1^5 - 466288Y_1^4 \\
&+ 523256Y_1^3 - 120031Y_1^2 - 38016Y_1 + 10791, \\
m_3 =\ & 24640Y_1^10 + 26144Y_1^9 - 62528Y_1^8 - 310684Y_1^7 + 47194Y_1^6 \\
&+ 520343Y_1^5 - 18353Y_1^4 - 295435Y_1^3 + 80617Y_1^2 + 10764Y_1 - 3798, \\
m_4 =\ & 10560Y_1^9 - 66112Y_1^8 - 26000Y_1^7 + 179432Y_1^6 + 368792Y_1^5 \\
&- 111830Y_1^4 - 170161Y_1^3 + 64113Y_1^2 + 8085Y_1 - 3927,
\end{aligned}
$$

and a_{ijkls}'s, b_{ijkls}'s and α_{mijk}'s are coefficients given in terms of k, and $\beta = (\beta_1, \beta_2, \beta_3)$.

It is easy to verify that

$$\det\left[\frac{\partial(\mu_1,\mu_2,\mu_3)}{\partial(\beta_1,\beta_2,\beta_3)}\right]_{\beta=0} = \frac{Y_1(2Y_1-1)^2}{(Y_1+1)^5(1-Y_1)}[Y_1(2Y_1-1)]^{\frac{2}{5}} > 0, \quad \text{for } Y_1 \in (Y_1^*, 1), \tag{3.52}$$

which shows that near the critical point $\mu = 0$, system (3.5) has the same bifurcation set with respect to μ as system (3.51) has with respect to β, up to a homeomorphism in the parameter space.

Now, following the method described in [6], and the computations in [36] we apply the method of normal forms and Abelian integral (or the Melnikov function method) to derive the bifurcations for the codimension-3 B-T bifurcation. In the following, we outline the proof.

The system (3.46) has two equilibrium solutions $\mathrm{E}_\pm$:

$$\mathrm{E}_\pm = (y_{1\pm}, 0), \quad \text{where} \quad y_{1\pm} = \pm\sqrt{-\beta_1} \quad \text{for} \quad \beta_1 < 0. \tag{3.53}$$

The stability of the equilibria $\mathrm{E}_\pm$ is determined from the Jacobian of (3.46), which is given by

$$J(y_1, y_2) = \begin{bmatrix} 0 & 1 \\ 2y_1 + 3y_1^2 y_2 + \beta_3 y_2 & \beta_2 + \beta_3 y_1 + y_1^3 \end{bmatrix}. \tag{3.54}$$

It is easy to see that the determinant of the J evaluated at $\mathrm{E}_\pm$ equals $\det(J(\mathrm{E}_\pm) = \mp 2y_{1\pm}$, implying that E_+ is a saddle. The saddle-node bifurcation arises from the critical surface determined from $y_{1\pm} = 0$, as

$$\mathrm{SN} = \{(\beta_1, \beta_2, \beta_3) \mid \beta_1 = 0\}, \tag{3.55}$$

excluding the origin in the parameter space. Since $\det(J(\mathrm{E}_-) = 2y_{1-} > 0$, the stability of E_- is determined by the trace:

$$\mathrm{Tr}(J(\mathrm{E}_-)) = \beta_2 - (\beta_3 - \beta_1)\sqrt{-\beta_1}, \quad (\beta_1 < 0).$$

E_- is asymptotically stable (either a focus or node) if $\mathrm{Tr}(J(\mathrm{E}_-)) < 0$ and unstable if $\mathrm{Tr}(J(\mathrm{E}_-)) > 0$. Hopf bifurcation arising from E_- occurs on the critical surface, determined by $\mathrm{Tr}(J(\mathrm{E}_-)) = 0$ as

$$\beta_2 = (\beta_3 - \beta_1)\sqrt{-\beta_1}, \quad (\beta_1 < 0). \tag{3.56}$$

Further, Hopf bifurcation theory can be applied to obtain the focus values by using the Maple program in [32] as follows:

$$v_1 = \frac{\beta_3 + 3\beta_1}{16\sqrt{-\beta_1}}$$
$$v_2 = \frac{5(\beta_3 - 3\beta_1)[2\sqrt{-\beta_1} - \beta_1(\beta_3 + 3\beta_1)(\beta_3 - 3\beta_1)]}{1152\beta_1^2}.$$

Hence, generalized Hopf bifurcation occurs from the curve which is the intersection of the Hopf bifurcation surface H and the critical surface, defined by $v_1 = 0$:

$$\beta_3 + 3\beta_1 = 0, \quad (\beta_1 < 0),$$

as

$$\beta_2 = -4\beta_1\sqrt{-\beta_1}, \quad \beta_3 = -3\beta_1, \quad (\beta_1 < 0), \tag{3.57}$$

from which two limit cycles can bifurcate. Moreover, since

$$v_2|_{v_1=0} = \frac{5}{96\sqrt{-\beta_1}} > 0,$$

the outer limit cycle is unstable, and the inner one stable, and both them enclose the unstable focus E_-.

Next, in order to find the homoclinic and degenerate homoclinic bifurcations, we apply the Melnikov function method [13]. To achieve this, introducing the following scaling:

$$y_1 = \varepsilon^{\frac{2}{5}} z_1, \;\; y_2 = \varepsilon^{\frac{3}{5}} z_2, \;\; \beta_1 = \varepsilon^{\frac{4}{5}}\gamma_1, \;\; \beta_2 = \varepsilon^{\frac{6}{5}}\gamma_2, \;\; \beta_3 = \varepsilon^{\frac{4}{5}}\gamma_3, \;\; \tau_1 = \varepsilon^{\frac{1}{5}}\tau, \;\; (0 < \varepsilon \ll 1), \tag{3.58}$$

together with the transformation,

$$z_1 = \bar{\gamma}_1 + w_1, \quad z_2 = \sqrt{2\bar{\gamma}_1}\, w_2, \quad \tau_2 = \sqrt{2\bar{\gamma}_1}\,\tau_1, \quad \gamma_1 = -\bar{\gamma}_1^2, \;\; (\bar{\gamma}_1 > 0), \tag{3.59}$$

into (3.46) we obtain

$$\begin{aligned} \frac{dw_1}{d\tau_2} &= w_2, \\ \frac{dw_2}{d\tau_2} &= w_1 + \frac{1}{2\bar{\gamma}_1} w_1^2 + \varepsilon\, q(w_1, w_2, \bar{\gamma}), \end{aligned} \tag{3.60}$$

where

$$q(w_1, w_2, \bar{\gamma}) = \frac{1}{\sqrt{2\bar{\gamma}_1}}\left[(\gamma_2 + \bar{\gamma}_1\gamma_3 + \bar{\gamma}_1^3)w_2 + (\gamma_3 + 3\bar{\gamma}_1^2)w_1 w_2 + 3\bar{\gamma}_1 w_1^2 w_2 + w_1^3 w_2\right], \tag{3.61}$$

with $\bar{\gamma} = (\bar{\gamma}_1, \gamma_2, \gamma_3)$.

When $\varepsilon = 0$, the system (3.60) is a Hamiltonian system with equilibrium points:

$$\widetilde{\mathrm{E}}_- = (-2\bar{\gamma}_1, 0) \quad \text{and} \quad \widetilde{\mathrm{E}}_0 = (0, 0). \tag{3.62}$$

$\widetilde{\mathrm{E}}_-$ is a center and $\widetilde{\mathrm{E}}_0$ is a saddle, and they correspond to the $\mathrm{E}_\pm$ defined in (3.46). The Hamiltonian of (3.60) can be written as

$$H(w_1, w_2) = \frac{1}{2}(w_2^2 - w_1^2) - \frac{1}{6\bar{\gamma}_1} w_1^3, \tag{3.63}$$

and the homoclinic orbit connecting E_0 is described by

$$\Gamma_0: \quad H(w_1, w_2) = \frac{1}{2}(w_2^2 - w_1^2) - \frac{1}{6\bar{\gamma}_1} w_1^3, \quad \text{with } H(0,0) = 0. \tag{3.64}$$

Note that $H(-2\bar{\gamma}_1, 0) = -\frac{2}{3}\bar{\gamma}_1^2$. Thus, any closed orbits of the Hamiltonian system $(3.60)|_{\varepsilon=0}$ within the homoclinic loop Γ_0 can be expressed by

$$\Gamma_{\mathrm{h}}: \quad H(w_1, w_2, h) = \frac{1}{2}(w_2^2 - w_1^2) - \frac{1}{6\bar{\gamma}_1} w_1^3 - h = 0, \quad h \in \Big(-\frac{2}{3}\bar{\gamma}_1^2, 0\Big). \tag{3.65}$$

Now, the (first-order) Melnikov function (or Abelian integral) for the perturbed system (3.60) is given by [13]

$$\begin{aligned} M(h,\gamma) &= \oint_{\Gamma_{\mathrm{h}}} q(w_1, w_2, \gamma)\, dw_1 - p(w_1, w_2, \gamma)\, dw_2 \,|_{\varepsilon=0} \qquad (p = 0) \\ &= \oint_{\Gamma_{\mathrm{h}}} q(w_1, w_2, \gamma)\,|_{\varepsilon=0}\ dw_1 = \oint_{\Gamma_{\mathrm{h}}} H_{w_2} q(w_1, w_2, \gamma)\,|_{\varepsilon=0}\ dt \\ &= \frac{1}{\sqrt{2\bar{\gamma}_1}} \oint_{\Gamma_{\mathrm{h}}} w_2^2 \left[\gamma_2 + \bar{\gamma}_1\gamma_3 + \bar{\gamma}_1^3 + (\gamma_3 + 3\bar{\gamma}_1^2) w_1 + 3\bar{\gamma}_1 w_1^2 + w_1^3\right] dt \\ &= M(h,\gamma) = C_0(\gamma) + C_1(\gamma)\, h \ln|h| + C_2(\gamma)\, h + C_3(h)\, h^2 \ln|h| + \cdots, \end{aligned} \tag{3.66}$$

for $0 < -h \ll 1$, where

$$\begin{aligned} C_0(\gamma) &= \frac{1}{\sqrt{2\bar{\gamma}_1}} \oint_{\Gamma_0} w_2^2 [\gamma_2 + \bar{\gamma}_1\gamma_3 + \bar{\gamma}_1^3 + (\gamma_3 + 3\bar{\gamma}_1^2) w_1 + 3\bar{\gamma}_1 w_1^2 + w_1^3]\, dt, \\ C_1(\gamma) &= a_{10} + b_{01}, \end{aligned} \tag{3.67}$$

in which a_{10} and b_{01} are derived from the coefficients in the functions $p(w_1, w_2, \gamma)$ and $q(w_1, w_2, \gamma)$ as

$$a_{10} = 0, \quad b_{01} = \frac{1}{\sqrt{2\bar{\gamma}_1}}(\gamma_2 + \bar{\gamma}_1\gamma_3 + \bar{\gamma}_1^3). \tag{3.68}$$

To compute $C_0(\gamma)$, introducing the following parametric transformation:

$$w_1(t) = -3\,\bar{\gamma}_1 \operatorname{sech}^2(t), \quad w_2(t) = 3\,\bar{\gamma}_1 \operatorname{sech}^2(t)\tanh(t), \tag{3.69}$$

into $C_0(\gamma)$ with a direct integration yields

$$C_0(\gamma) = \frac{6\bar{\gamma}_1\sqrt{2\bar{\gamma}_1}}{5}\left[\gamma_2 - \frac{5}{7}\bar{\gamma}_1\gamma_3 - \frac{103}{77} b_1 \bar{\gamma}_1^3\right]. \tag{3.70}$$

Finally, $C_0(\gamma)$ and $C_1(\gamma)$ can be expressed in terms of the original perturbation parameters β_j by using

$$\bar{\gamma}_1 = \sqrt{-\gamma_1} = \sqrt{-\varepsilon^{-\frac{4}{5}}\beta_1} = \varepsilon^{-\frac{2}{5}}\sqrt{-\beta_1}, \quad \gamma_2 = \varepsilon^{-\frac{6}{5}}\beta_2, \quad \gamma_3 = \varepsilon^{-\frac{4}{5}}\beta_3,$$

as

$$\begin{aligned} C_0(\beta) &= \frac{6\bar{\gamma}_1\sqrt{2\bar{\gamma}_1}}{5}\,\varepsilon^{-\frac{6}{5}}\Big[\beta_2 - \Big(\frac{5}{7}\beta_3 - \frac{103}{77}\beta_1\Big)\sqrt{-\beta_1}\Big], \\ C_1(\beta) &= \frac{1}{\sqrt{2\bar{\gamma}_1}}\,\varepsilon^{-\frac{6}{5}}\left[\beta_2 + (\beta_3 - \beta_1)\sqrt{-\beta_1}\,\right]. \end{aligned} \tag{3.71}$$

Therefore, the homoclinic loop bifurcation occurs from the critical surface, defined by $C_0(\beta) = 0$, as

$$\beta_2 = \Big(\frac{5}{7}\beta_3 - \frac{103}{77}\beta_1\Big),$$

while the degenerate homoclinic loop bifurcation happens on the curve, which is the intersection of the homoclinic loop bifurcation surface and the critical surface defined by $C_1(\beta) = 0$:

$$\beta_2 + (\beta_3 - \beta_1)\sqrt{-\beta_1} = 0,$$

as

$$\beta_2 = -\frac{4}{11}\beta_1\sqrt{-\beta_1}, \quad \beta_3 = \frac{15}{11}\beta_1, \quad (\beta_1 < 0).$$

Finally, it is known from [6] that double limit cycle bifurcation occurs from a critical surface, which is tangent to the Hopf bifurcation surface H on the critical curve GH, and tangent to the homoclinic bifurcation surface HL on the critical curve DHL. However, no formulas have been obtained for this surface, nor numerical approaches have been developed for plotting this surface. □

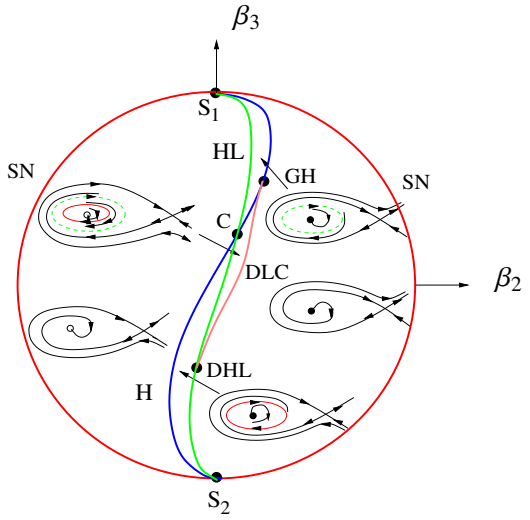

Figure 3.3: Bifurcation diagram for the codimension-3 B-T bifurcation based on the normal form (3.46), displayed in the intersection of the cone and the 2-sphere $\beta_1^2 + \beta_2^2 + \beta_3^2 = \sigma^2$, with the red color curve for saddle-node, the blue curve for Hopf and the green curve for homoclinic loop bifurcations, respectively. The GH and DHL represent the generalized Hopf critical point and the degenerate homoclinic critical point, respectively.

The bifurcation diagram projected on a 2-sphere is shown in Figure 2.4 with typical phase portraits, which is similar to Figure 3 in [6] and Figure 2 in [18].

Chapter 4

Conclusion and future work

Human health has been severely endangered throughout history by infectious diseases, the natural enemies of humans. Many researchers have successfully predicted and evaluated patterns of transmission of infectious diseases based on their etiology and transmission routes. Other non-pathological infectious diseases, such as the spread of computer viruses, the proliferation of information on the Internet, alcoholism, smoking, apoptosis, gene sequencing, and other forms of non-pathological infectious diseases, may also benefit from the application of infectious disease modeling, which is not limited to the study of pathological infectious diseases.

Bifurcation analysis is necessary in the study of disease models in order to explore complex dynamics which may happen in reality. The analysis provides a global picture of the qualitative dynamical behaviors of the models, thus helping them design, predict, and control diseases. Hopf bifurcation and Bogdanov-Takens (B-T) bifurcation are two well-known bifurcation phenomena, yielding complex dynamical behaviors such as jumping between equilibrium solutions and periodic oscillations (limit cycles), as well as homoclinic and heteroclinic loop motions. These different dynamical patterns may reflect the complex situations of patients. In fact, almost all scientific articles devoted to studying disease models pay attention to these two bifurcations. However, it has been shown that even for simple 2-d disease models, the bifurcation analysis becomes extremely difficult, caused by complicated computation, such that traditional approaches are not applicable. In many published articles related to disease systems, Hopf bifurcation analysis is not complete and B-T bifurcation is even not discussed. Recently, a hierarchical parametric analysis has been proposed to attack the difficulty [39], in which a simple epidemic model is used to demonstrate that this new approach is efficient when traditional methods are not applicable.

In this paper, we have applied dynamical system theory, in particular, stability and bifurcation theory, to further study the dynamics of two infectious disease models, which were investigated in [22, 29], however, these analyses are far from completion regarding the important Hopf and B-T bifurcations. We follow the new hierarchical parametric approach to provide

a complete analysis on the Hopf and B-T bifurcations of the two models.

Two disease models are investigated in this paper: one is an infectious disease SIR model with a saturated treatment function, introduced by Wang *et al.* [29], and another one is an SIRS model with a generalized incidence function, studied by Rao *et al.* [22]. Our analysis confirms that the disease-free equilibrium $E_0 = (0, 0$ is always a saddle point (which only exists in the model [29]), while another disease-free equilibrium $E_1 = (1, 0)$ (which exists in both the two models) is asymptotically stable for the basic reproduction number, $R_0 < 1$, and unstable for $R_0 > 1$, with a transcritical bifurcates to occur at the critical point $R_0 = 1$. We determined the conditions necessary for forward, backward, Hopf, and B-T bifurcation to analyze the nature of these bifurcations, especially for the conditions to the codimension of Hopf and B-T bifurcations. We showed how to determine the codimension of Hopf and B-T bifurcations using this epidemic model and the dynamical behavior around the equilibrium points. Furthermore, for the codimension-3 B-T bifurcation, we used a one-step transformation methodology suggested by [38], which is superior to the usual six-step strategy. Based on numerical simulations, several limit cycle bifurcations are demonstrated, which are in excellent agreement with theoretical predictions.

Future works mainly focus on the following tasks:

(1) To perform numerical simulation for the B-T bifurcation of the Rao's model, which is much more difficult than that for Hopf bifurcation;

(2) To carry out the Hopf and B-T bifurcations for the Rao's model with different death rates μ_i;

(3) To improve the hierarchical parametric analysis to be applicable for general nonlinear dynamical models;

(4) To develop combined symbolic and numerical Maple software package for Hopf and B-T bifurcation analyses.

Bibliography

[1] Algaba, E. Freire, E. Gamero, Hypernormal form for the Hopf-zero bifurcation, Int. J. Bifurcation and Chaos 8 (1998) 1857–1887.

[2] Baider and J. A. Sanders, Unique normal forms: the nilpotent Hamiltonian case, J. Differ. Equ. 92 (1991) 282–304.

[3] Buonomo, B. & Lacitignola, D. On the backward bifurcation of a vaccination model with nonlinear incidence. *Nonlinear Analysis: Modelling And Control*. **16**, 30-46 (2011)

[4] Cai, Y., Kang, Y., Banerjee, M. & Wang, W. A stochastic SIRS epidemic model with infectious force under intervention strategies. *Journal Of Differential Equations*. **259**, 7463-7502 (2015)

[5] Dhooge, W. Govaerts, Yu. A. Kuznetsov, MATCONT: A MATLAB package for numerical bifurcation analysis of ODEs, ACM Trans. Math. Software, 29 (2003) 141–164.

[6] Dumortier, R. Roussarie, J. Sotomayor, Generic 3-parameter families of vector fields on the plane, unfolding a singularity with nilpotent linear part. The cusp case of codimension 3, Ergodic Theory Dynam. Systems 7 (1987) 375–413.

[7] Gazor, M. Moazeni, Parametric normal forms for Bogdanov-Takens singularity; the generalized saddle-node case, Discrete Contin. Dyn. Syst. Ser. A 35 (2015) 205–224.

[8] Gazor, P. Yu, Formal decomposition method and parametric normal form, Int. J. Bifurcation and Chaos 20 (2010) 3487–3415.

[9] Gazor, P. Yu, Spectral sequences and parametric normal forms, J. Differ. Equ. 252 (2012) 1003–1031.

[10] Guckenheimer, P. Holmes, Nonlinear Oscillations, Dynamical Systems, and Bifurcations of Vector Fields (4th Ed.), Springer, New York, 1993.

[11] Gumel, A., Moghadas, S., Yuan, Y. & Yu, P. Bifurcation and stability analyses of a 13-D SEIC model using normal form reduction and numerical simulation. *DYNAMICS*

OF CONTINUOUS DISCRETE AND IMPULSIVE SYSTEMS SERIES B. **10** pp. 317-330 (2003)

[12] Han, Bifurcation of limit cycles and the cusp of order *n*, Acta Math. Sinica 13 (1997) 64–75.

[13] Han, P. Yu, Normal Forms, Melnikov Functions, and Bifurcations of Limit Cycles, Springer-Verlag, London, 2012.

[14] Hu, Z., Ma, W. & Ruan, S. Analysis of SIR epidemic models with nonlinear incidence rate and treatment. *Mathematical Biosciences*. **238**, 12-20 (2012)

[15] Kermack, W. & McKendrick, A. Contributions to the mathematical theory of epidemics. II.—The problem of endemicity. *Proceedings Of The Royal Society Of London. Series A, Containing Papers Of A Mathematical And Physical Character*. **138**, 55-83 (1932)

[16] Kendall, D. Deterministic and stochastic epidemics in closed populations. *Proceedings Of The Third Berkeley Symposium On Mathematical Statistics And Probability*. **4** pp. 149-165 (1956)

[17] Lahrouz, A., Omari, L., Kiouach, D. & Belmaâti, A. Complete global stability for an SIRS epidemic model with generalized non-linear incidence and vaccination. *Applied Mathematics And Computation*. **218**, 6519-6525 (2012)

[18] Li, J. Li, Z. Ma, Codimension 3 B-T bifurcations in an epidemic model with a nonlinear incidence, Discrete Contin. Dyn. Syst. Ser. B 20 (2015) 1107–1116.

[19] Li, Y. Zhou, J. Wu, Z. Ma, Complex dynamics of a simple epidemic model with a nonlinear incidence, Discrete Contin. Dyn. Syst. Ser. B 8 (2007) 161–173.

[20] Li, C., Li, J. & Ma, Z. Codimension 3 BT bifurcations in an epidemic model with a nonlinear incidence. *Discrete Continuous Dynamical Systems-B*. **20**, 1107 (2015)

[21] Marsden, M. McCracken, The Hopf bifurcation and Its Applications, Springer-Verlag, New York, 1976.

[22] Rao, F., Mandal, P. & Kang, Y. Complicated endemics of an SIRS model with a generalized incidence under preventive vaccination and treatment controls. *Applied Mathematical Modelling*. **67** pp. 38-61 (2019)

[23] Ross, R. An application of the theory of probabilities to the study of a priori pathometry.—Part I. *Proceedings Of The Royal Society Of London. Series A, Containing Papers Of A Mathematical And Physical Character*. **92**, 204-230 (1916)

[24] Ross, R. & Hudson, H. An application of the theory of probabilities to the study of a priori pathometry.—part iii. *Proceedings Of The Royal Society Of London. Series A, Containing Papers Of A Mathematical And Physical Character*. **93**, 225-240 (1917)

[25] Roussel, Nonlinear Dynamics - A Hands-On Introductory Survey, Morgan and Claypool, San Rafael, California, 2019

[26] Takens, Singularities of vector fields, Publ. Math. IHES 43 (1974) 47–100.

[27] Ushiki, Normal forms for singularities of vector fields, Japan J. Appl. Math. 1 (1984) 1–37.

[28] Wang, W. Backward bifurcation of an epidemic model with treatment. *Mathematical Biosciences*. **201**, 58-71 (2006)

[29] Wang, J., Liu, S., Zheng, B. & Takeuchi, Y. Qualitative and bifurcation analysis using an SIR model with a saturated treatment function. *Mathematical And Computer Modelling*. **55**, 710-722 (2012)

[30] Xiao, D. & Ruan, S. Global analysis of an epidemic model with nonmonotone incidence rate. *Mathematical Biosciences*. **208**, 419-429 (2007)

[31] Yu. A. Kuznetsov, Elements of Applied Bifurcation Theory (2nd Ed.), Springer, New York, 1998.

[32] Yu, Computation of normal forms via a perturbation technique, J. Sound Vib. 211 (1998) 19–38.

[33] Yu, Simplest normal forms of Hopf and generalized Hopf bifurcations, Int. J. Bifurcation and Chaos 9 (1999) 1917–1939.

[34] Yu, A. Y. L. Leung, The simplest normal form of Hopf bifurcation, Nonlinearity 16 (2003) 277–300.

[35] Yu, P., Zhang, W. & Wahl, L. Dynamical analysis and simulation of a 2-dimensional disease model with convex incidence. *Communications In Nonlinear Science And Numerical Simulation*. **37** pp. 163-192 (2016)

[36] Yu, W. Zhang, Complex dynamics in a unified SIR and HIV disease model: A bifurcation theory approach, J. Nonlinear Sci. 29 (2019) 2447–2500.

[37] Zhang, X. & Liu, X. Backward bifurcation of an epidemic model with saturated treatment function. *Journal Of Mathematical Analysis And Applications*. **348**, 433-443 (2008)

[38] Zeng, S. Deng, P. Yu, Bogdanov-Takens bifurcation in predator-prey systems, Discrete Contin. Dyn. Syst. Ser. S 13 (2020) 3253–3269.

[39] Zeng, P. Yu, A hierarchical parametric analysis on Hopf bifurcation of an epidemic model, Discrete Contin. Dyn. Syst. Ser. S (2022) (online since March 23, 2022).

[40] Guckenheimer, J. & Kuznetsov, Y. Bogdanov-takens bifurcation. *Scholarpedia*., http://www.scholarpedia.org/article/Bogdanov-Takens_bifurcation

[41] Wikipedia contributors Compartmental models in epidemiology — Wikipedia, The Free Encyclopedia. (https://en.wikipedia.org/w/index.php?title=Compartmental_models_in_epidemiologyoldid=1094997436,2022)